CONFIDENTIAL

Copy
RM L57L18

NACA

RESEARCH MEMORANDUM

AN INVESTIGATION OF SUPERSONIC STORE INTERFERENCE IN THE VICINITY OF A 22° SWEPT-WING–FUSELAGE CONFIGURATION AT MACH NUMBERS OF 1.61 AND 2.01

By Douglas J. Geier

Langley Aeronautical Laboratory
Langley Field, Va.

NATIONAL ADVISORY COMMITTEE
FOR AERONAUTICS

WASHINGTON

February 24, 1958

CONFIDENTIAL

NATIONAL ADVISORY COMMITTEE FOR AERONAUTICS

RESEARCH MEMORANDUM

AN INVESTIGATION OF SUPERSONIC STORE INTERFERENCE IN THE VICINITY OF A 22° SWEPT-WING—FUSELAGE CONFIGURATION AT MACH NUMBERS OF 1.61 AND 2.01

By Douglas J. Geier

SUMMARY

An investigation has been conducted in the Langley 4- by 4-foot supersonic pressure tunnel at Mach numbers of 1.61 and 2.01 in which separate forces and moments were measured on a store (five components), on a 22° swept wing (three components), and on a 22° swept-wing—fuselage combination (three components) for a wide range of store positions. The interference effects for a 22° swept wing are similar to those effects for a 45° swept wing (NACA RM L55A13a) and a 60° delta wing (NACA RM L55I27a). The store side forces are large for all three wings with the magnitudes increasing toward the wing tip, and the largest magnitude occurs in the presence of the 22° swept wing.

INTRODUCTION

Wind-tunnel investigations on supersonic store interference have shown that, due to interference between various configuration components, large performance penalties and large loads can occur.

Previous research on store interference at the Langley 4- by 4-foot supersonic pressure tunnel includes tests on detached stores in the presence of a 45° swept-wing—fuselage configuration at Mach numbers of 1.61 and 2.01 (refs. 1, 2, and 3) and a 60° delta-wing—fuselage configuration at a Mach number of 1.61 (ref. 4).

More recent work (refs. 5 and 6) has been aimed at calculating forces on detached stores and store-pylon configurations for correlation with experimental programs.

The present paper presents the results of an investigation of detached store forces and moments in the presence of a 22° swept-wing—fuselage combination. Separate forces and moment were measured at Mach numbers of 1.61 and 2.01 on a sting-supported store (five components) and on the wall-mounted semispan-wing—fuselage combination (three components).

SYMBOLS

$C_{D,w}$ drag coefficient of the wing, $\frac{\text{Drag}}{qS}$

$C_{L,w}$ lift coefficient of the wing, $\frac{\text{Lift}}{qS}$

$C_{m,w}$ pitching-moment coefficient of the wing about $\frac{\bar{c}}{4}$, $\frac{\text{Pitching moment}}{qS\bar{c}}$

$C_{D,wf}$ drag coefficient of the wing-fuselage combination, $\frac{\text{Drag}}{qS}$

$C_{L,wf}$ lift coefficient of the wing-fuselage combination, $\frac{\text{Lift}}{qS}$

$C_{m,wf}$ pitching-moment coefficient of the wing-fuselage combination about $\frac{\bar{c}}{4}$, $\frac{\text{Pitching moment}}{qS\bar{c}}$

$C_{D,t}$ total drag coefficient of complete configuration (wing and fuselage plus store) based on wing area, $C_{D,wf} + C_{D,s}\left(\frac{F}{S}\right)$

$C_{L,t}$ total lift coefficient of complete configuration (wing and fuselage plus store) based on wing area, $C_{L,wf} + C_{L,s}\left(\frac{F}{S}\right)$

$C_{D,s}$ drag coefficient of store based on frontal area, $\frac{\text{Drag}}{qF}$

$C_{L,s}$ lift coefficient of store, $\frac{\text{Lift}}{qF}$

$C_{m,s}$ pitching-moment coefficient of store about store nose, $\frac{\text{Pitching moment}}{qFl}$

$C_{Y,s}$ side-force coefficient of store (for left wing panel, positive side force is toward the wing root), $\frac{\text{Side force}}{qF}$

$C_{n,s}$ yawing-moment coefficient of store about store nose, $\frac{\text{Yawing moment}}{qFl}$

$\bar{c}$ mean aerodynamic chord of wing, in.

α angle of attack measured with respect to free stream, deg

S total area of wing semispan, 0.5 sq ft

F maximum frontal area of store, 0.0123 sq ft

q dynamic pressure, lb/sq ft

l store length, 12 in.

x chordwise position of store midpoint, measured from nose of fuselage (see fig. 1), in.

y spanwise position of store midpoint measured from fuselage center line (see fig. 1), in.

z vertical position of store center line, measured from wing chord plane (see fig. 1), in.

M Mach number

Subscripts:

w wing

wf wing-fuselage combination

s store

i interference-free coefficient

APPARATUS AND TESTS

Models and Equipment

The principal dimensions of the models and the general arrangement of the test setup are shown in figure 1. Pertinent model dimensions are given in table I. The semispan-wing—fuselage combination was designed to simulate a 22° swept-wing heavy bomber-type airplane. The wing and fuselage were constructed of metal and were mounted on a boundary-layer bypass plate $10\frac{3}{4}$ inches from the tunnel wall. The wing is swept approximately 22° about the 25-percent chord (the 75-percent chord is unswept).

The fuselage and store are the same as were used in previous store tests and are described in detail in reference 1, together with a description of the test equipment. Pertinent remarks on support interference are also included in reference 1. The wing-fuselage angle of attack was set at 0° and 4° while the store angle of attack remained constant at 0°. Tests were made with the store at various spanwise, chordwise, and vertical positions (at $\alpha = 0°$, $z = 1.15$ inches and 2.09 inches; at $\alpha = 4°$, $z = 2.09$ inches). The tests were made with the store in the presence of the wing and wing-fuselage combination at $M = 1.61$ but only in the presence of the wing-fuselage combination at $M = 2.01$.

The store was run in conjunction with the wing and the wing-fuselage combination in all spanwise and vertical positions shown in figure 1 and at chordwise positions of 15, 18, 21, 24, and 27 inches for the store with wing and at chordwise positions of 12, 15, 18, 21, 24, 27, 30, and 33 inches for the store with the wing-fuselage combination.

All tests were run with boundary-layer transition fixed on all components as described in reference 1 and with no support pylons or model tail surfaces.

The tests were performed in the Langley 4- by 4-foot supersonic pressure tunnel at Mach numbers of 1.61 and 2.01 and corresponding Reynolds numbers per foot of 4.20×10^6 and 3.62×10^6.

Accuracy of Data

An estimate of the relative accuracy of the present data as determined from an inspection of repeat test points and static-deflection calibration is presented as follows:

Store position:	
x, in.	±0.025
y, in.	±0.05
z, in.	±0.05
Store characteristics:	
$C_{D,s}$	±0.005
$C_{L,s}$	±0.010
$C_{m,s}$	±0.005
$C_{Y,s}$	±0.010
$C_{n,s}$	±0.005
α, s, deg	±0.2
Wing-fuselage combination:	
$C_{D,wf}$	±0.0005
$C_{L,wf}$	±0.005
$C_{m,wf}$	±0.002
α, wf, deg	±0.1

PRESENTATION AND DISCUSSION OF DATA

Interference-Free Data

Store.- The drag, lift, and pitching-moment coefficients for the isolated store at angles of attack from 0° to 12° are shown in figure 2 for M = 1.61 and 2.01. Also shown for comparison in the figure are the isolated store data from references 1, 2, and 3. The data for the store pitching-moment coefficient are presented herein computed about the store nose.

Wing and wing-fuselage combination.- The isolated wing and wing-fuselage drag, lift, and pitching-moment coefficients are presented in figure 3, for angles of attack from 0° to 14° at M = 1.61 and M = 2.01.

Basic Data

The basic data are presented in contour-plot form. Contour plots of the store (five components) and of the wing and the wing-fuselage forces and moments (three components) are presented in figures 4 to 31.

Contour plots have been made for each coefficient covering two vertical heights and two angles of attack (three plots in all). The store midpoint is the reference point (the point at which the force coefficient is plotted) for all contour plots.

Store drag, lift, and pitching-moment coefficients.- Figures 4 and 9 show the drag coefficient of the store (based on store frontal area) in the presence of the wing and wing-fuselage combination. Figure 4(a) shows that the influence of the wing on store drag coefficient is to increase the drag as much as 25 percent as the store moves inboard under the wing at a vertical location of 1.15 inches. As the store is moved outboard, forward or rearward of these positions, the store drag coefficient decreases rapidly, in some cases to values below the value for the isolated store, and a favorable wing interference effect on the store drag coefficient is indicated. There is a decrease in magnitude of store drag coefficient due to an increase in the vertical displacement between the store and wing. (See figs. 9(a) and 9(b).)

The effect of changing the wing or wing-fuselage angle of attack (fig. 9(c)) is to increase the maximum store drag coefficient and to decrease the minimum store drag coefficient and shift the maximum values rearward near the trailing edge of the wing.

Figure 22 shows that the trends of the store drag coefficients at $M = 2.01$ are similar to those previously discussed for $M = 1.61$. The store drag coefficients at $M = 2.01$ are smaller than those at $M = 1.61$, and the regions of maximum drag are shifted rearward somewhat.

Lift coefficients for the store in the presence of the wing and wing-fuselage combination are presented in figures 5 and 10. A comparison of figures 5 and 10 shows that the effect of adding the fuselage is small. It can be seen in figure 10(a) that the store experiences positive lift coefficients at all store positions in the vicinity of the wing. Positions of maximum lift interference are located inboard under the wing. The effects of increasing the vertical displacement between the wing and the store are small. (See fig. 10(b).)

Increasing the wing-fuselage angle of attack from 0° to 4° increases the negative lift coefficient along the leading edge of the wing, decreases the positive lift interference at the inboard stations, and slightly increases the interference near the wing tip.

Figure 23 shows that the lift coefficients are smaller at a Mach number of 2.01 than at the lower Mach number and the maximum values are shifted slightly rearward.

The pitching-moment coefficients (figs. 6 and 11) for $M = 1.61$ and those at $M = 2.01$ (fig. 24) are computed about the store nose and reflect primarily the lift on the store.

Store side-force and yawing-moment coefficients.- Negative (toward the wing tip) side force is shown in figure 12(a) for all store positions in the region of the wing. The effect of increasing the vertical displacement between the store and the wing (fig. 12(b)) is small.

An increase in wing-fuselage angle of attack (fig. 12(c)) causes a large increase in the value of negative side-force coefficients with the maximum value of side-force coefficient occurring near the wing tip. Comparison of figures 7 and 12 shows that the effect of the fuselage is small.

The magnitudes of the side-force coefficients for a Mach number of 2.01 (fig. 25) are generally smaller than those for a Mach number of 1.61. The store yawing-moment coefficient (computed about the nose of the store in figs. 8, 13, and 26) reflects largely the variation in the side-force coefficient.

Wing-fuselage and total-drag coefficients.- Contour plots of the wing drag and wing-fuselage drag coefficients (based on wing area) in the presence of the store are presented in figures 14 and 17. The drag coefficients of the wing and the wing-fuselage show a maximum increase in drag coefficient of about 20 percent due to store interference. Maximum drag-coefficient values occur inboard from the midsemispan position.

Comparison of figures 14 and 17 shows a wing-fuselage drag coefficient slightly higher than the wing drag coefficient in the immediate vicinity of the wing. Vertical displacement of the store had no appreciable effect on the wing or wing-fuselage drag coefficients.

Figure 27 shows that at a Mach number of 2.01 the wing-fuselage drag-coefficient trends are generally the same as those at a Mach number of 1.61.

Figure 20 presents the total-drag coefficients of the complete configuration. Although no pylon drag or interference is included in $C_{D,t}$, the total-drag coefficient is of interest in evaluating the net or overall interference on a complete configuration (wing-fuselage combination plus store).

The total-drag coefficient of the complete configuration is higher than the sum of the free-air drag of the components (0.0193) for all store positions on or near the wing except for the tip positions. The regions for maximum interference drag are near the wing midchord, inboard. At the wing tip, the store induced a favorable interference-drag effect.

Increasing the vertical displacement (fig. 20(b)) decreases the values of total-drag coefficient in the vicinity of the wing, but unfavorable drag interference remains over essentially the same areas. Increasing the angle of attack increases the mutual interference.

As seen in figure 30, the total-drag coefficient at $M = 2.01$ shows the same general trends as those discussed for a Mach number of 1.61.

Wing-fuselage and total-lift coefficients.- The lift coefficients of the wing and wing-fuselage combination in the presence of the store are shown in figures 15 and 18. By comparison of these two figures, it can be seen that the interference lift produced by the addition of the fuselage is small.

When the store is at its closest proximity to the wing (fig. 15(a)), there is favorable lift interference for all store positions rearward from the 40-percent chord, with the maximum value equal approximately to that produced by 1.2° angle of attack of the wing.

Increasing the vertical displacement between the wing and the store (fig. 15(b)) tends to shift the zero-lift contour a small distance forward toward the leading edge of the wing, although the magnitudes of the lift coefficients remain the same. The magnitudes of the wing-fuselage lift coefficient change when the angle of attack is increased from 0° to 4°, but the interference lift coefficient remains approximately the same.

Figure 21 presents the total-lift coefficients of the complete configuration (wing-fuselage combination plus store). These data show only small variations from the results previously shown for the wing-fuselage lift coefficients. Thus, the effect of the store on total-lift coefficient is relatively small.

Figures 28 and 31 present the wing-fuselage and total-lift coefficients at a Mach number of 2.01. These data show only small variations from the results previously given for the lower Mach number data.

Wing-fuselage pitching-moment coefficients.- Figures 16 and 19 ($M = 1.61$) and figure 29 ($M = 2.01$) present the pitching-moment coefficients of the wing and wing-fuselage combination in the presence of the store $\left(\text{moments computed about } \frac{\bar{c}}{4}\right)$. These figures show that the pitching-moment interferences are small and are predominantly those felt by the wing. The effects of vertical displacement and angle of attack are similar to those noted previously for other coefficients.

COMPARISON PLOTS

A comparison of the contour plots of store drag and total-drag coefficients ($z = 2.09$, $\alpha = 0^\circ$) for the 22° swept-wing combination, a 60° delta-wing combination, and the 45° swept-wing combination is shown in figure 32. Although there are large differences in the wing plan forms, the maximum value of store drag coefficient produced on the store by all three wing-fuselage combinations tends to be similar in magnitude.

The values of high store drag coefficients for all three wing combinations occur in the same region, inboard on the wing.

Although the values of total-drag coefficient are different for the three wing combinations, the maximum incremental drag produced by interference is of similar magnitude and occurs in the same regions, inboard on the wing.

Comparison of the contour plots of the store lift and total-lift coefficients for the three wing-fuselage combinations is presented in figure 33. The data show that the magnitudes of store lift coefficient produced by the 45° swept wing, 60° delta wing, and the 22° swept wing on the store are comparable. Contour plots of the total-lift coefficients show that the magnitudes of the total-lift coefficients are similar for all three wing combinations. The maximum total-lift interference occurred for all three wing combinations in the vicinity of the wing trailing edge near the inboard store positions.

Figure 34 shows a comparison of the side-force coefficients for the store in presence of the three wing-fuselage combinations. Although the data in references 5 and 6 show the pylon to be the major cause of high side force on a store-pylon combination, a comparison of store side force can give some indication as to the magnitudes and direction of store side force.

Figure 34(a) shows small side forces in the direction of the wing tip for all store positions in the vicinity of the 22° swept wing. Store

side forces toward the wing root, however, are shown near the wing leading edges for the store in presence of the 45° swept wing and the 60° delta wing.

At 4° angle of attack (fig. 34(b)), there are tipward side forces for the store positions in the vicinity of all three wings. The magnitudes of the side-force coefficients increase greatly when the store is moved toward the wing tip, the largest values being with the 22° swept wing.

CONCLUSIONS

An investigation has been conducted in the Langley 4- by 4-foot supersonic pressure tunnel at Mach numbers of 1.61 and 2.01 in which separate forces were measured on a detached store in the presence of a 22° swept wing and a 22° swept-wing—fuselage combination for a wide range of store positions. The results are compared with similar tests of the store in the presence of a 45° swept-wing—fuselage combination and a 60° delta-wing—fuselage combination and indicate the following conclusions:

1. Significant changes in store forces and moments may occur with small changes in store chordwise and spanwise position.

2. The interference forces measured at a Mach number of 2.01 were smaller in magnitude but had characteristics similar to those measured at a Mach number of 1.61.

3. The total-interference drag and lift produced by the 45° swept wing, the 60° delta wing, and the 22° swept-wing—fuselage combinations were of similar magnitude and characteristics. The store positions for high drag and lift coefficients for the three wing combinations occurred in the same regions - inboard on the wing, in the case of drag, and inboard along the trailing edge of the wing, in the case of lift.

4. For all three wing-fuselage combinations, the store experienced large negative side forces over most of the wing plan form with the magnitudes of negative side force increasing toward the wing tip and the largest side-force coefficients occurring in the presence of the 22° swept wing.

Langley Aeronautical Laboratory,
National Advisory Committee for Aeronautics,
Langley Field, Va., December 4, 1957.

REFERENCES

1. Smith, Norman F., and Carlson, Harry W.: The Origin and Distribution of Supersonic Store Interference From Measurement of Individual Forces on Several Wing-Fuselage-Store Configurations. I.- Swept-Wing Heavy-Bomber Configuration With Large Store (Nacelle). Lift and Drag; Mach Number, 1.61. NACA RM L55A13a, 1955.

2. Smith, Norman F., and Carlson, Harry W.: The Origin and Distribution of Supersonic Store Interference From Measurement of Individual Forces on Several Wing-Fuselage-Store Configurations. II.- Swept-Wing Heavy-Bomber Configuration With Large Store (Nacelle). Lateral Forces and Pitching Moments; Mach Number, 1.61. NACA RM L55E26a, 1955.

3. Carlson, Harry W., and Geier, Douglas J.: The Origin and Distribution of Supersonic Store Interference From Measurement of Individual Forces on Several Wing-Fuselage-Store Configurations. V.- Swept-Wing Heavy-Bomber Configuration With Large Store (Nacelle). Mach Number 2.01. NACA RM L55K15, 1956.

4. Morris, Odell A.: The Origin and Distribution of Supersonic Store Interference From Measurement of Individual Forces on Several Wing-Fuselage-Store Configurations. IV.- Delta-Wing Heavy-Bomber Configuration With Large Store. Mach Number, 1.61. NACA RM L55I27a, 1955.

5. Bobbitt, Percy J., Carlson, Harry W., and Pearson, Albin O.: Calculation of External-Store Loads and Correlation With Experiment. NACA RM L57D30a, 1957.

6. Morris, Odell A., Carlson, Harry W., and Geier, Douglas J.: Experimental and Theoretical Determination of Forces and Moments on a Store and on a Store-Pylon Combination Mounted on a 45° Swept-Wing—Fuselage Configuration at a Mach number of 1.61. NACA RM L57K18, 1958.

TABLE I.- PERTINENT MODEL DIMENSIONS

Store:	
Maximum diameter, in.	1.5
Maximum frontal area, sq ft	0.0123
Base diameter, in.	0.96
Base area, sq ft	0.005
Overall length, in.	12
Nose fineness ratio	3
Afterbody fineness ratio	1.82
Overall fineness ratio	8
Ratio of wing area to store maximum frontal area	40.6
Fuselage:	
Maximum diameter, in.	2.75
Maximum frontal area (semicircle), sq ft	0.0206
Base diameter, in.	1.372
Base area (semicircle), sq ft	0.0051
Overall length, in.	35.75
Nose fineness ratio	4.75
Afterbody fineness ratio	3
Overall fineness ratio	13
22° swept wing:	
Semispan, in.	10.39
Mean aerodynamic chord, in.	7.759
Area (semispan) sq ft	0.50
Aspect ratio	1.5
Center-line chord, in.	11.058
Section	4-percent circular-arc

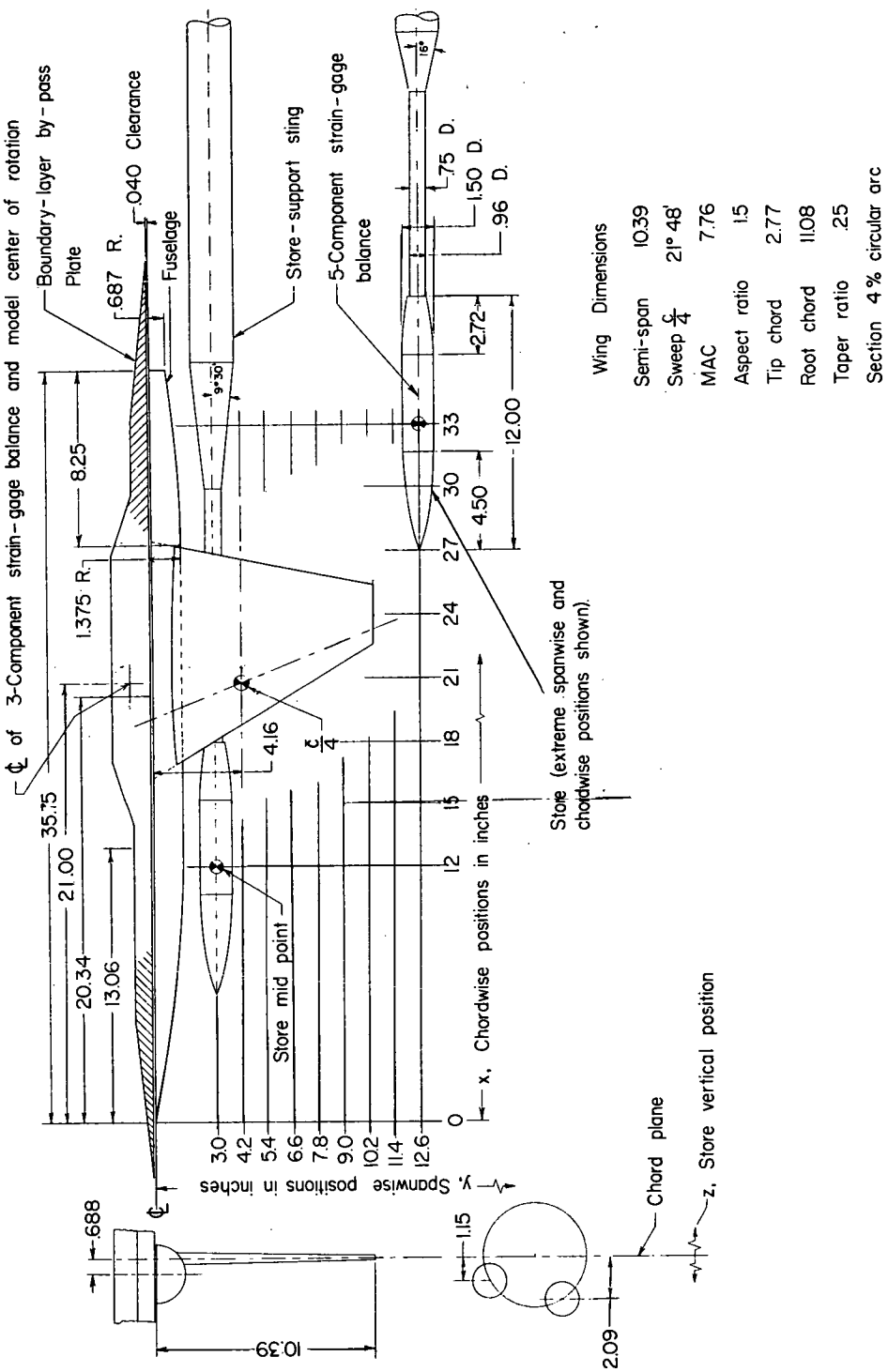

Figure 1.- Layout of models showing dimensions of components and ranges of store positions investigated. Fuselage and store nose and afterbody are ogive bodies of revolution. Center sections are cylindrical. All dimensions are in inches.

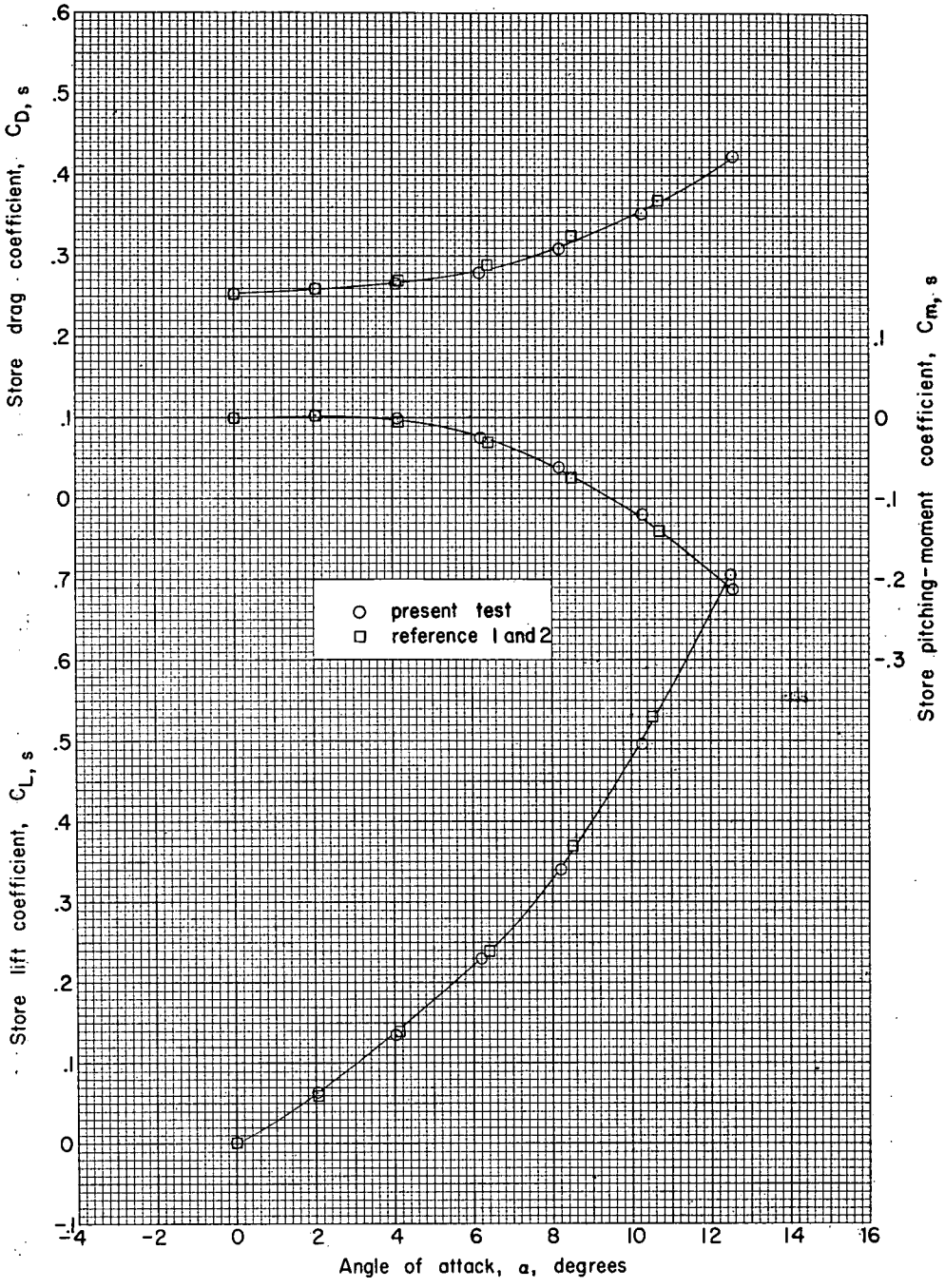

(a) M = 1.61.

Figure 2.- Aerodynamic characteristics of the isolated store.

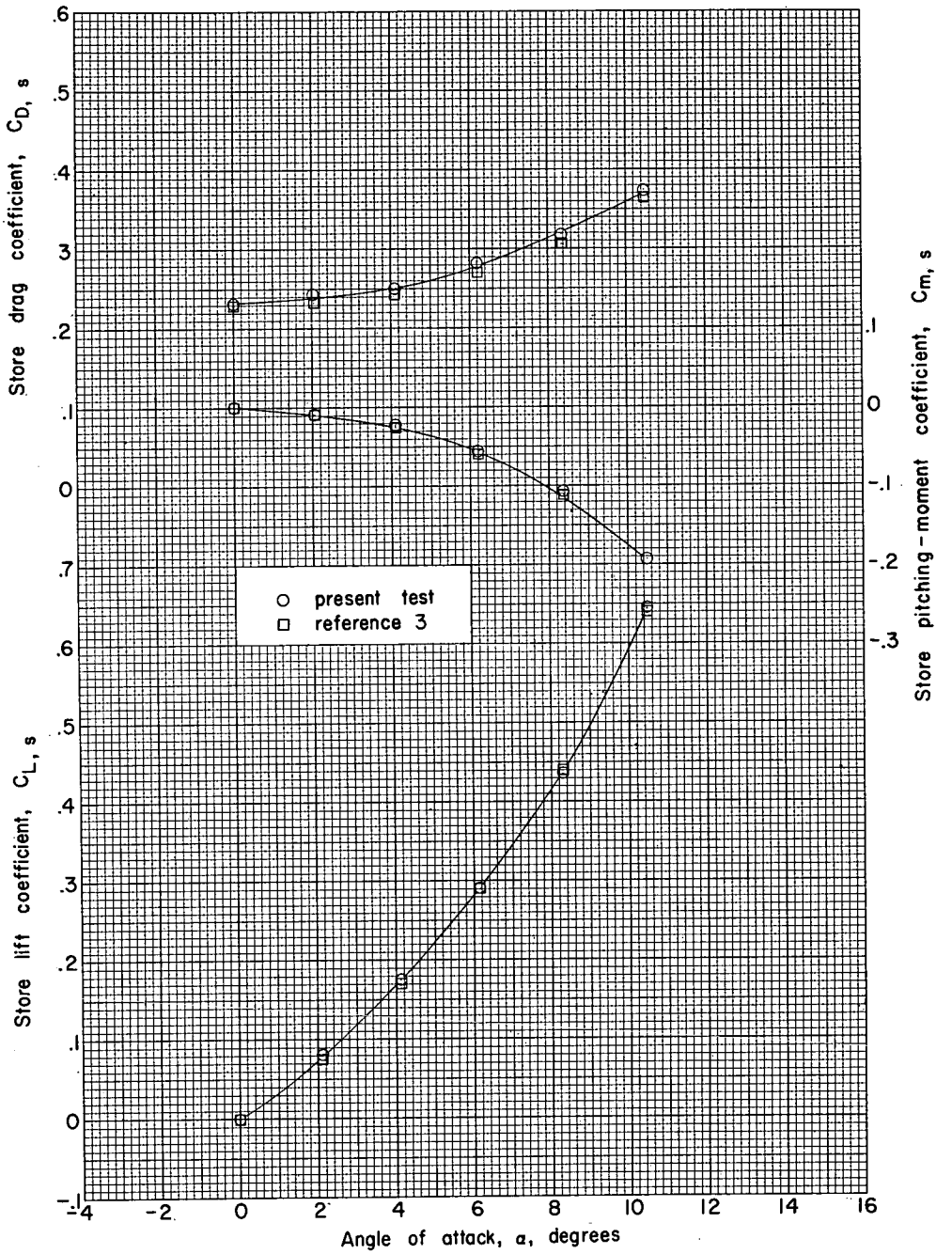

(b) M = 2.01.

Figure 2.- Concluded.

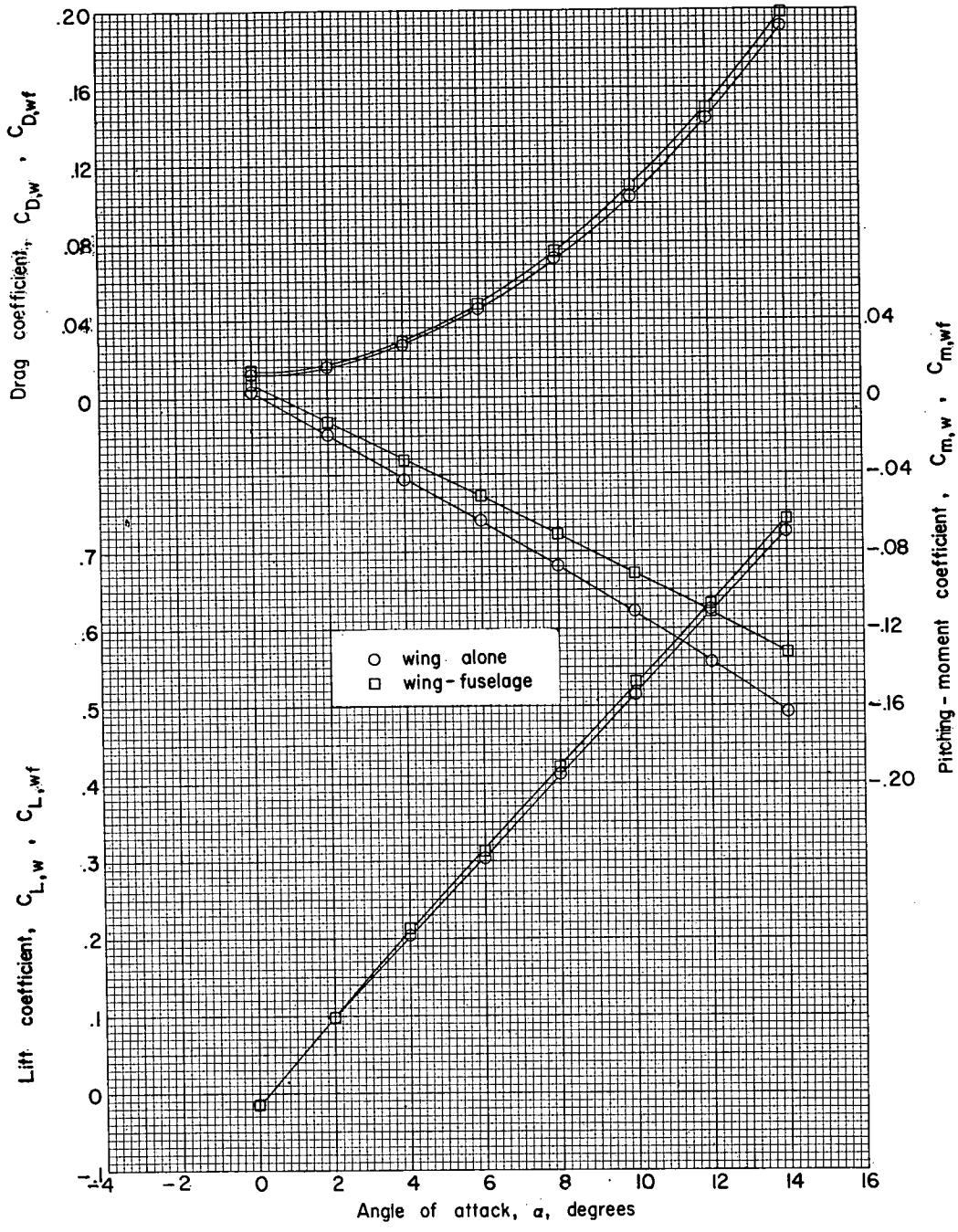

(a) M = 1.61.

Figure 3.- Aerodynamic characteristics of the isolated wing and wing-fuselage combination.

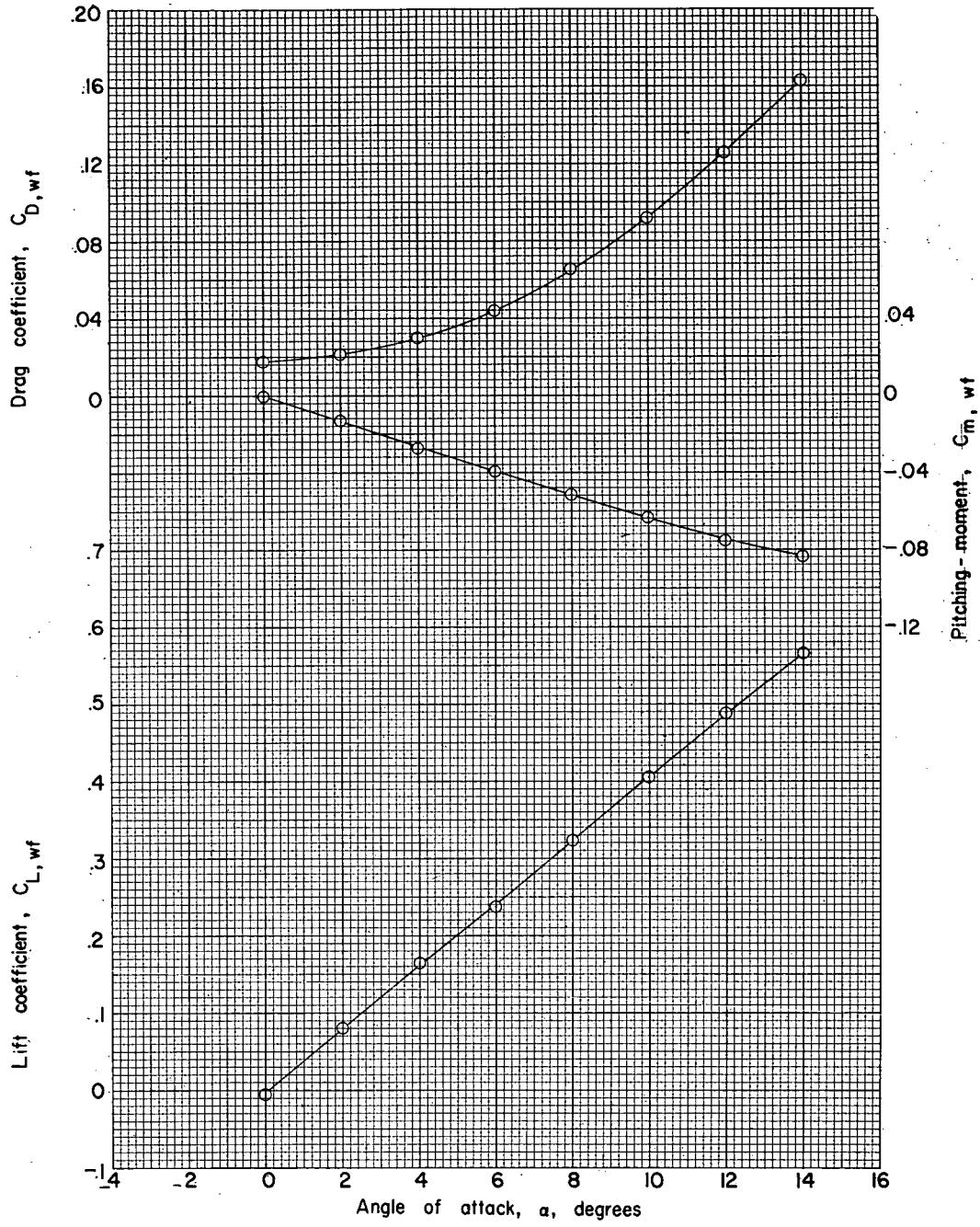

(b) M = 2.01.

Figure 3.- Concluded.

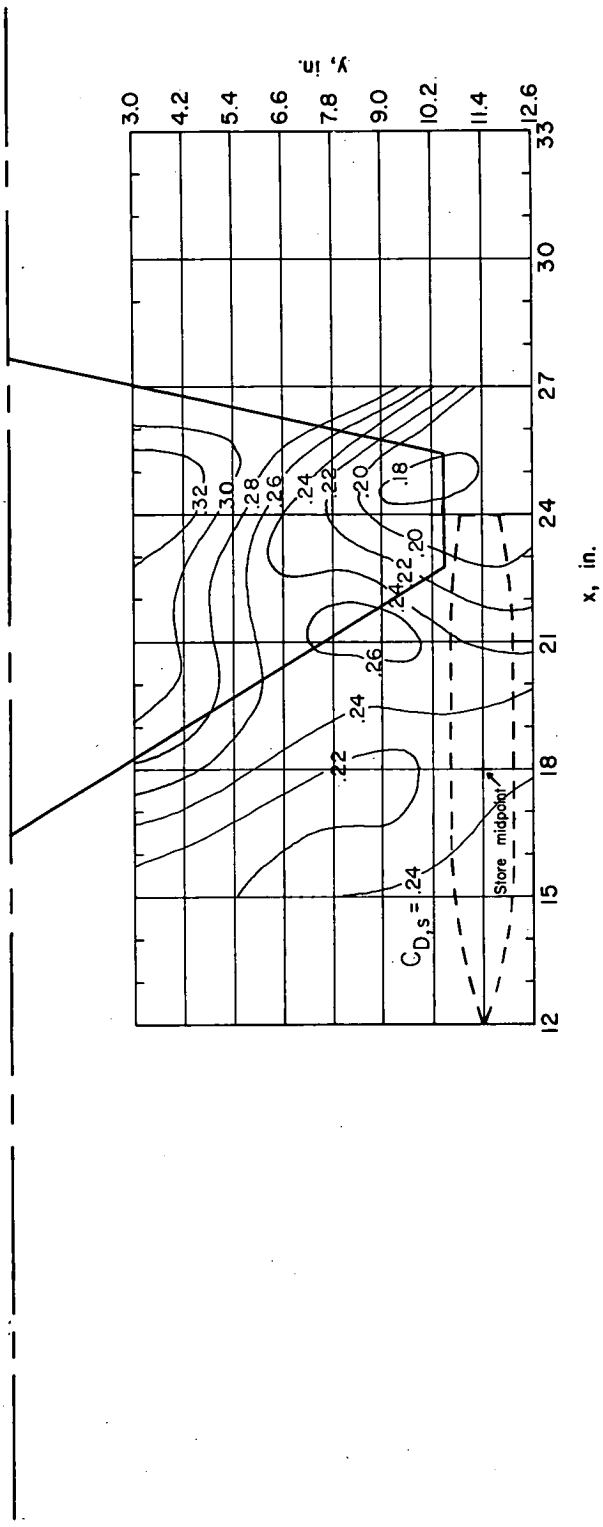

(a) z = 1.15 in.; $\alpha = 0^{\circ}$.

Figure 4.- Contour plot of the drag coefficients of store in presence of the wing at M = 1.61. Drag coefficients of the isolated store ($\alpha = 0^{\circ}$, $C_{D,i} = 0.2520$; $\alpha = 4^{\circ}$, $C_{D,i} = 0.2650$).

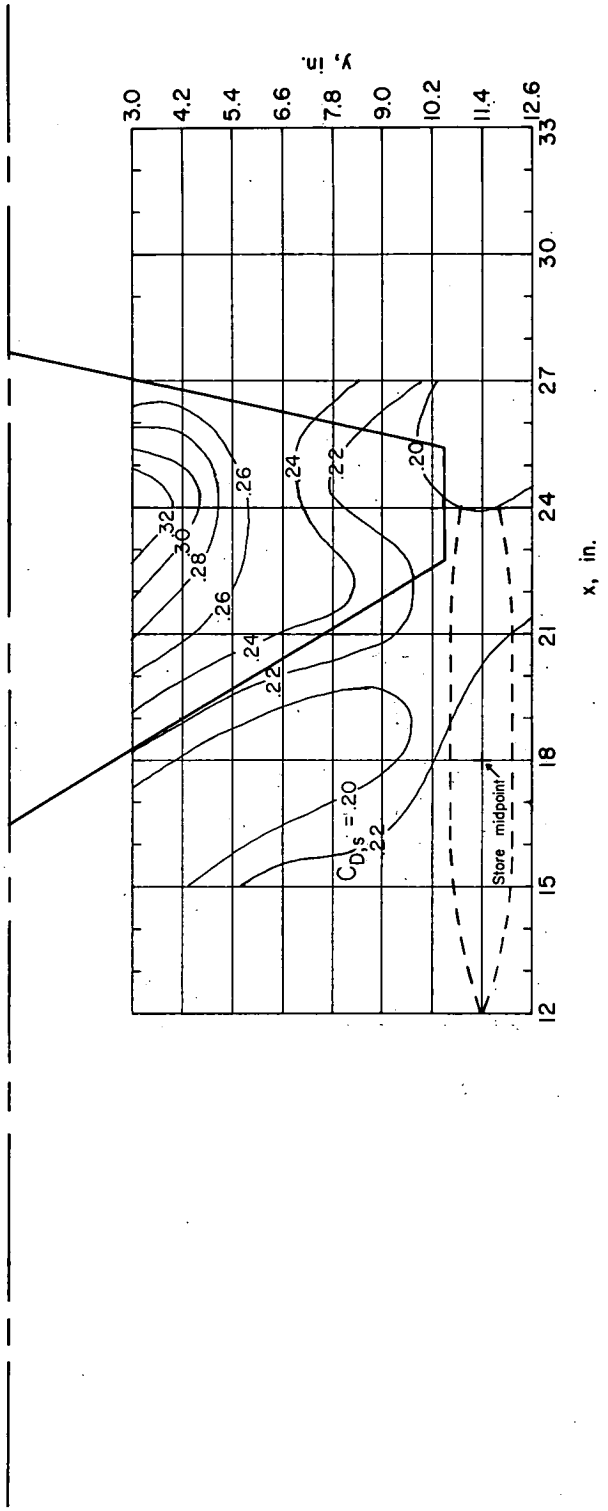

(b) $z = 2.09$ in.; $\alpha = 0^{\circ}$.

Figure 4.- Continued.

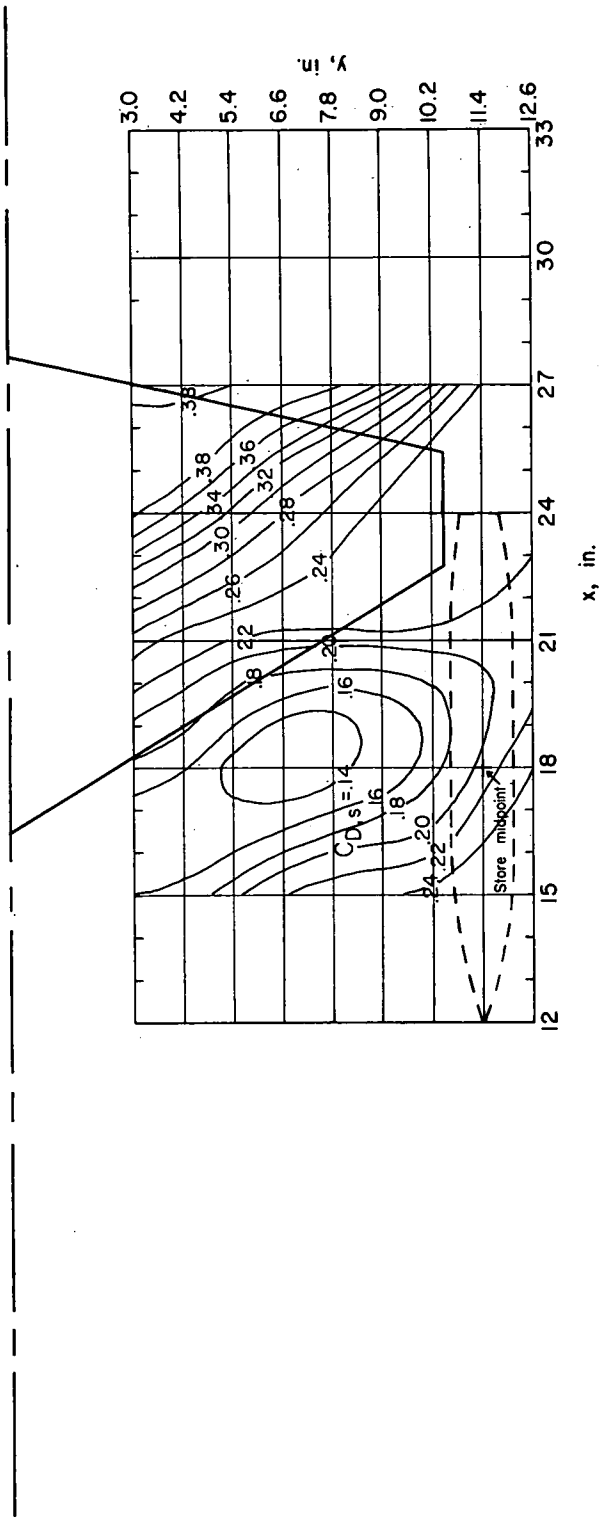

(c) z = 2.09 in.; $\alpha = 4^{\circ}$.

Figure 4.- Concluded.

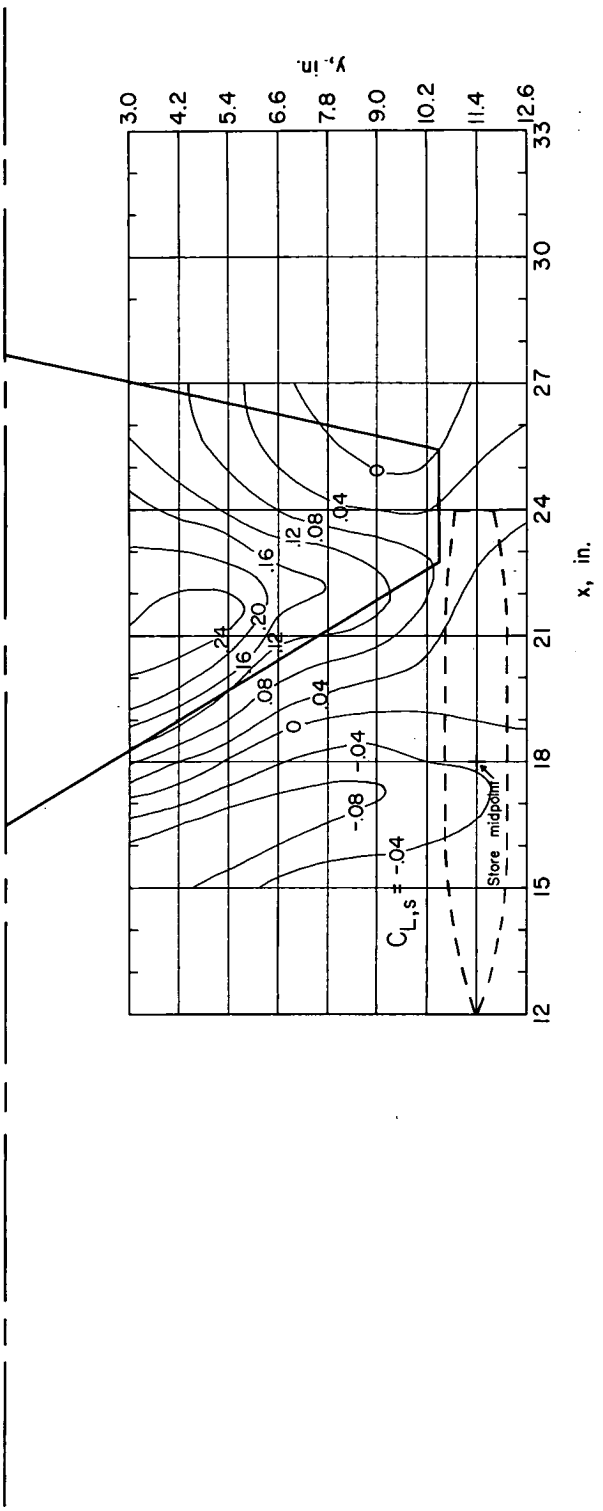

(a) z = 1.15 in.; $\alpha = 0^{\circ}$.

Figure 5.- Contour plot of the lift coefficients of the store in presence of the wing at M = 1.61. Lift coefficients for the isolated store ($\alpha = 0^{\circ}$, $C_{L,i} = 0.000$; $\alpha = 4^{\circ}$, $C_{L,i} = 0.135$).

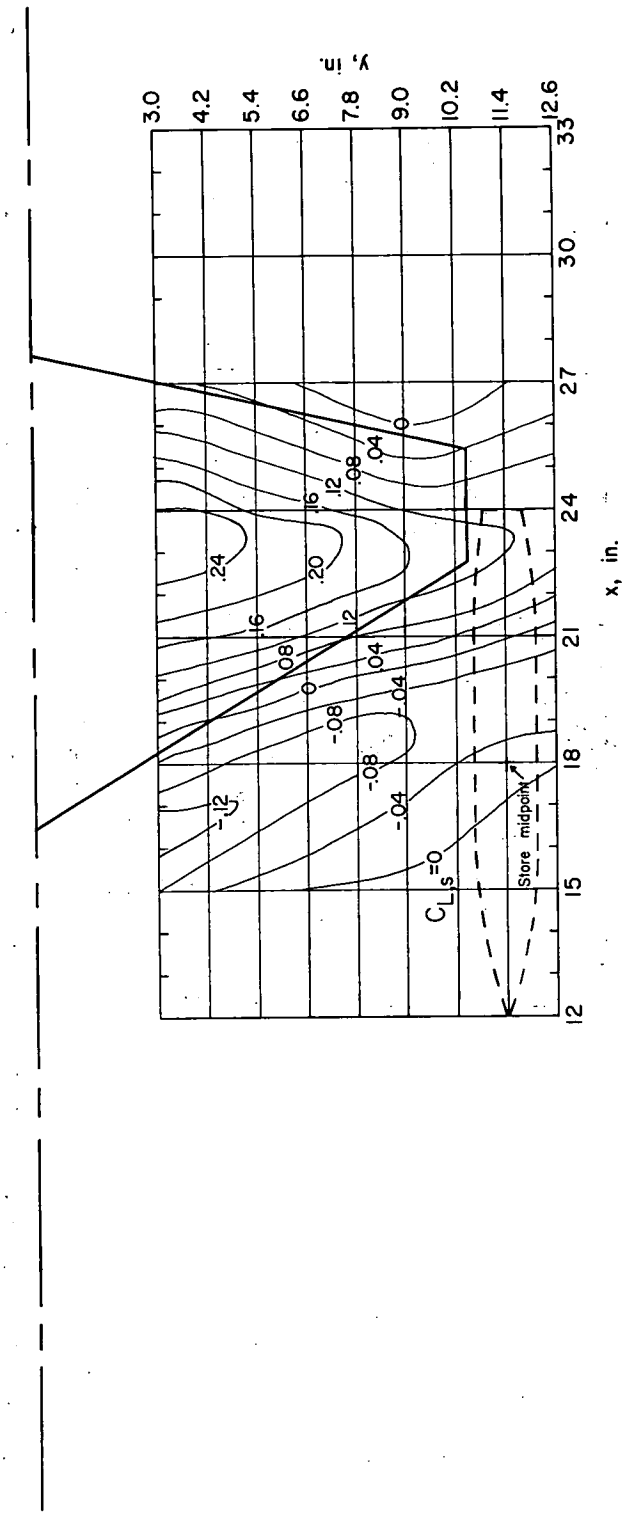

(b) z = 2.09 in.; $\alpha = 0^{\circ}$.

Figure 5.- Continued.

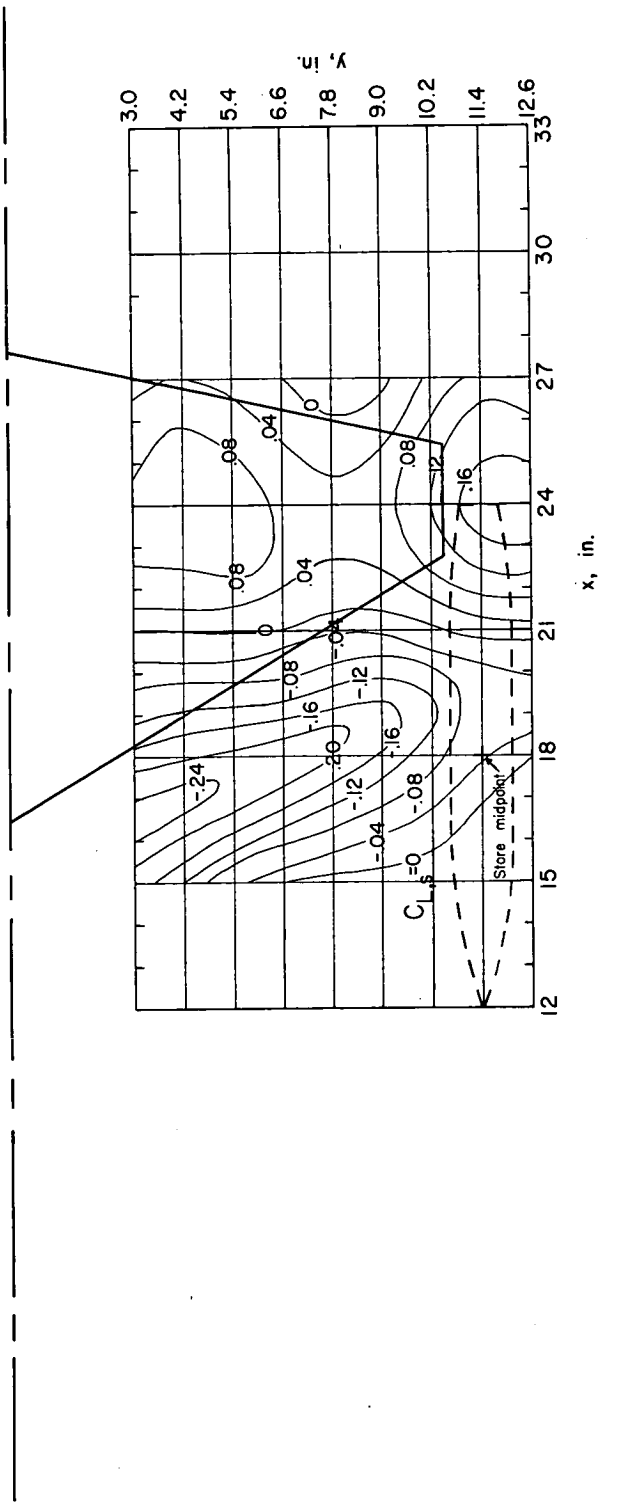

(c) $z = 2.09$ in.; $\alpha = 4^{\circ}$.

Figure 5.- Concluded.

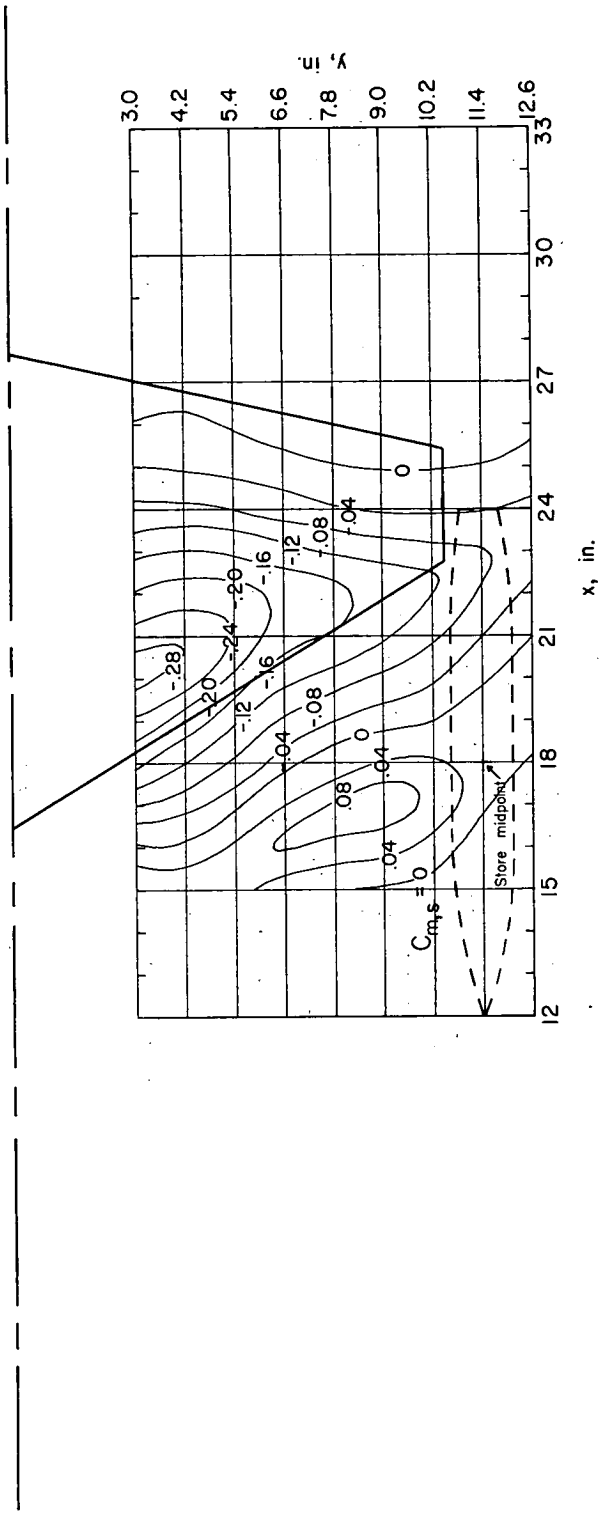

(a) $z = 1.15$ in.; $\alpha = 0^\circ$.

Figure 6.- Contour plot of pitching-moment coefficients of the store in presence of the wing at $M = 1.61$. Pitching-moment coefficients for the isolated store $\left(\alpha = 0^\circ,\ C_{m,i} = 0.000;\right.$ $\left.\alpha = 4^\circ,\ C_{m,i} = -0.002\right)$.

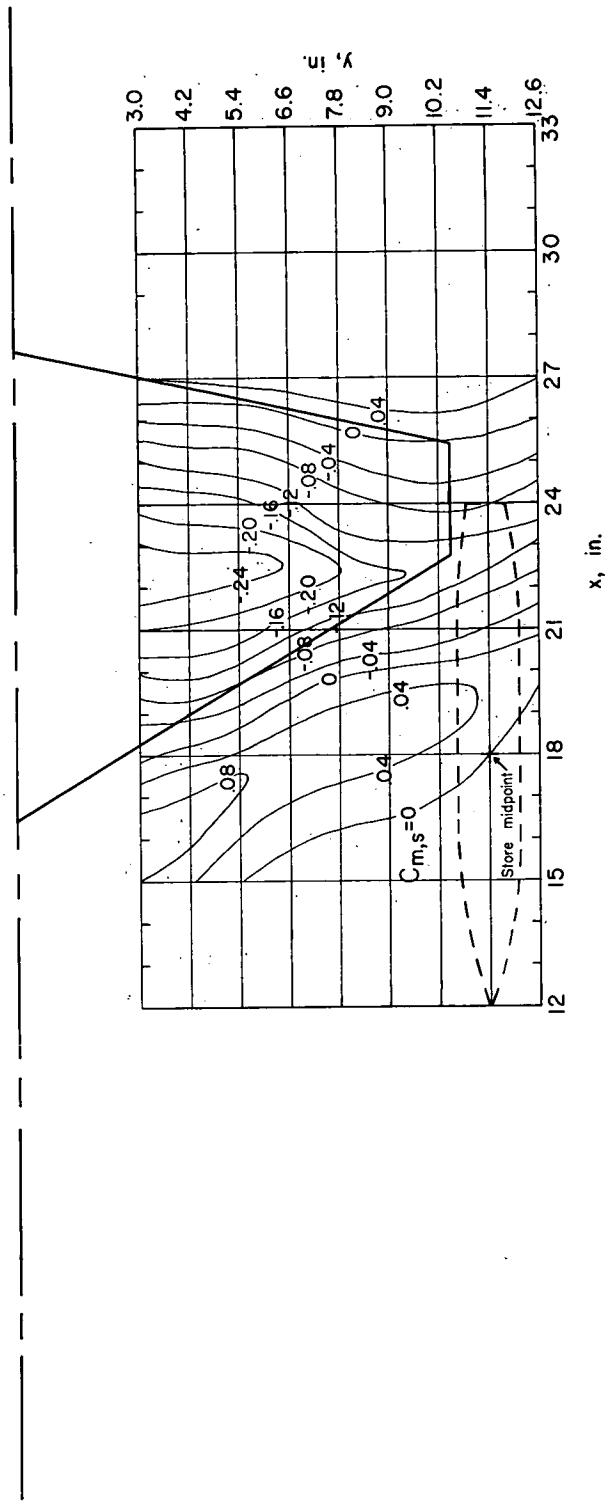

(b) $z = 2.09$ in.; $\alpha = 0^{\circ}$.

Figure 6.- Continued.

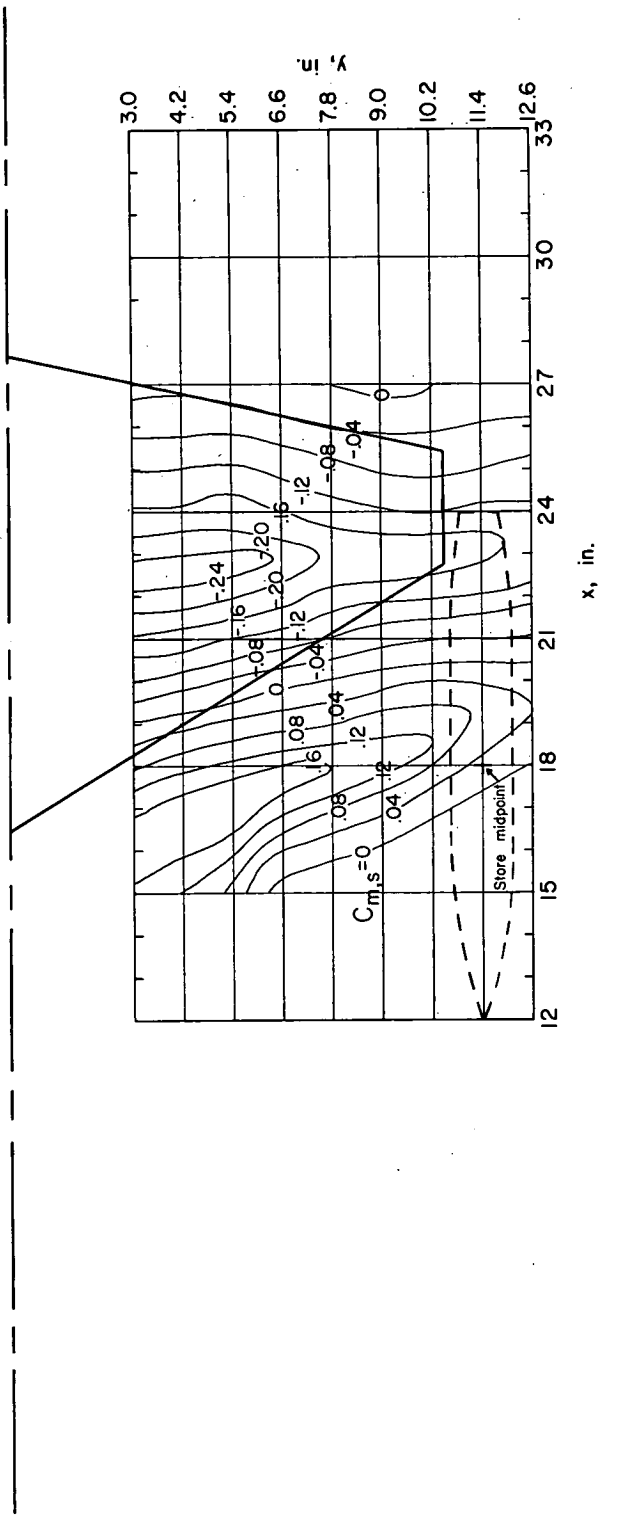

(c) z = 2.09 in.; $\alpha = 4^{\circ}$.

Figure 6.- Concluded.

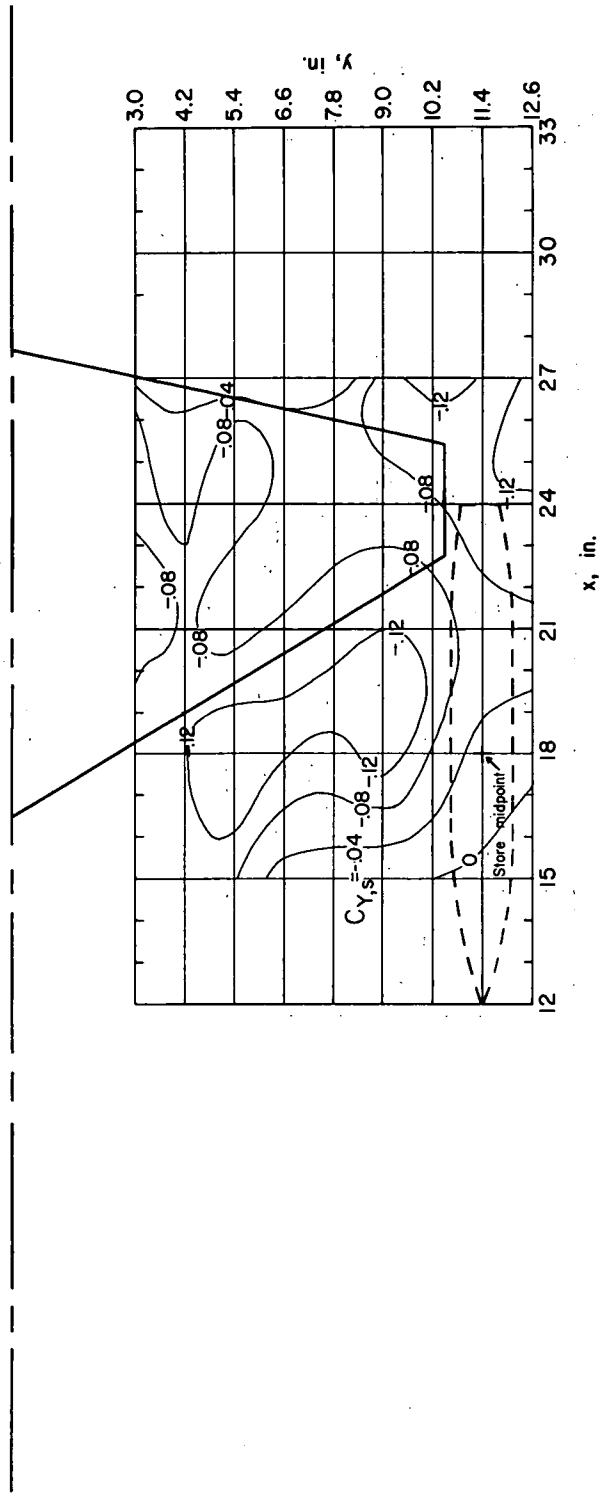

(a) z = 1.15 in.; $\alpha = 0^{\circ}$.

Figure 7.- Contour plot of side-force coefficients of the store in presence of the wing at M = 1.61.

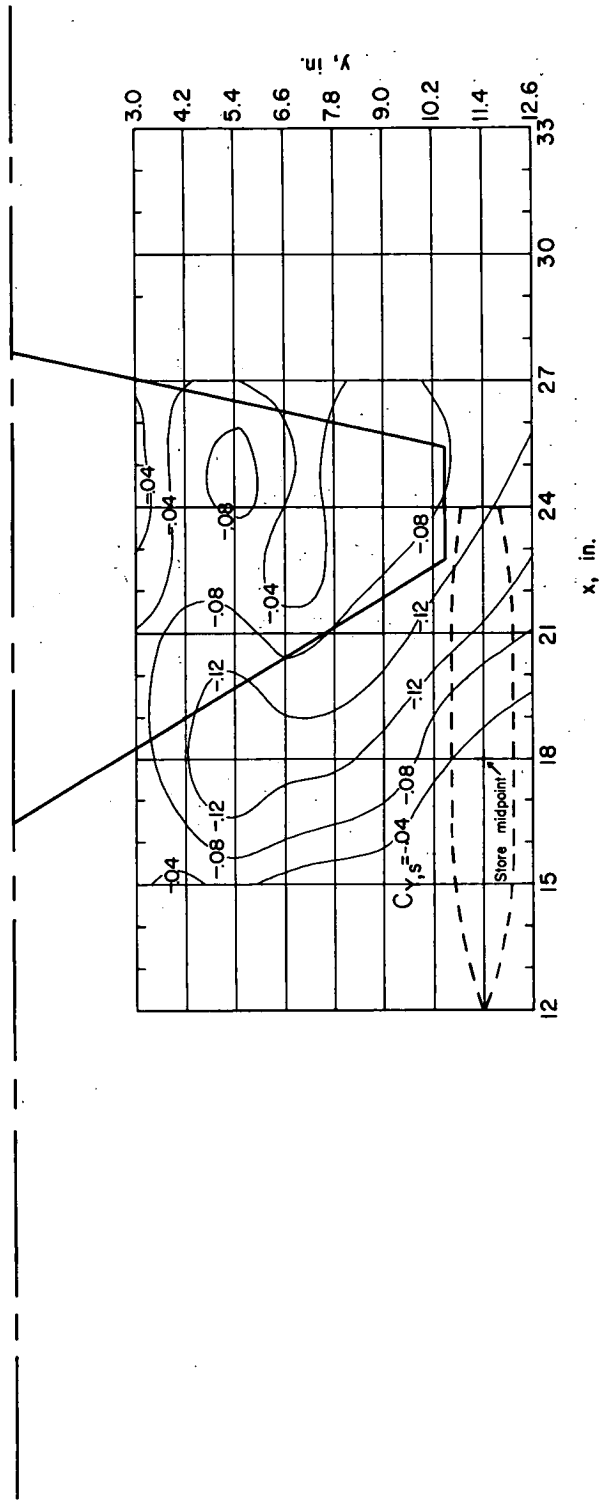

(b) z = 2.09 in.; $\alpha = 0^{\circ}$.

Figure 7.- Continued.

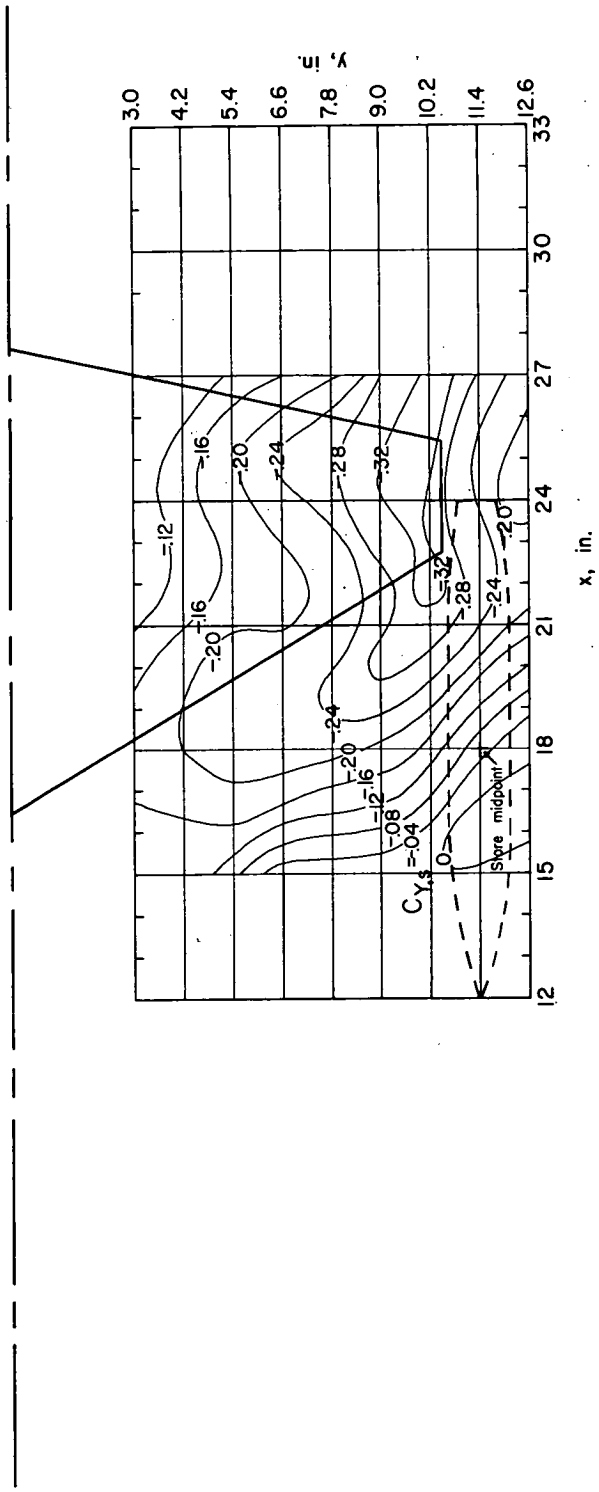

(c) $z = 2.09$ in.; $\alpha = 4^{\circ}$.

Figure 7.- Concluded.

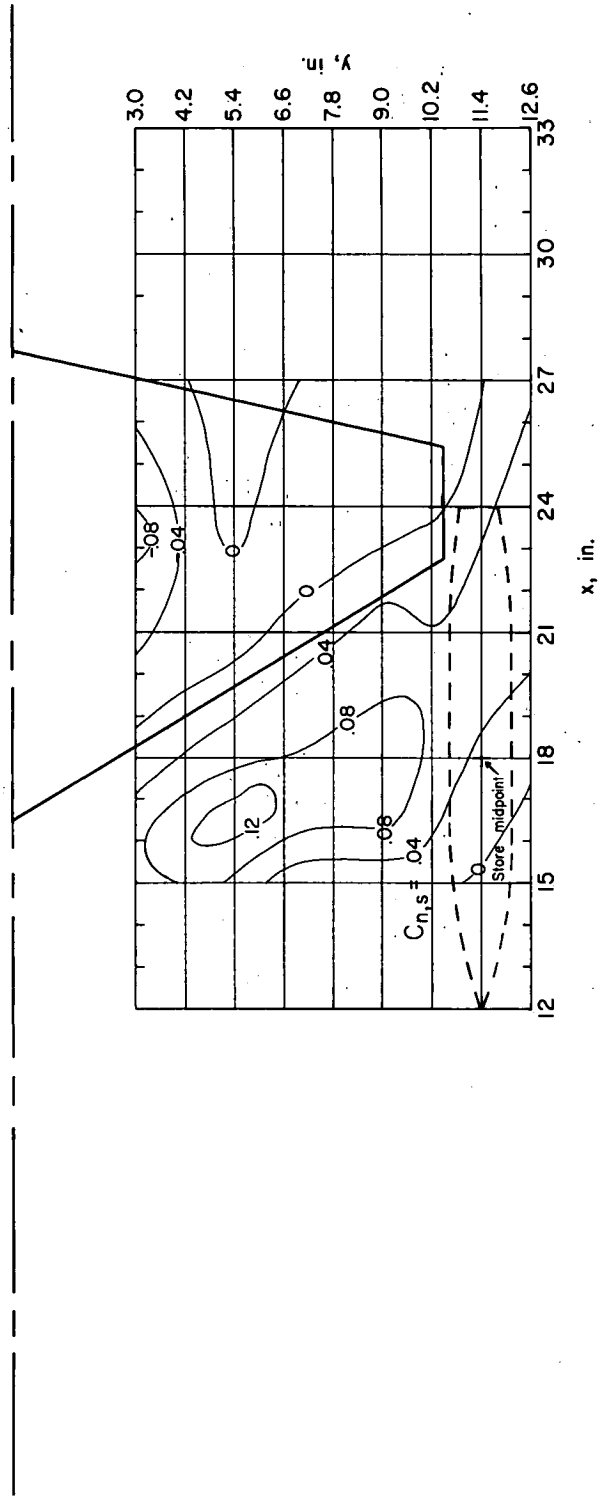

(a) $z = 1.15$ in.; $\alpha = 0^{\circ}$.

Figure 8.- Contour plot of yawing-moment coefficients of the store in presence of the wing at $M = 1.61$.

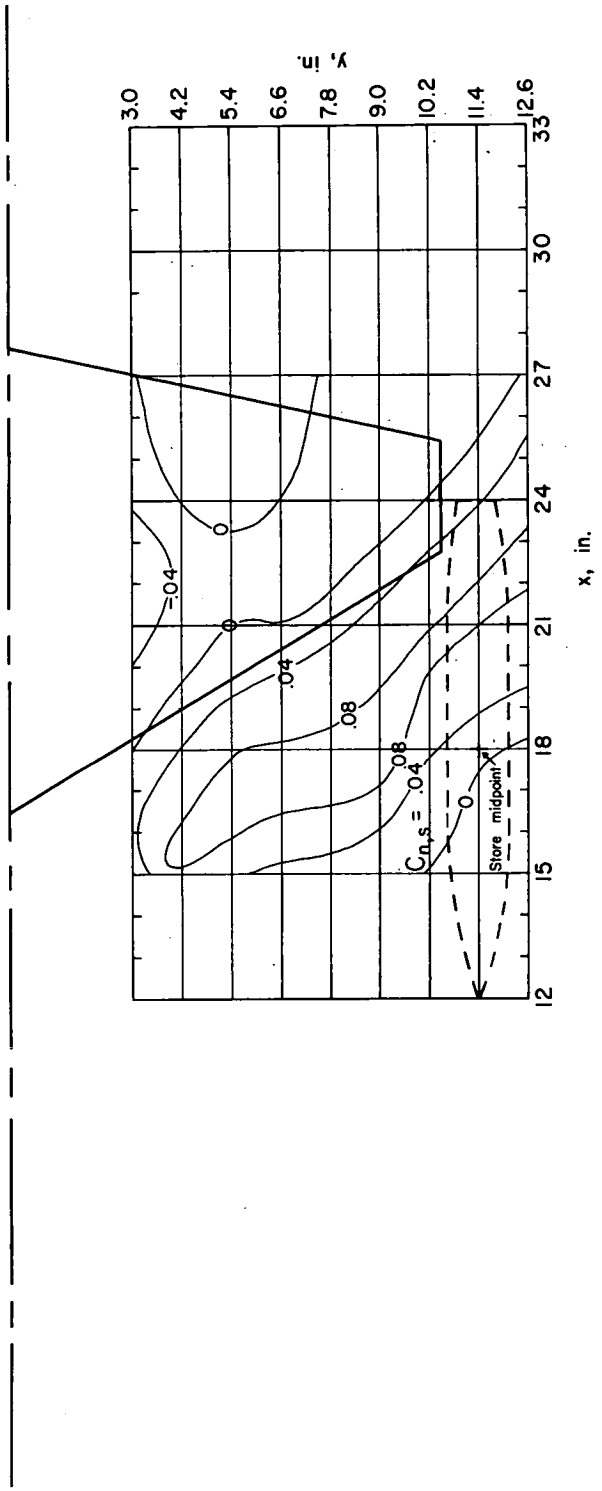

(b) z = 2.09 in.; $\alpha = 0^{\circ}$.

Figure 8.- Continued.

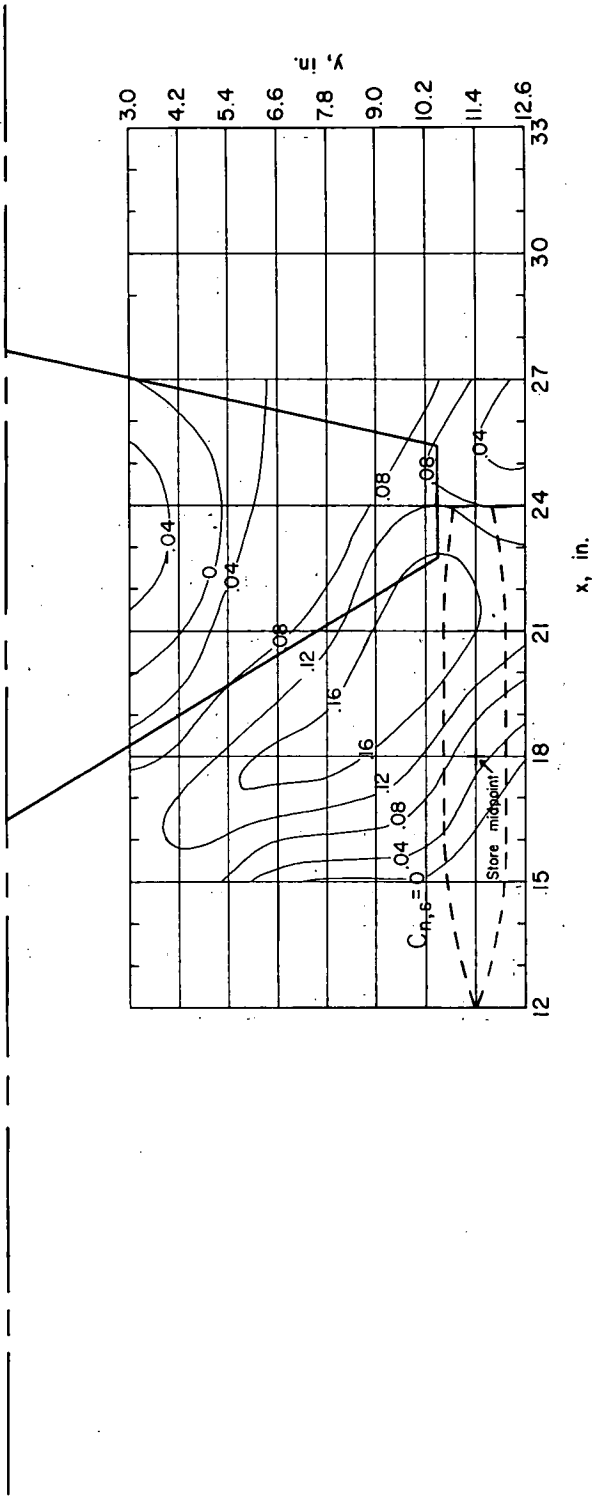

(c) $z = 2.09$ in.; $\alpha = 4^{\circ}$.

Figure 8.- Concluded.

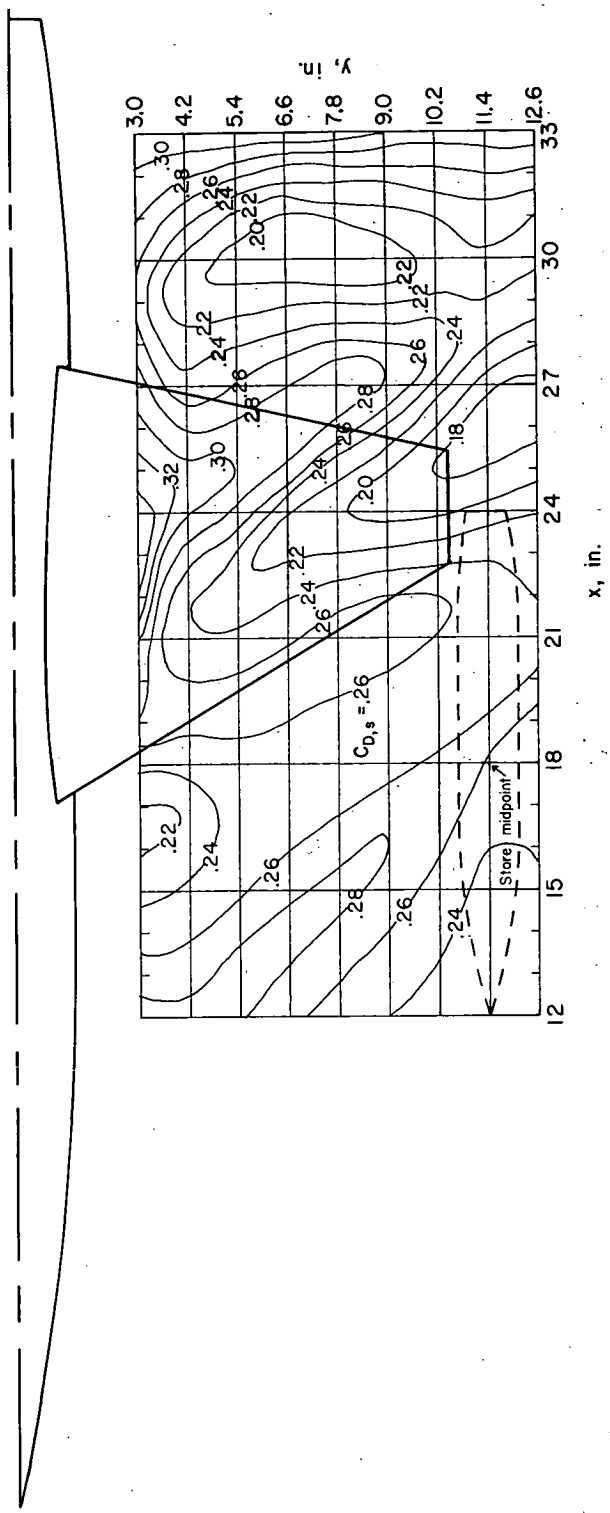

(a) $z = 1.15$ in.; $\alpha = 0^\circ$.

Figure 9.- Contour plot of the drag coefficients of the store in presence of the wing-fuselage combination at $M = 1.61$. Drag coefficients of isolated store $\left(\alpha = 0^\circ, C_{D,i} = 0.252; \alpha = 4^\circ, C_{D,i} = 0.265\right)$.

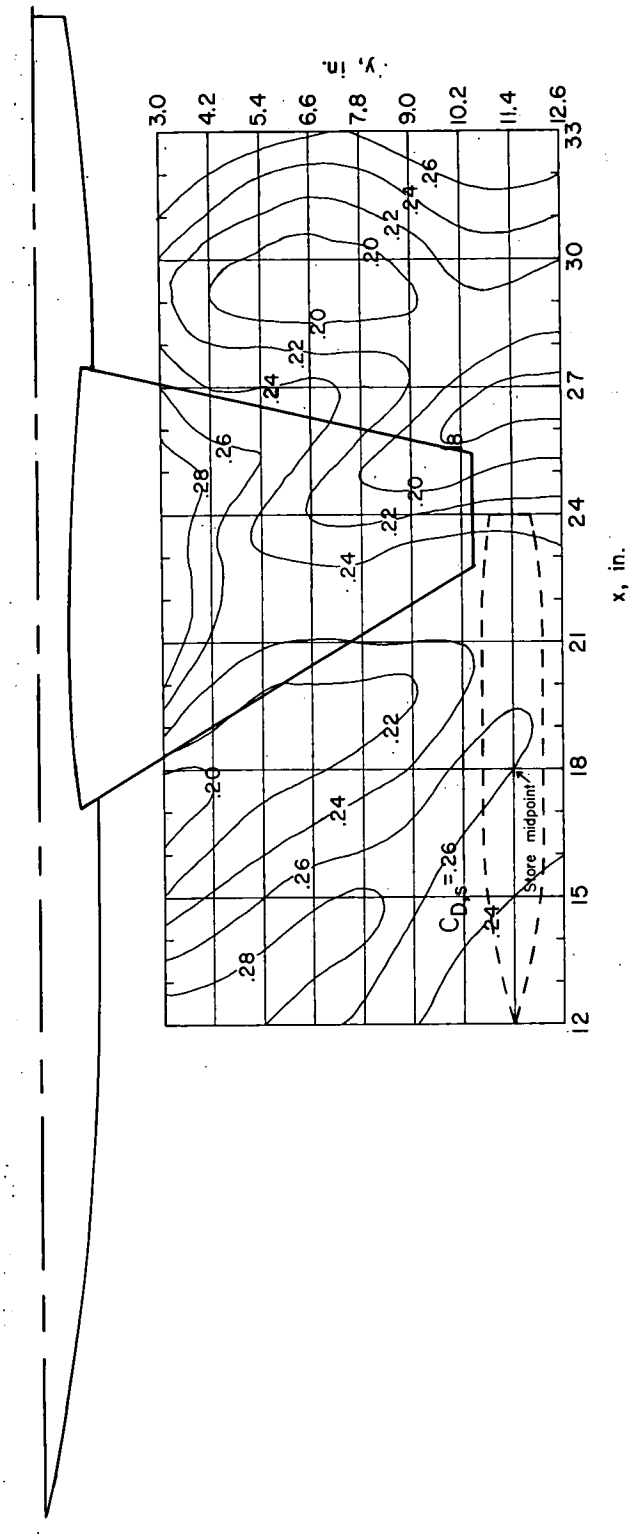

(b) z = 2.09 in.; $\alpha = 0^{\circ}$.

Figure 9.- Continued.

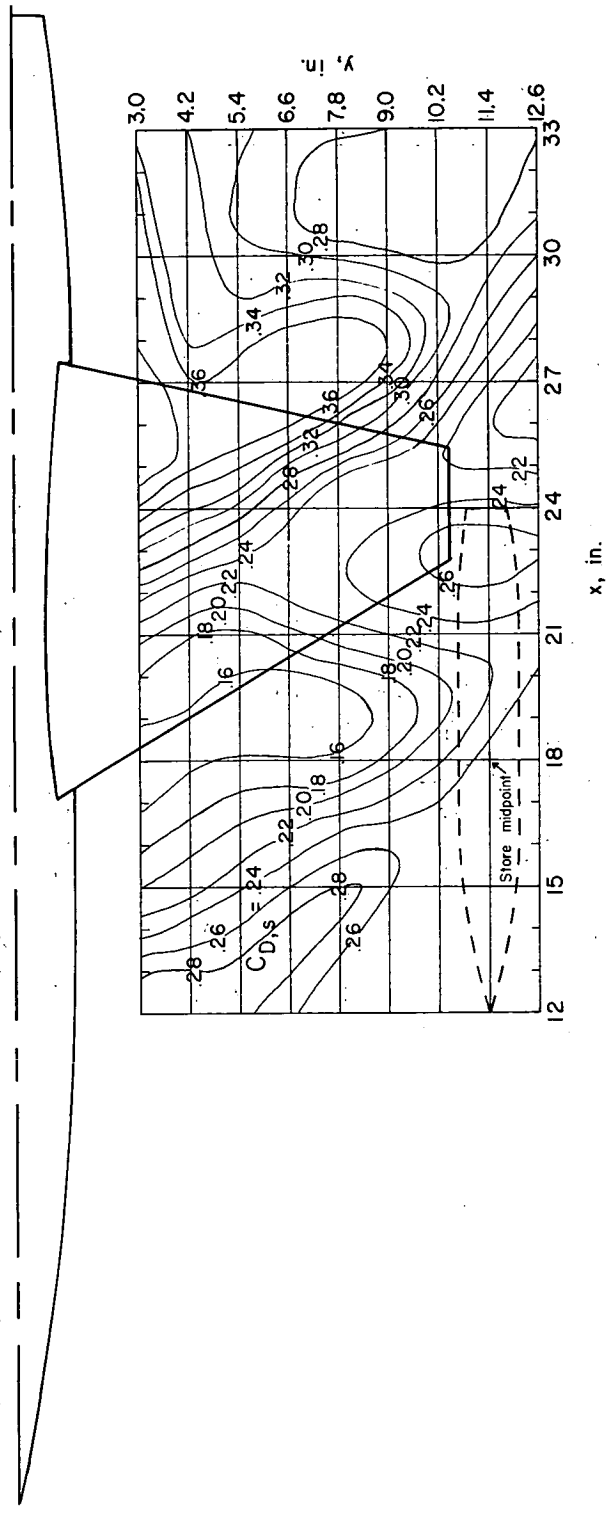

(c) $z = 2.09$ in.; $\alpha = 4^{\circ}$.

Figure 9.- Concluded.

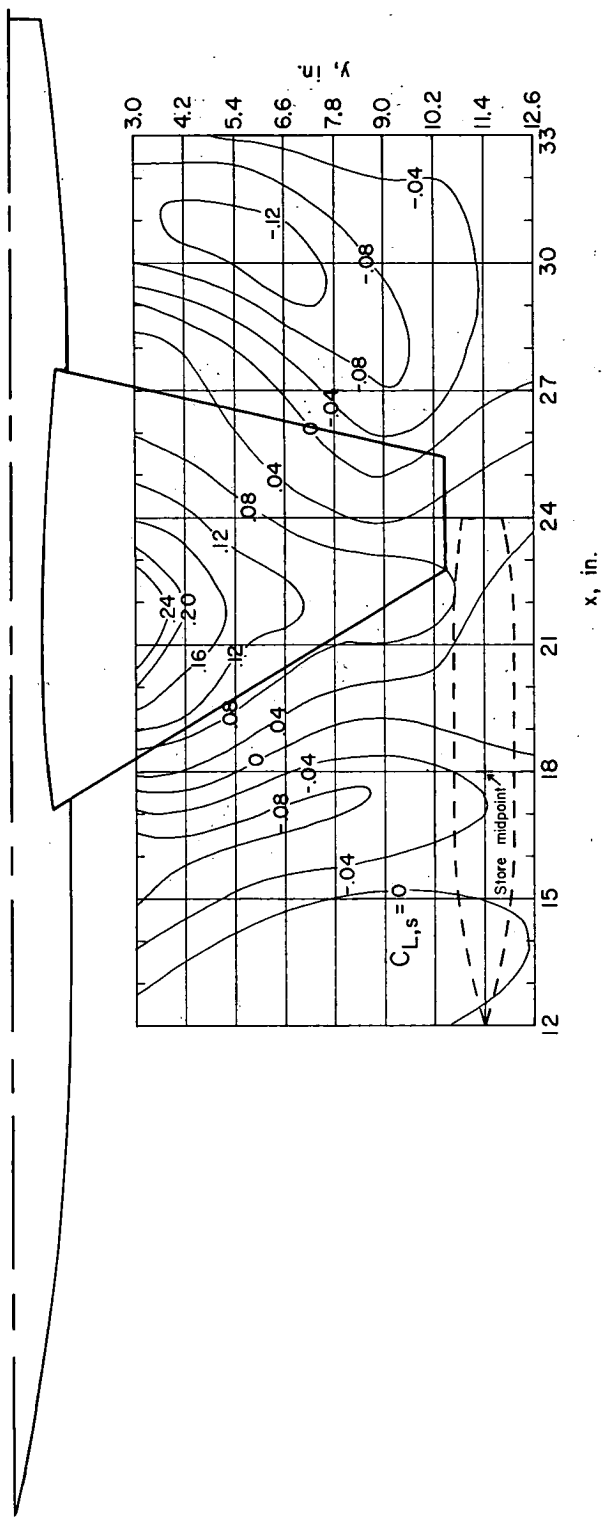

(a) z = 1.15 in.; $\alpha = 0^{\circ}$.

Figure 10.- Contour plot of lift coefficients of store in presence of the wing-fuselage combination at M = 1.61. Lift coefficients of the isolated store ($\alpha = 0^{\circ}$, $C_{L,i} = 0.000$; $\alpha = 4^{\circ}$, $C_{L,i} = 0.0135$).

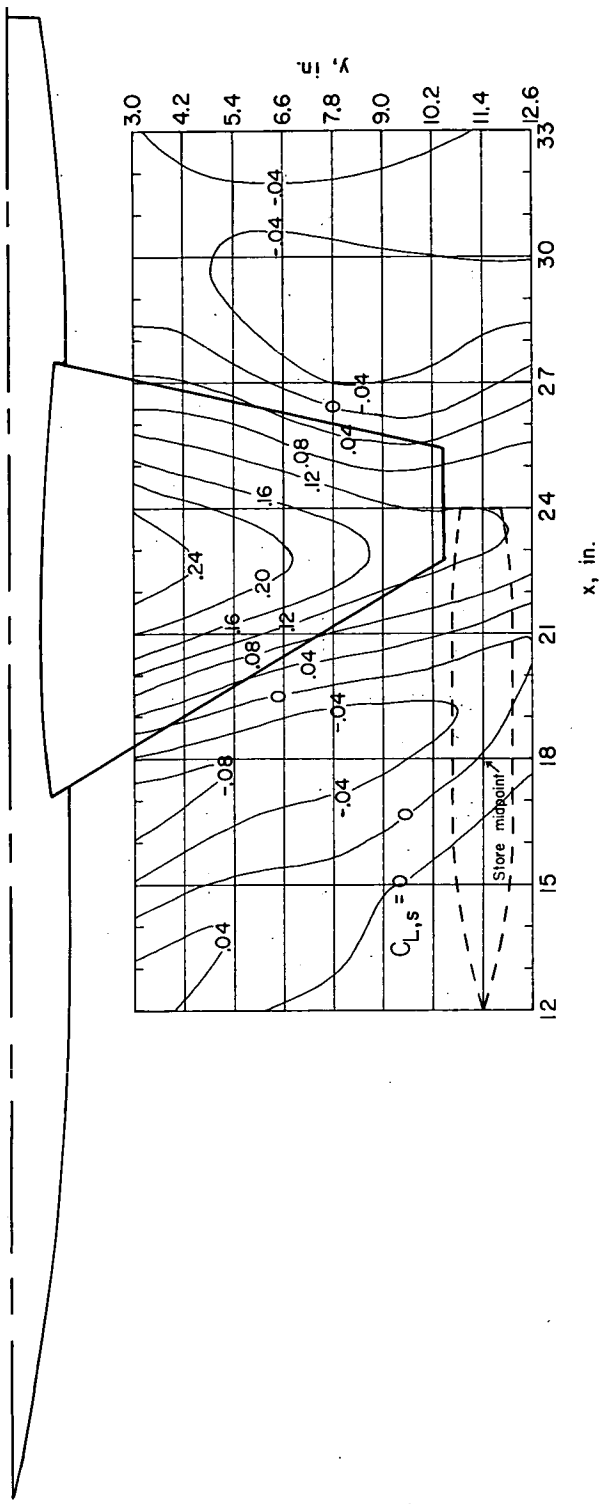

(b) z = 2.09 in.; $\alpha = 0^{\circ}$.

Figure 10.- Continued.

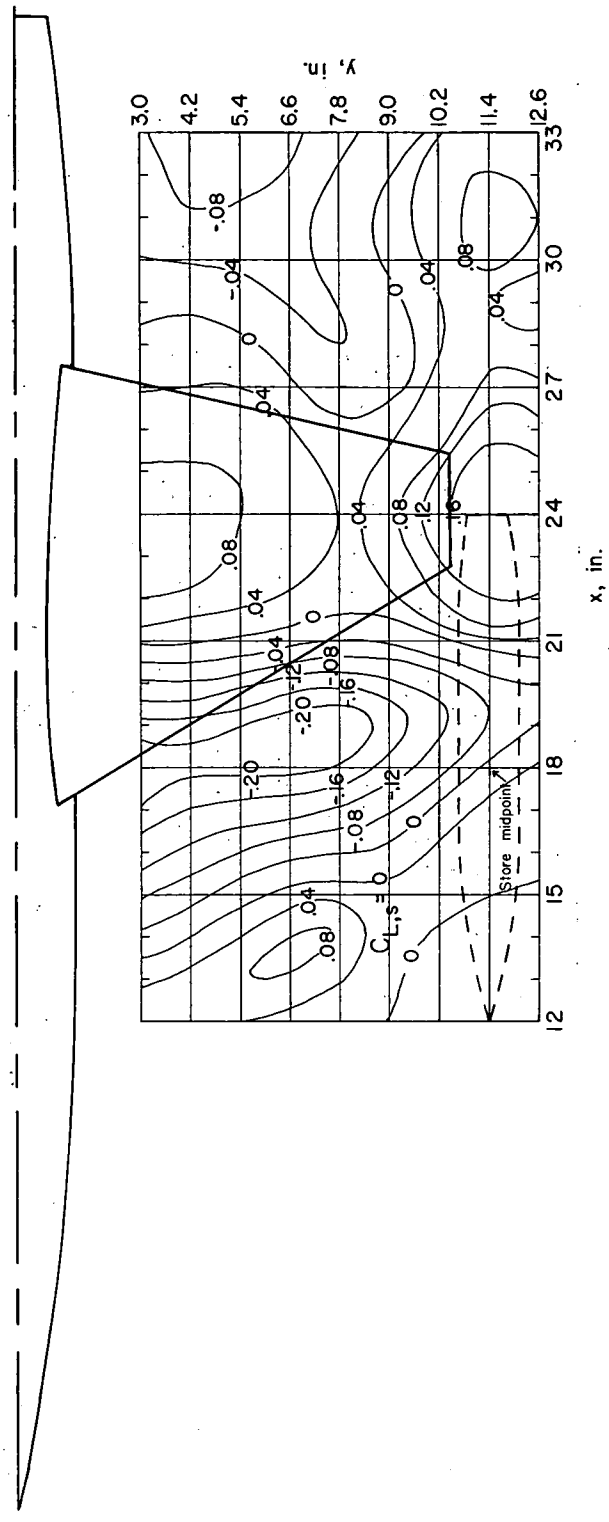

(c) $z = 2.09$ in.; $\alpha = 4^{\circ}$.

Figure 10.- Concluded.

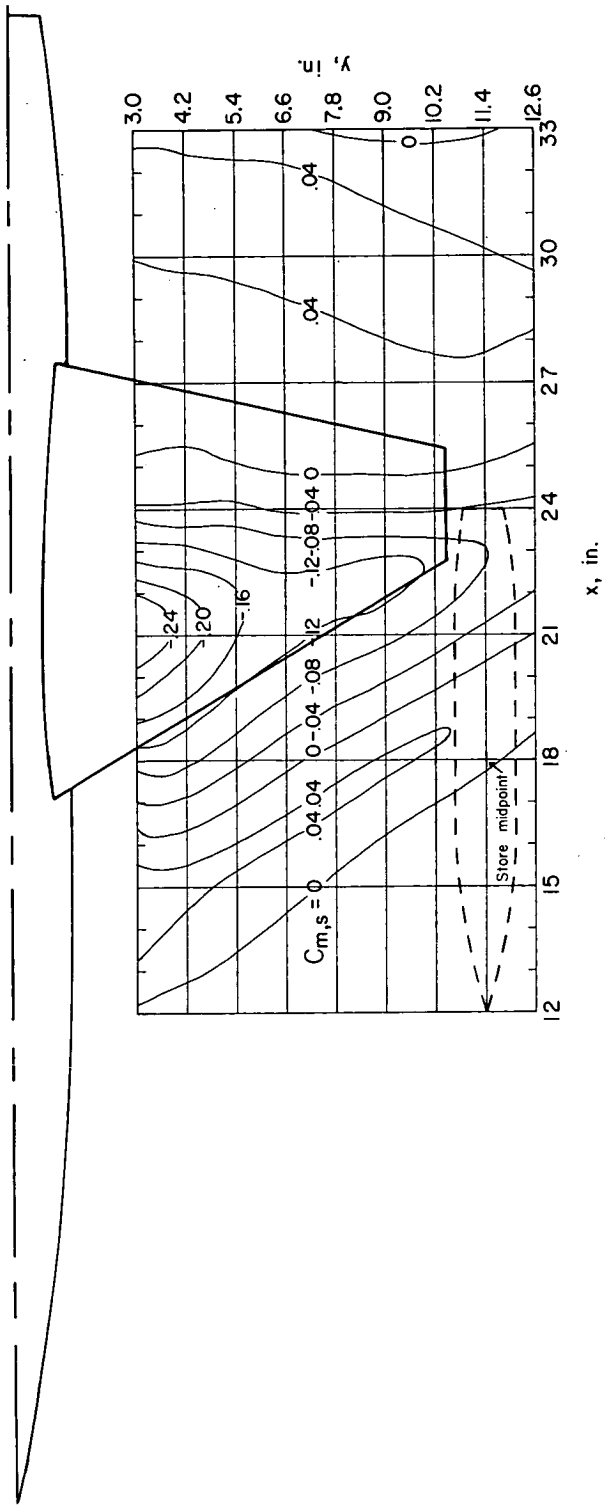

(a) $z = 1.15$ in.; $\alpha = 0^{\circ}$.

Figure 11.- Contour plot of pitching-moment coefficients of store in the presence of the wing-fuselage combination at $M = 1.61$. Pitching-moment coefficients for the isolated store $\left(\alpha = 0^{\circ}, C_{m,1} = 0.000; \alpha = 4^{\circ}, C_{m,1} = -0.002\right)$.

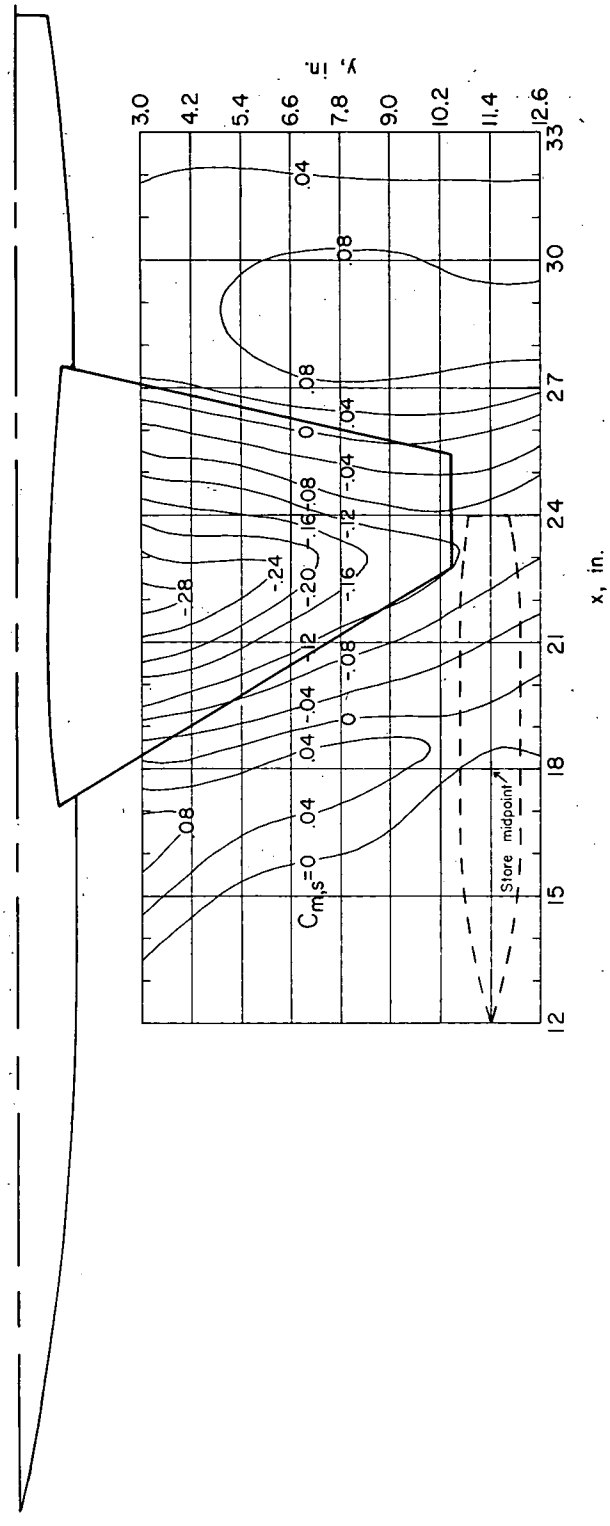

(b) z = 2.09 in.; $\alpha = 0^{\circ}$.

Figure 11.- Continued.

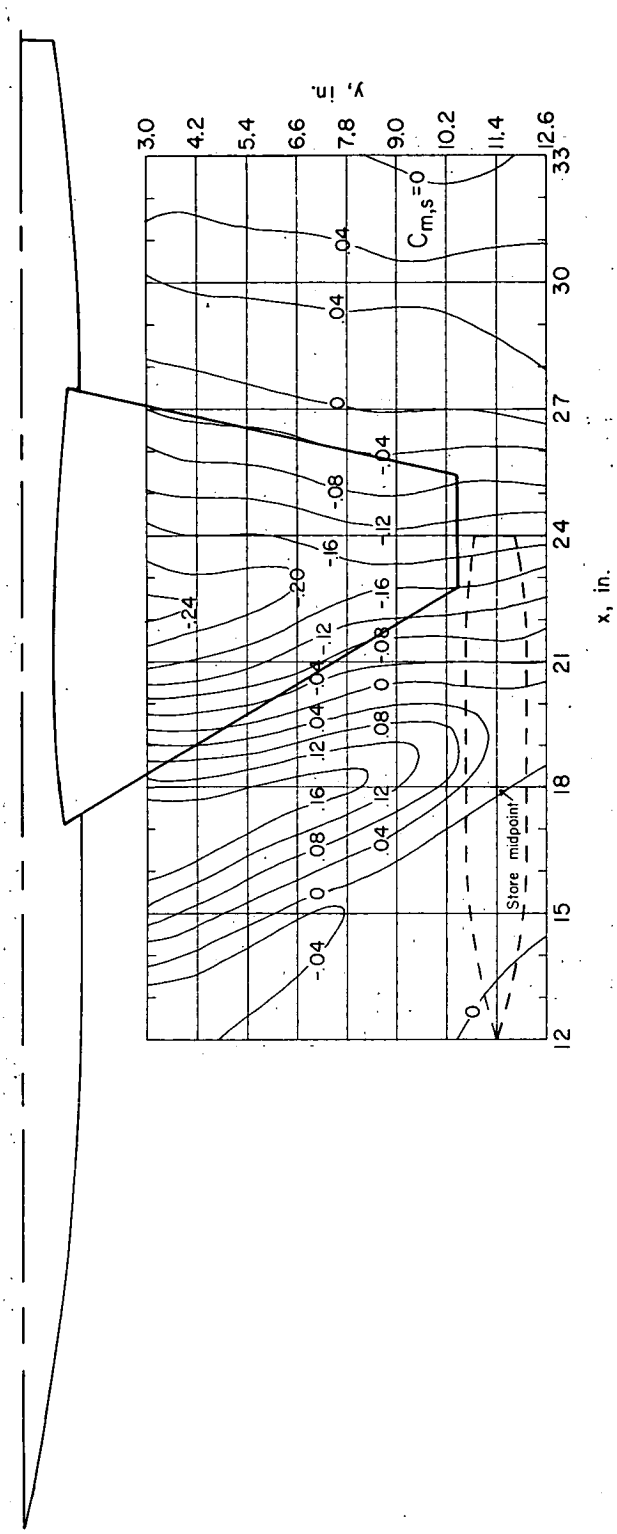

(c) $z = 2.09$ in.; $\alpha = 4^{\circ}$.

Figure 11.- Concluded.

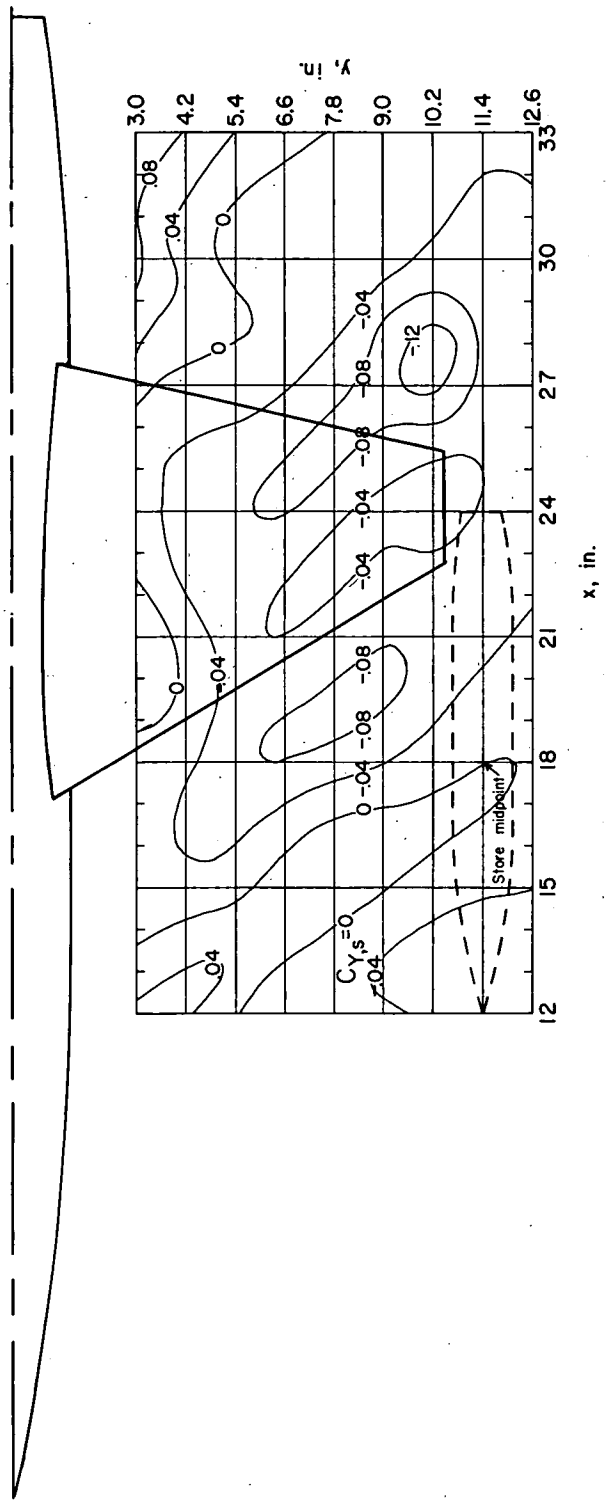

(a) $z = 1.15$ in.; $\alpha = 0^{\circ}$.

Figure 12.- Contour plot of side-force coefficients of the store in the presence of the wing-fuselage combination at $M = 1.61$.

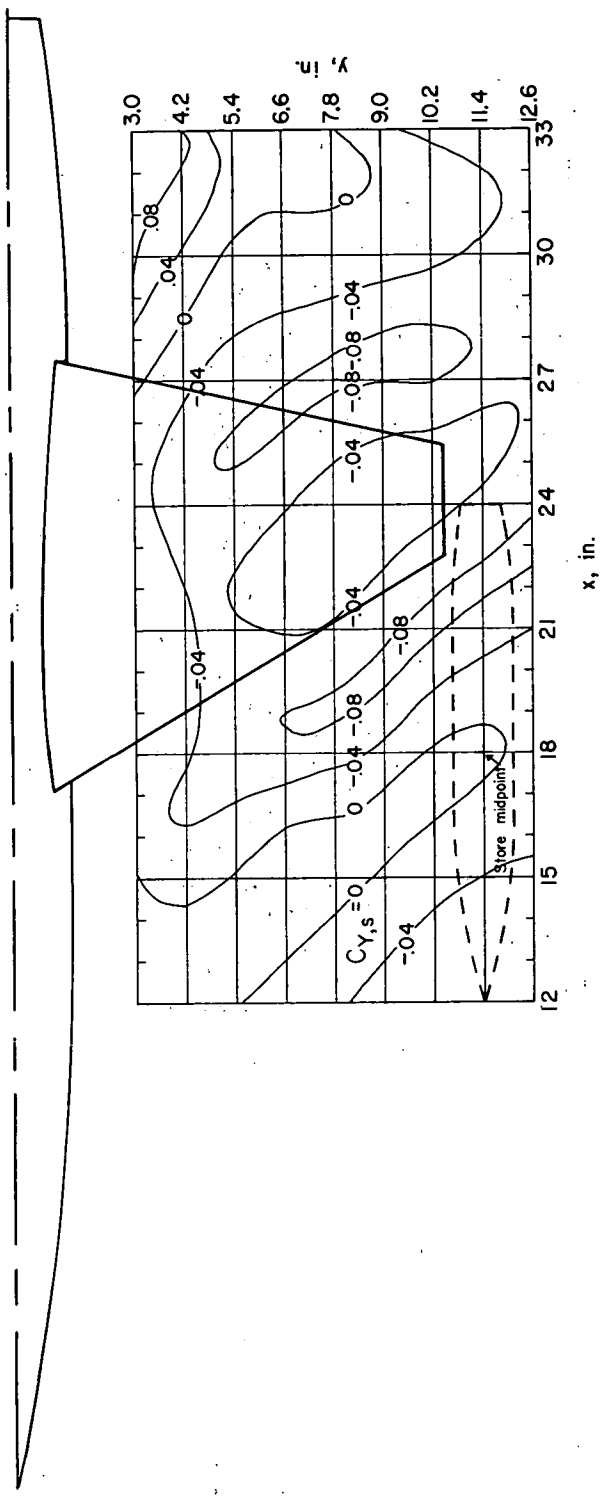

(b) z = 2.09 in.; $\alpha = 0^{\circ}$.

Figure 12.- Continued.

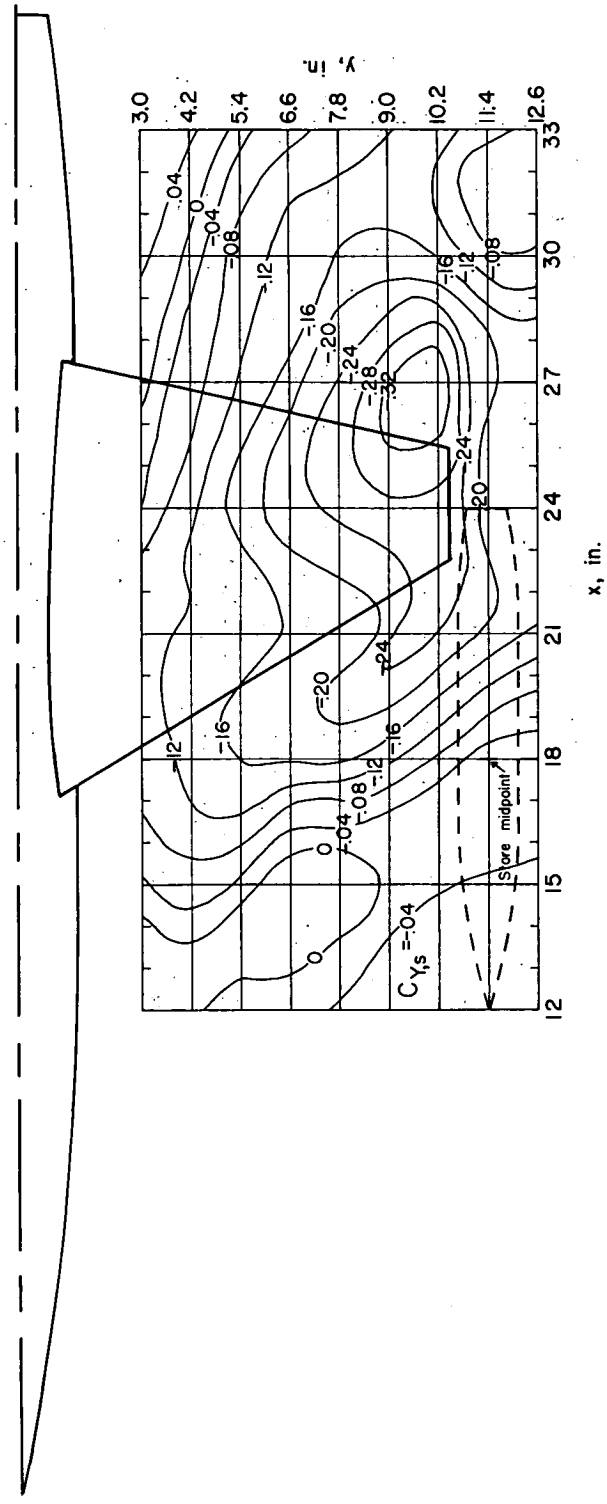

(c) z = 2.09 in.; $\alpha = 4^{\circ}$.

Figure 12.- Concluded.

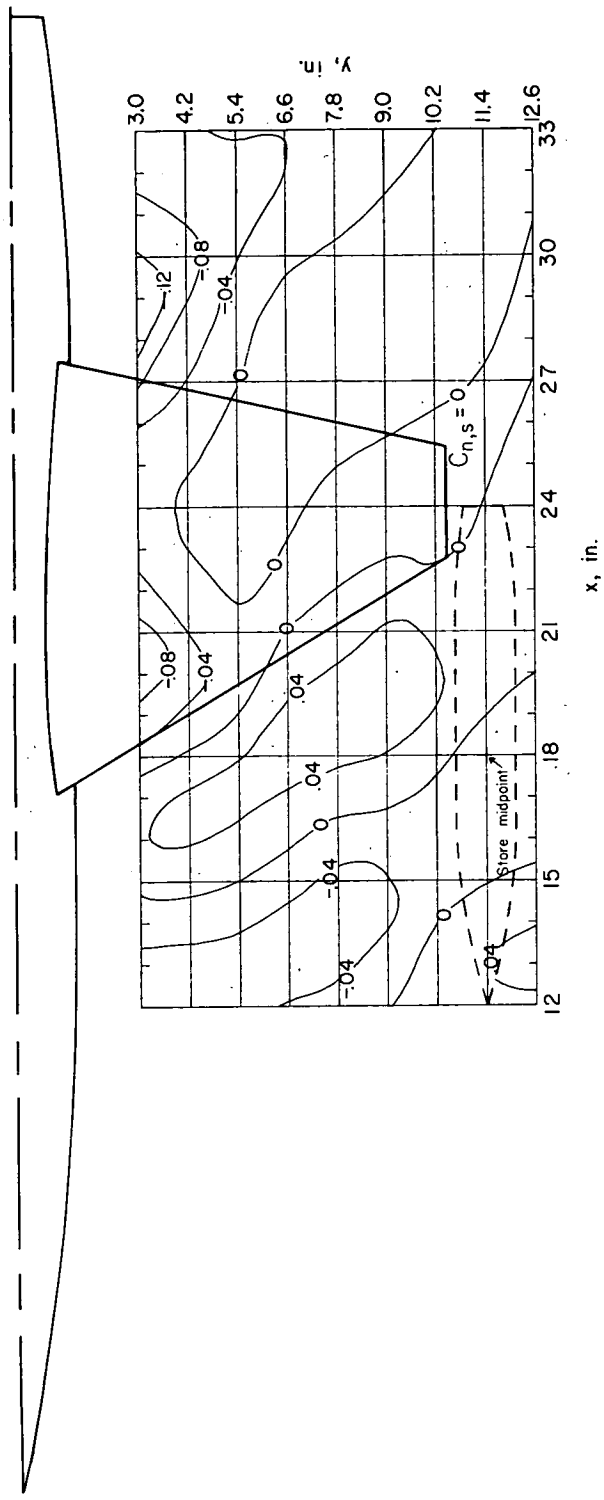

(a) z = 1.15 in.; $\alpha = 0^{\circ}$.

Figure 13.- Contour plot of yawing-moment coefficients of store in presence of the wing-fuselage combination at M = 1.61.

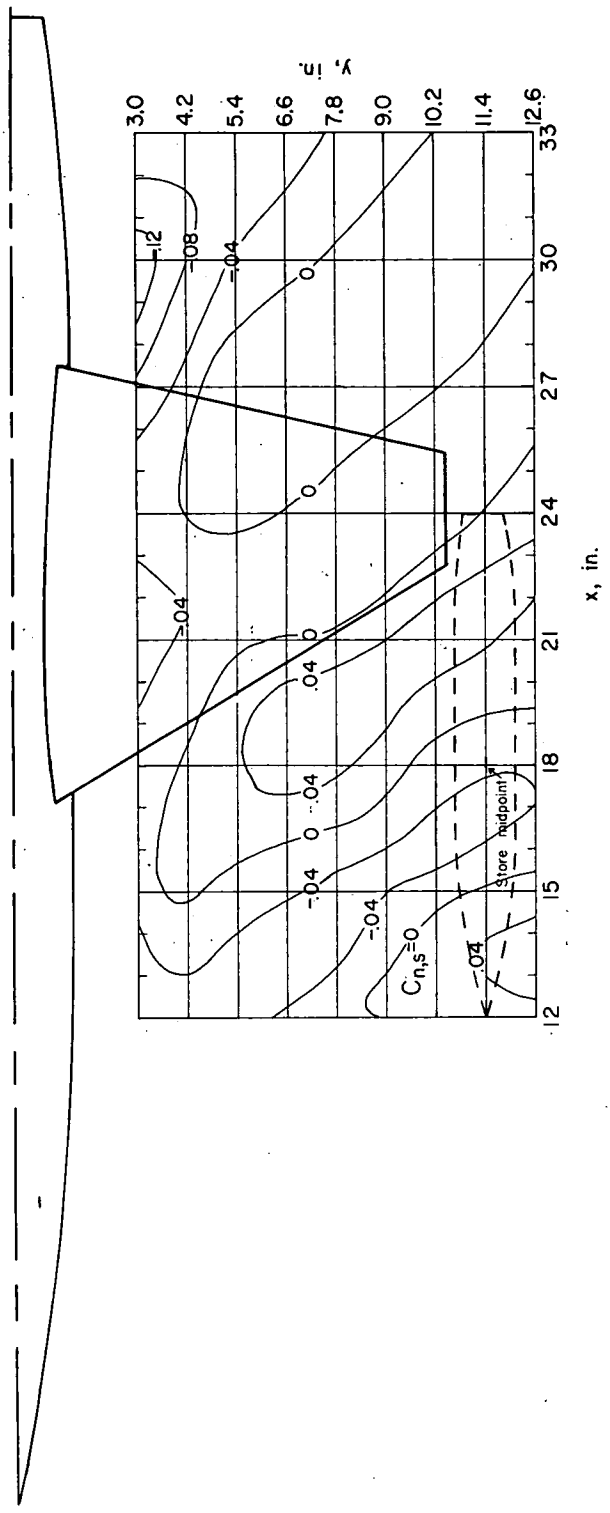

(b) $z = 2.09$ in.; $\alpha = 0^{\circ}$.

Figure 13.- Continued.

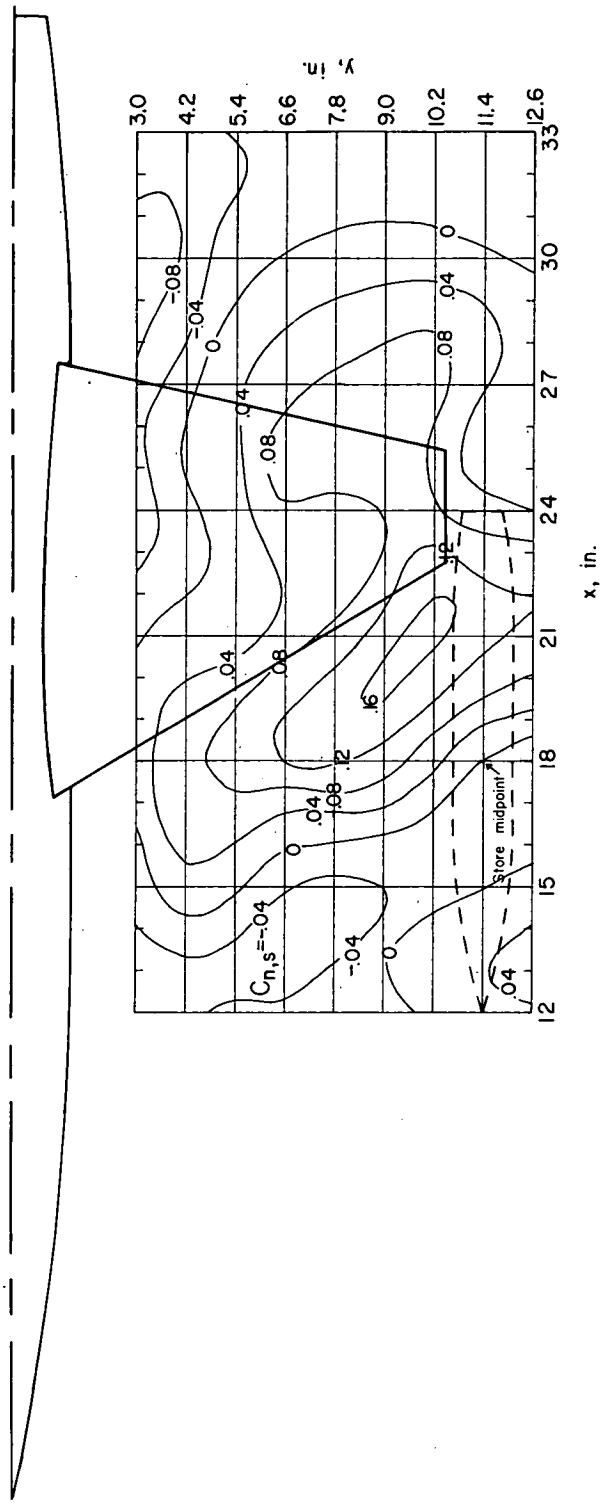

(c) z = 2.09 in.; $\alpha = 4^{\circ}$.

Figure 13.- Concluded.

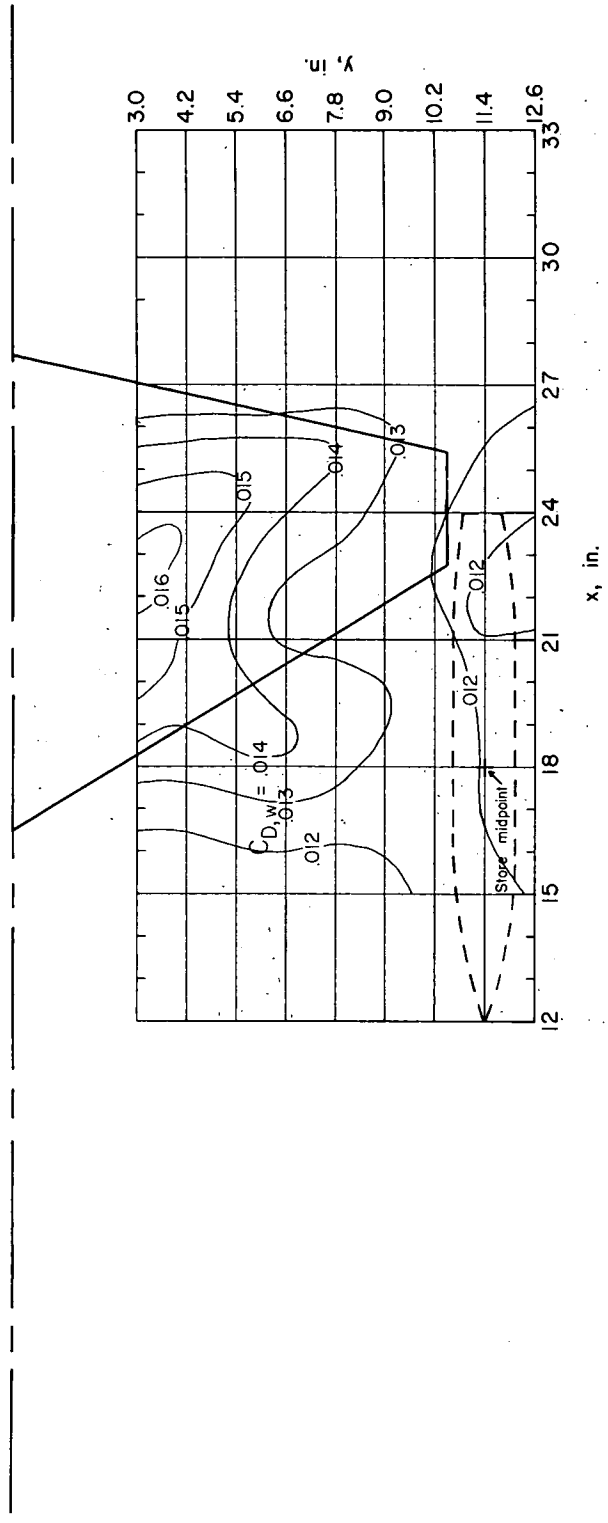

(a) z = 1.15 in.; $\alpha = 0^\circ$.

Figure 14.- Contour plot of drag coefficients of the wing in the presence of the store at M = 1.61. Drag coefficients of the isolated wing ($\alpha = 0^\circ$, $C_{D,i} = 0.0122$; $\alpha = 4^\circ$, $C_{D,i} = 0.0279$).

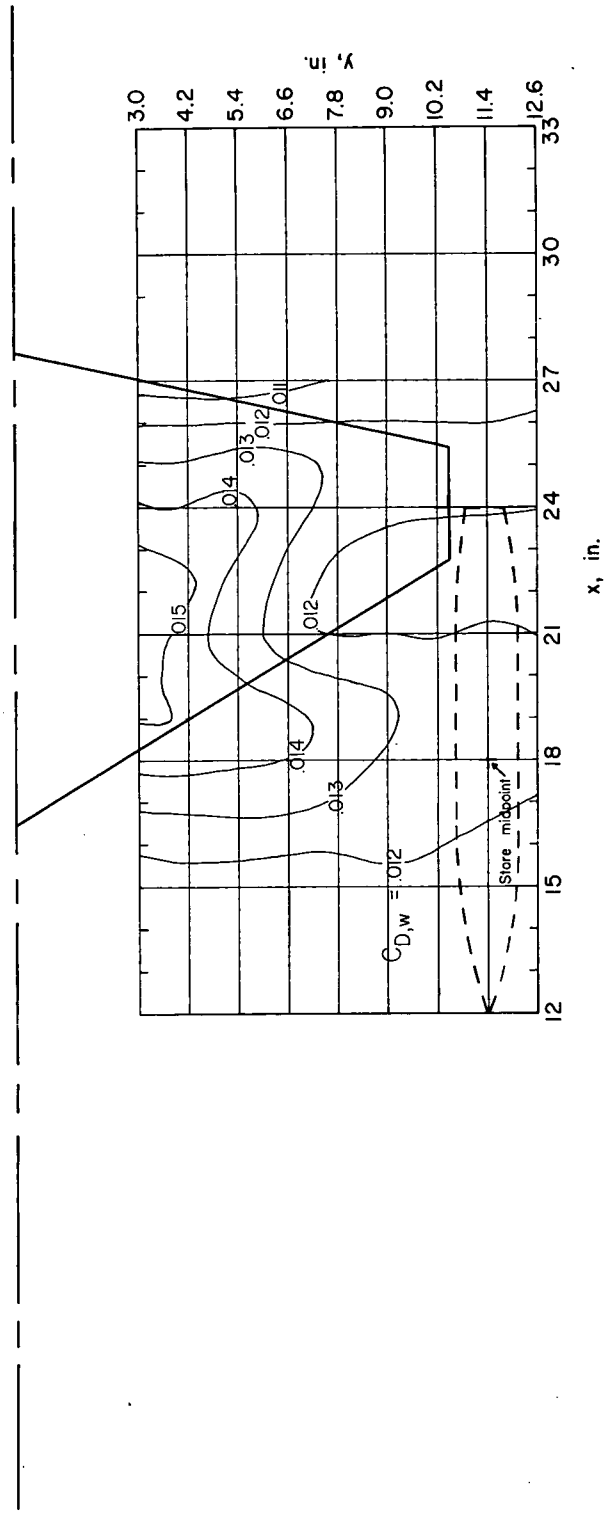

(b) z = 2.09 in.; $\alpha = 0^{\circ}$.

Figure 14.- Continued.

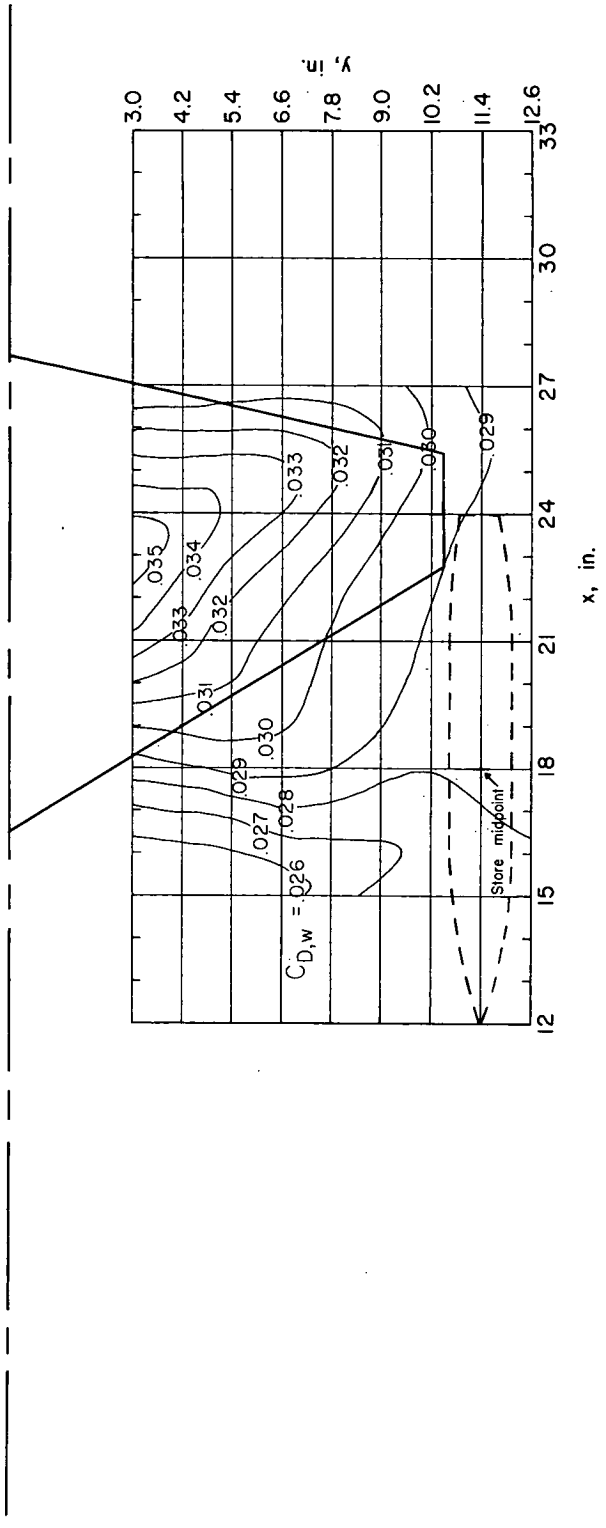

(c) z = 2.09 in.; $\alpha = 4^{\circ}$.

Figure 14.- Concluded.

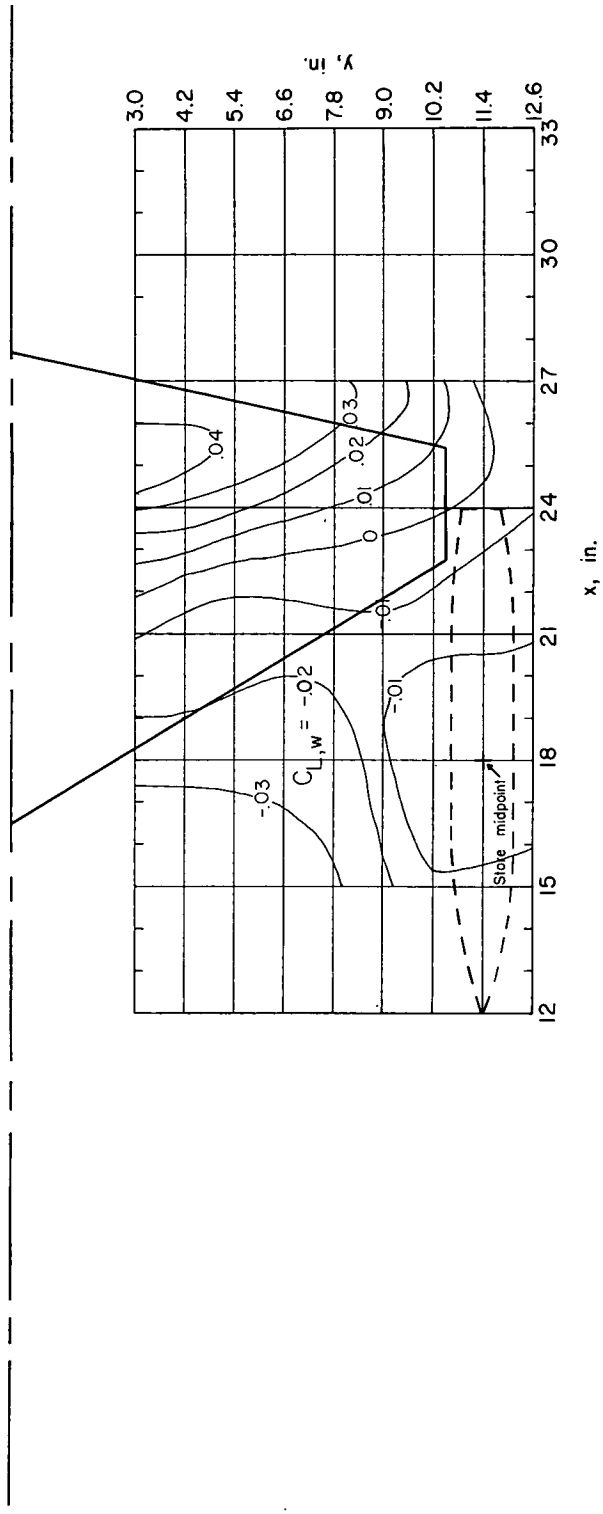

(a) z = 1.15 in.; $\alpha = 0^\circ$.

Figure 15.- Contour plot of the lift coefficients of wing in presence of the store at M = 1.61. Lift coefficient of the isolated wing $\left(\alpha = 0^\circ;\ C_{L,i} = -0.0145;\ \alpha = 4^\circ,\ C_{L,i} = 0.2058\right)$.

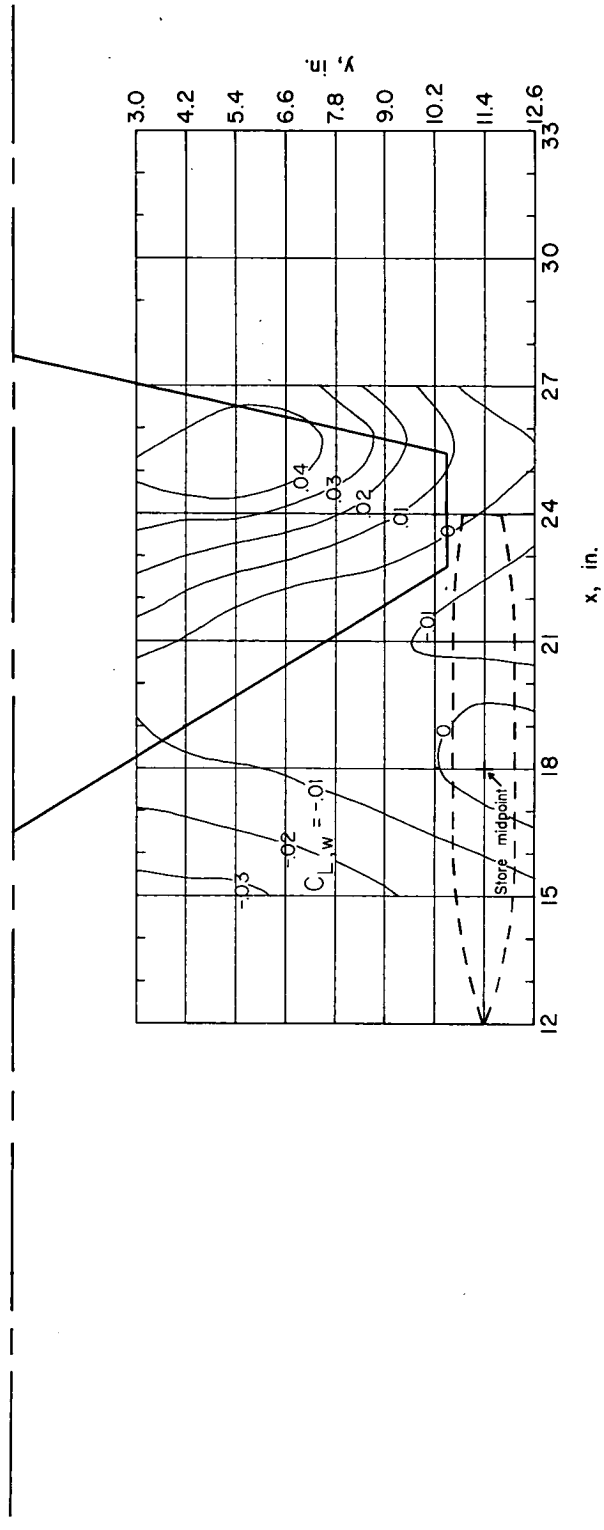

(b) z = 2.09 in.; $\alpha = 0^{\circ}$.

Figure 15.- Continued.

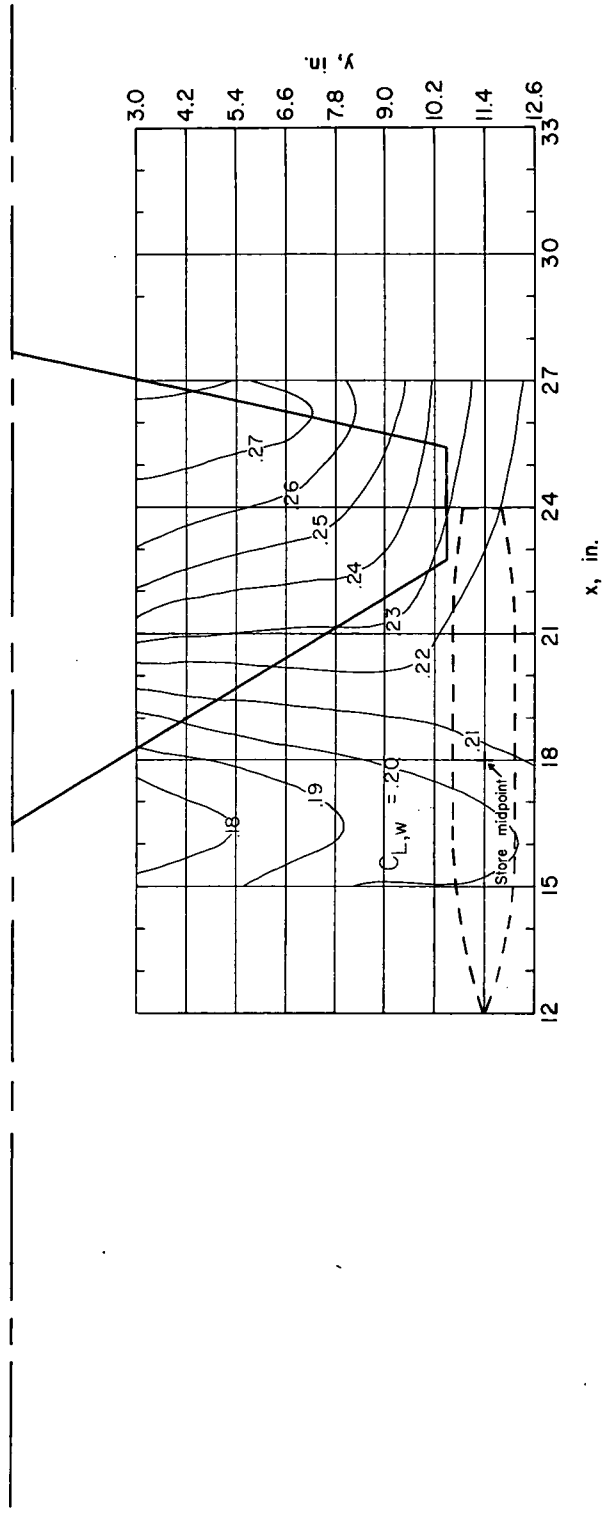

(c) $z = 2.09$ in.; $\alpha = 4^{\circ}$.

Figure 15.- Concluded.

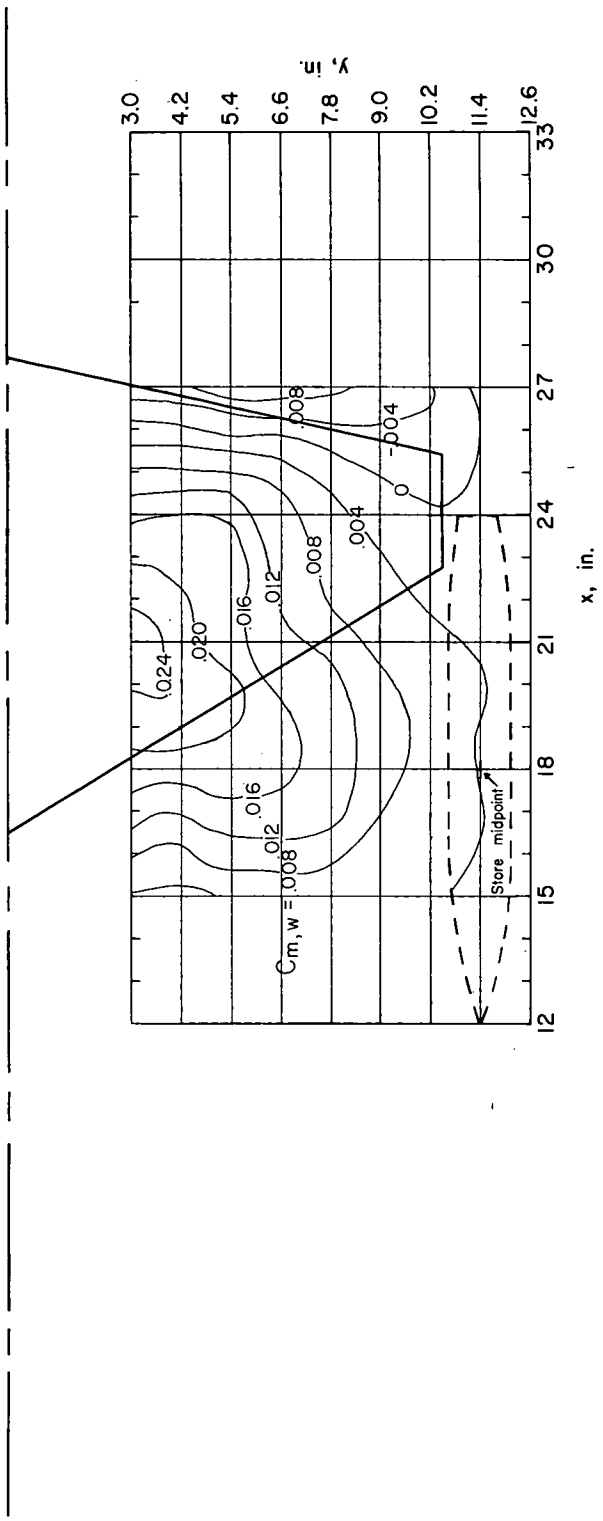

(a) $z = 1.15$ in.; $\alpha = 0^\circ$.

Figure 16.- Contour plot of pitching-moment coefficients of the wing in presence of the wing at $M = 1.61$. Pitching-moment coefficients for the isolated wing ($\alpha = 0^\circ$, $C_{m,i} = 0.0035$; $\alpha = 4^\circ$, $C_{m,i} = -0.0428$).

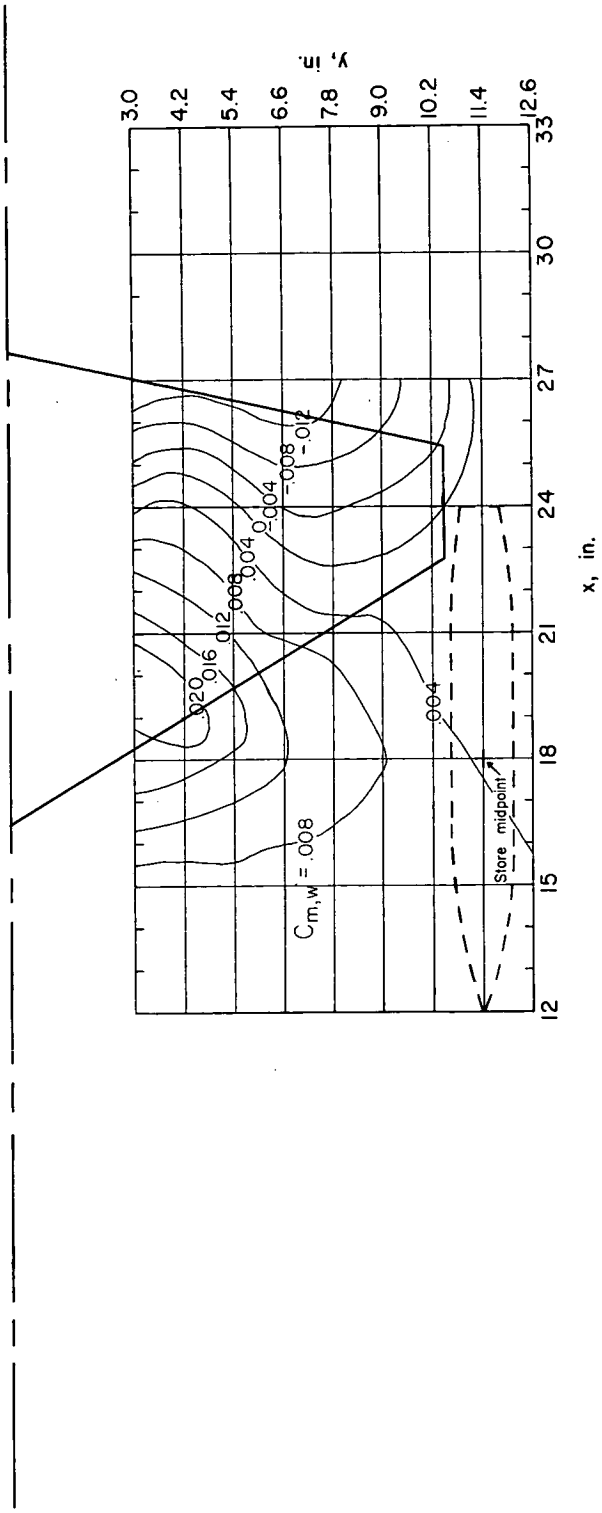

(b) z = 2.09 in.; $\alpha = 0^{\circ}$.

Figure 16.- Continued.

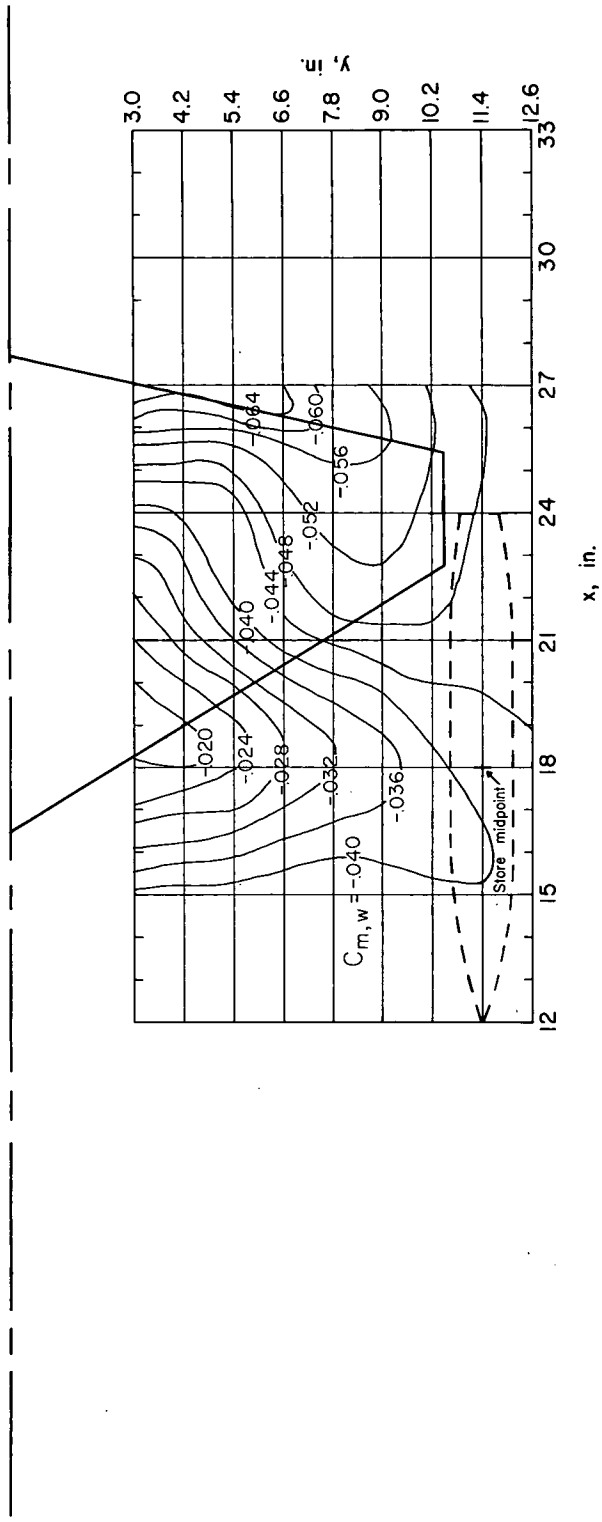

(c) $z = 2.09$ in.; $\alpha = 4^\circ$.

Figure 16.- Concluded.

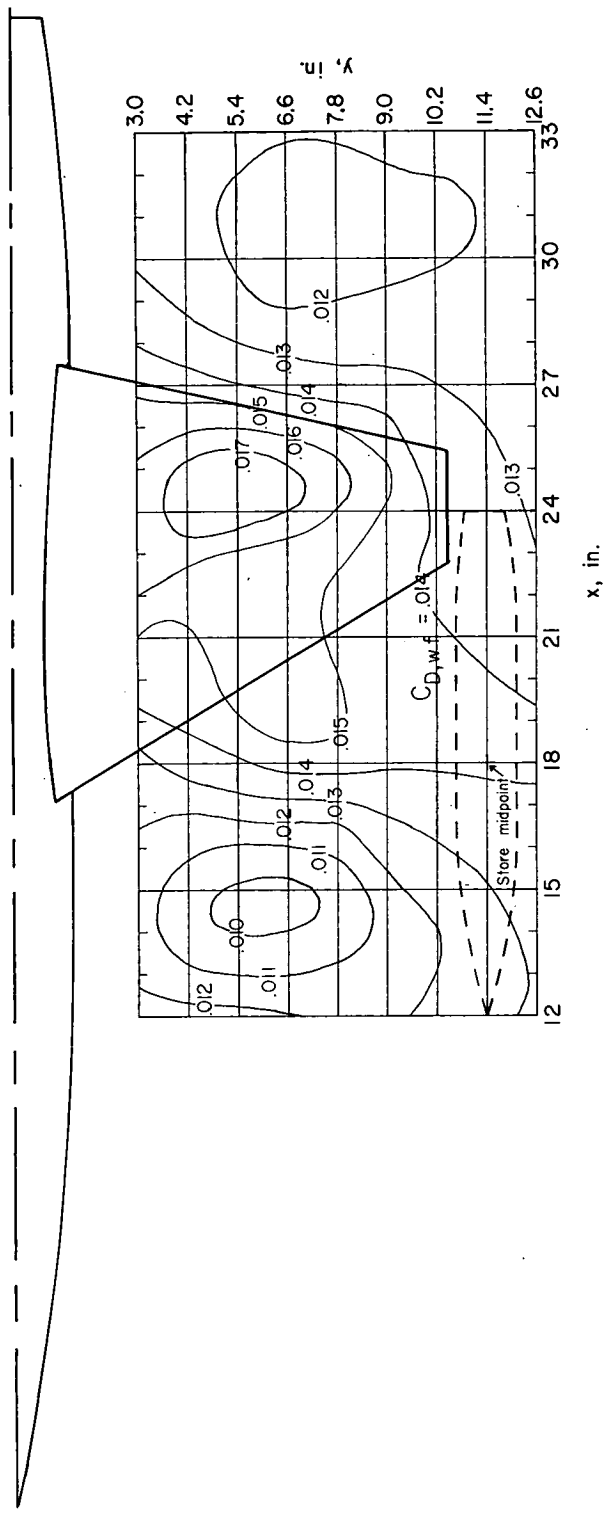

(a) $z = 1.15$ in.; $\alpha = 0^\circ$.

Figure 17.- Contour plot of the drag coefficients of wing-fuselage combination in presence of the store at $M = 1.61$. Drag coefficients for the isolated-wing—fuselage combination ($\alpha = 0^\circ$, $C_{D,i} = 0.013$; $\alpha = 4^\circ$, $C_{D,i} = 0.0296$).

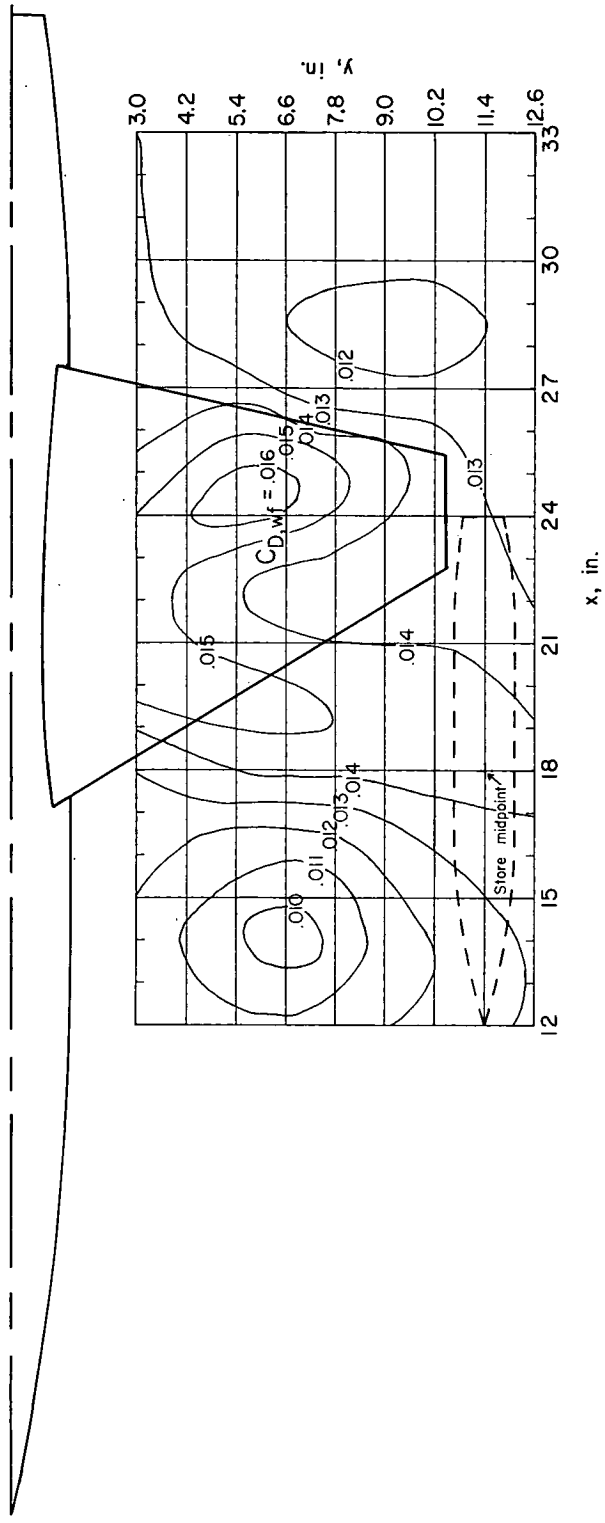

(b) z = 2.09 in.; $\alpha = 0^{\circ}$.

Figure 17.- Continued.

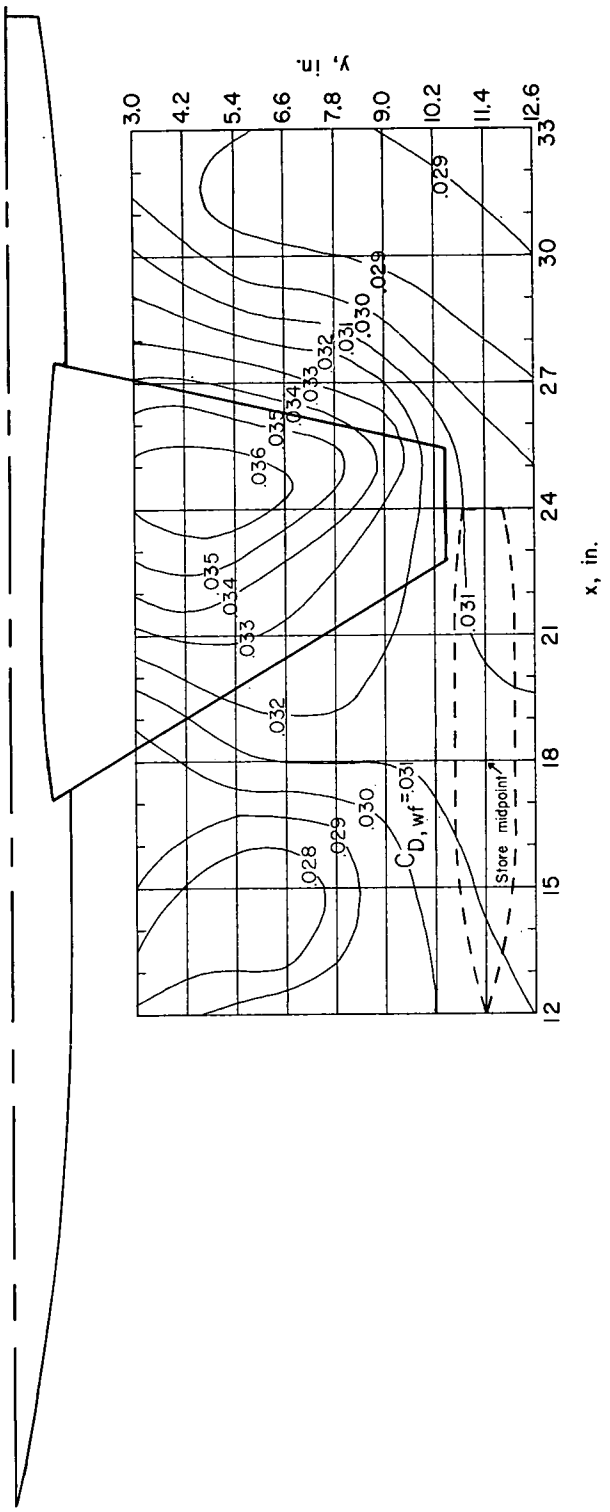

(c) $z = 2.09$ in.; $\alpha = 4^{\circ}$.

Figure 17.- Concluded.

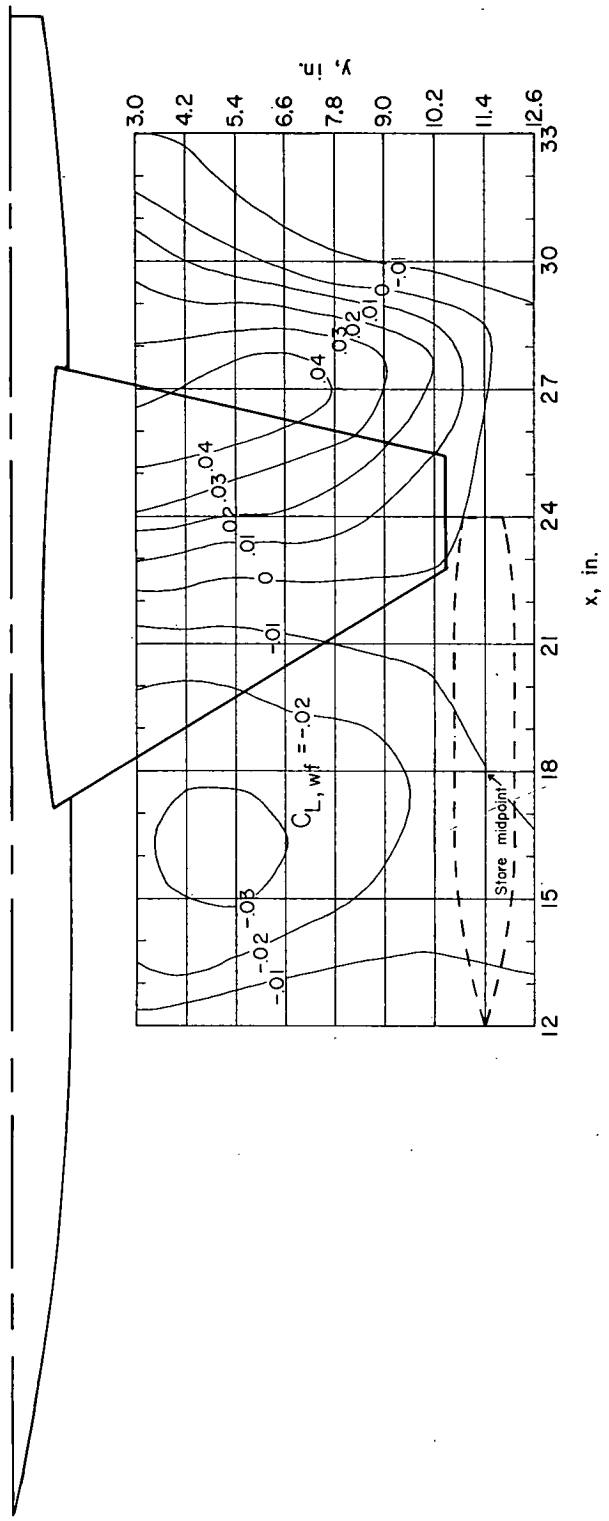

(a) z = 1.15 in.; $\alpha = 0^{\circ}$.

Figure 18.- Contour plot of the lift coefficients of wing-fuselage combination in presence of the store at M = 1.61. Lift coefficients of the isolated-wing—fuselage combination ($\alpha = 0^{\circ}$, $C_{L,i} = -0.0162$; $\alpha = 4^{\circ}$, $C_{L,i} = 0.2121$).

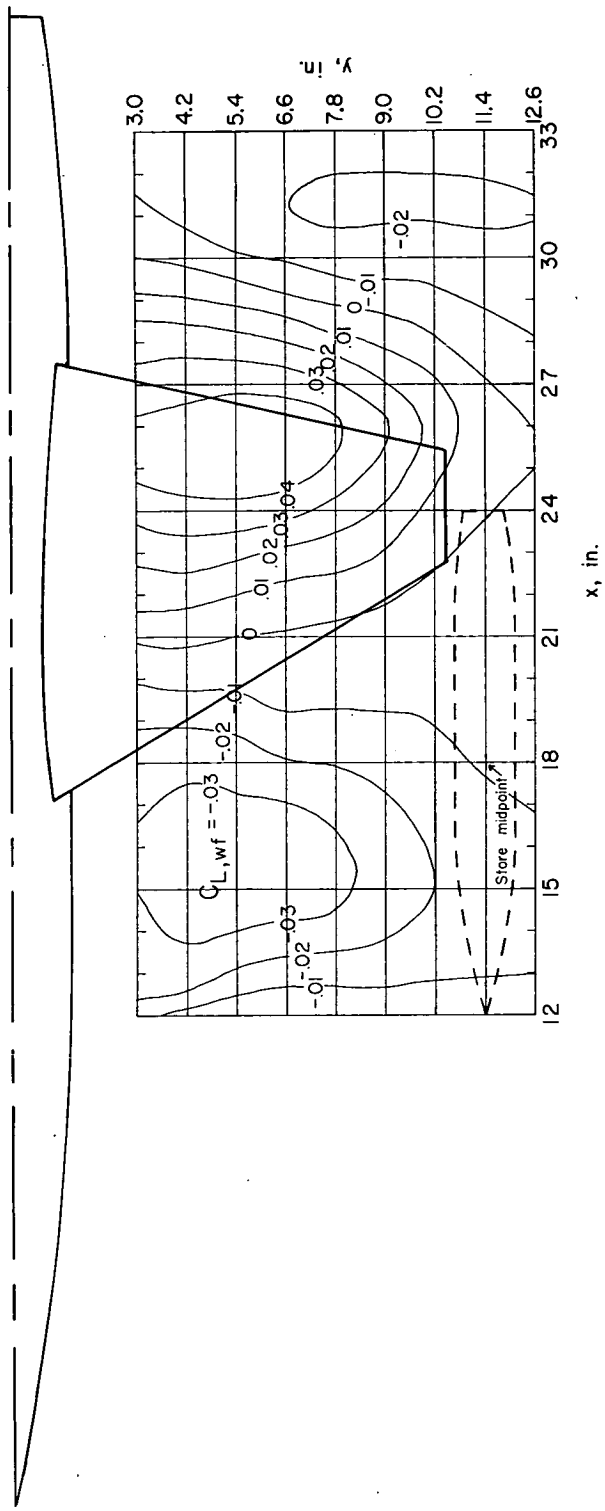

(b) z = 2.09 in.; $\alpha = 0^{\circ}$.

Figure 18.- Continued.

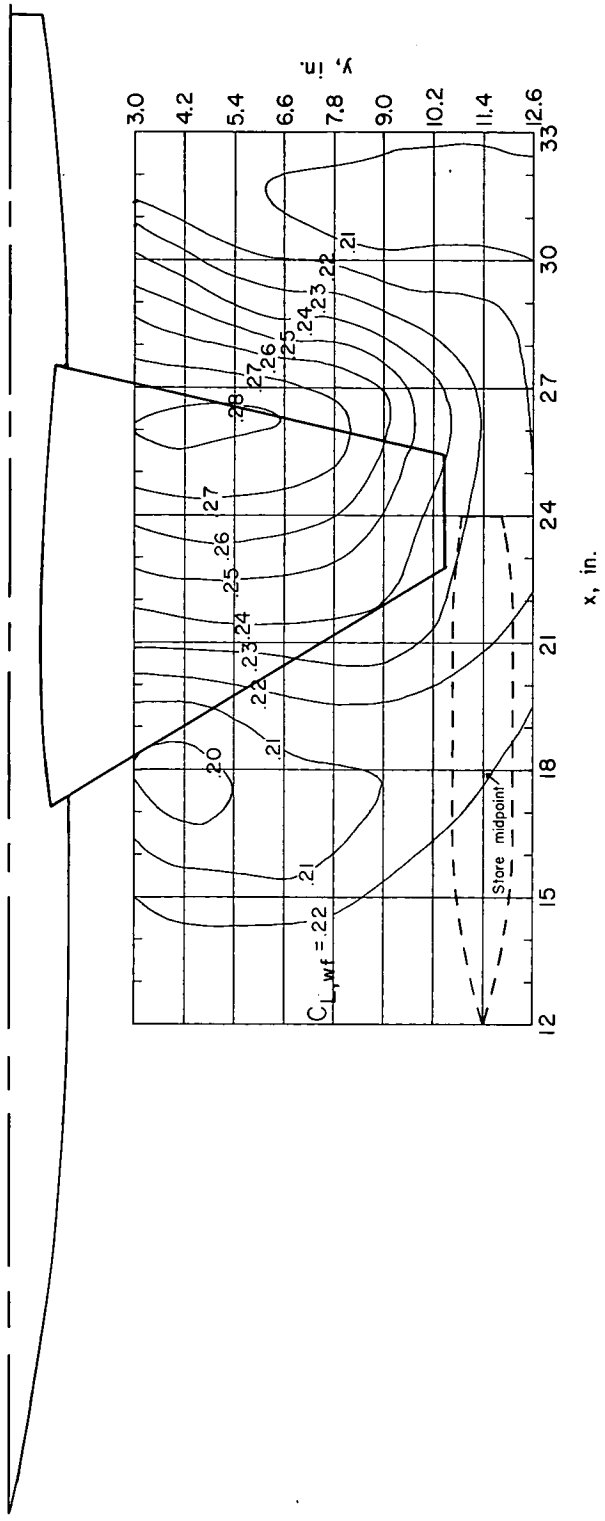

(c) z = 2.09 in.; $\alpha = 4^{\circ}$.

Figure 18.- Concluded.

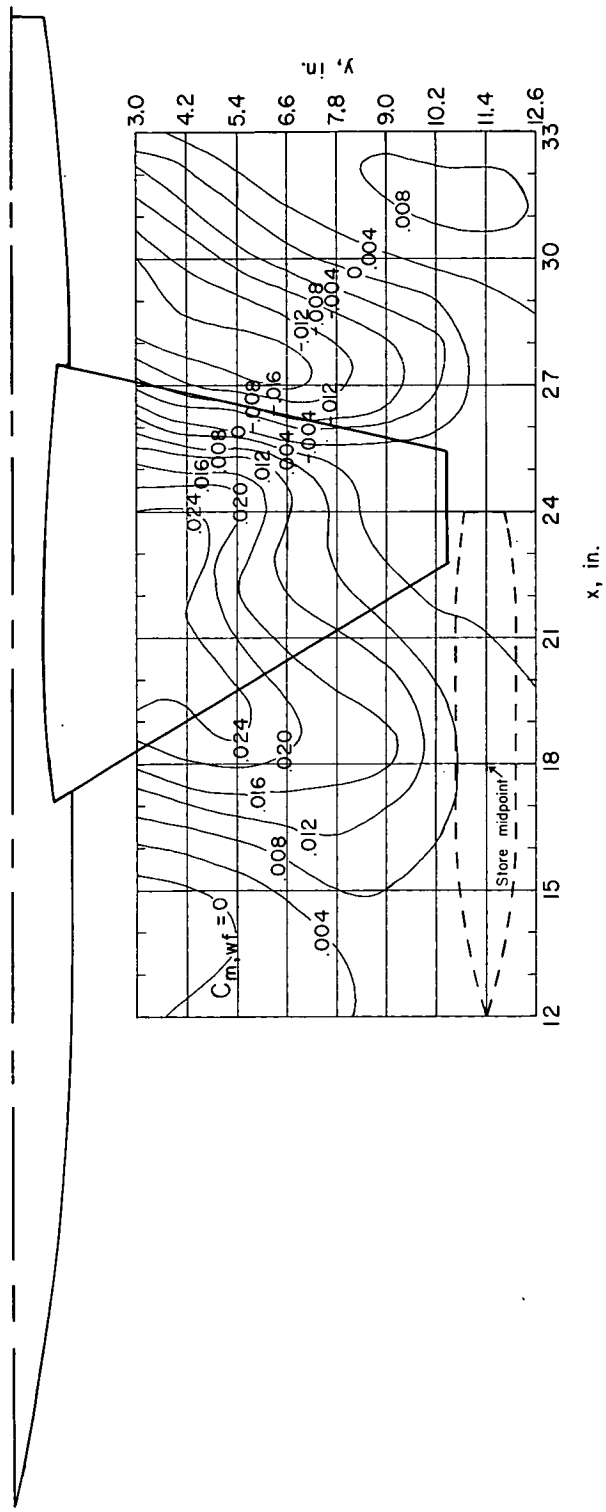

(a) $z = 1.15$ in.; $\alpha = 0^{\circ}$.

Figure 19.- Contour plot of the pitching-moment coefficients of wing-fuselage combination in presence of the store at $M = 1.61$. Pitching-moment coefficients for the isolated-wing—fuselage combination ($\alpha = 0^{\circ}$, $C_{m,i} = 0.0072$; $\alpha = 4^{\circ}$, $C_{m,i} = -0.0330$).

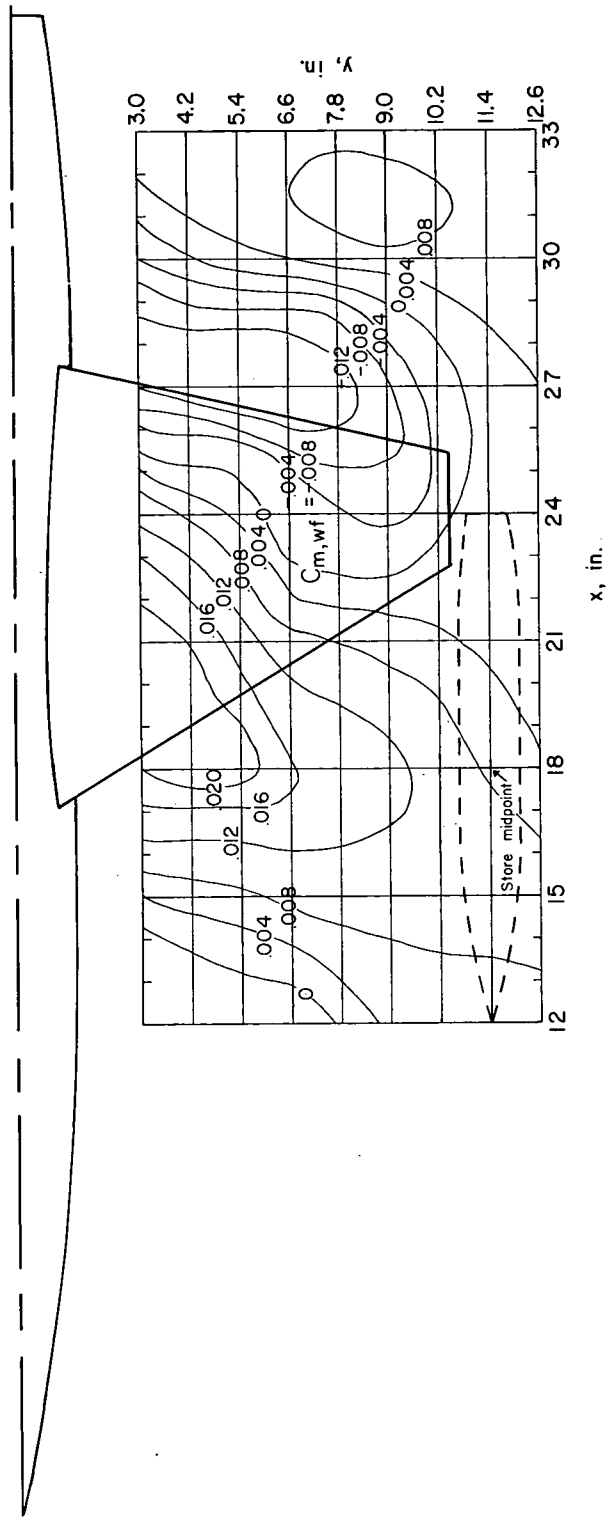

(b) z = 2.09 in.; $\alpha = 0^{\circ}$.

Figure 19.- Continued.

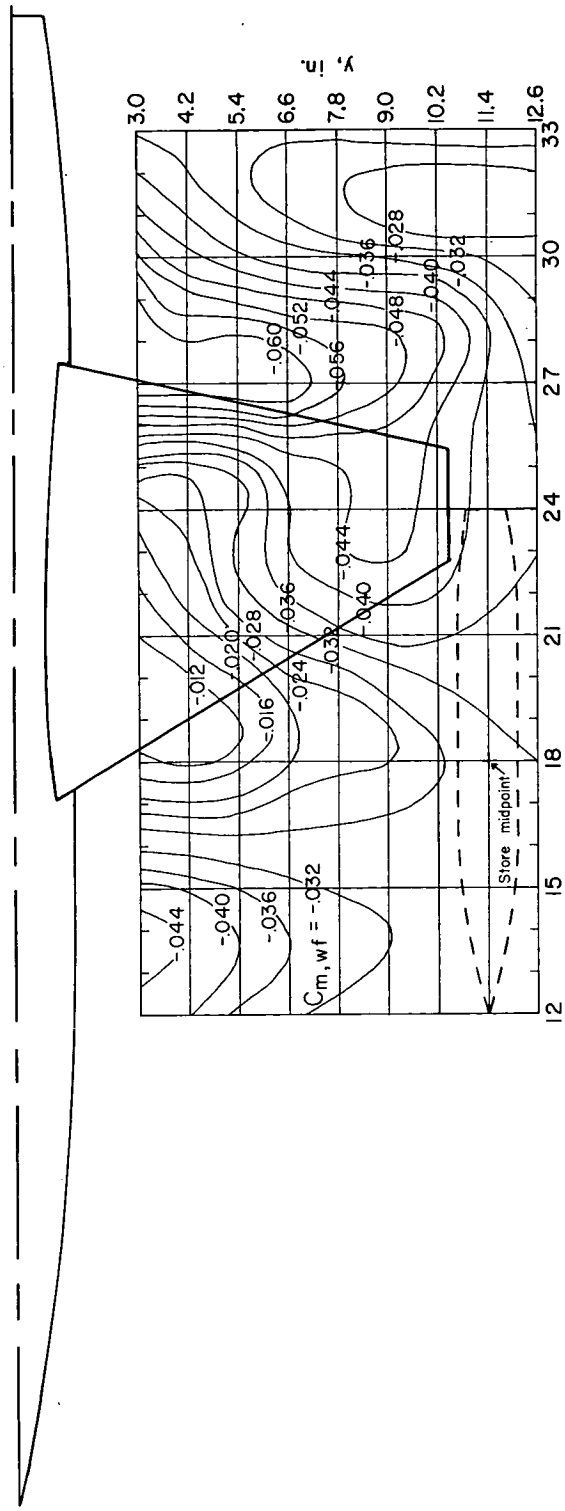

(c) z = 2.09 in.; $\alpha = 4^{\circ}$.

Figure 19.- Concluded.

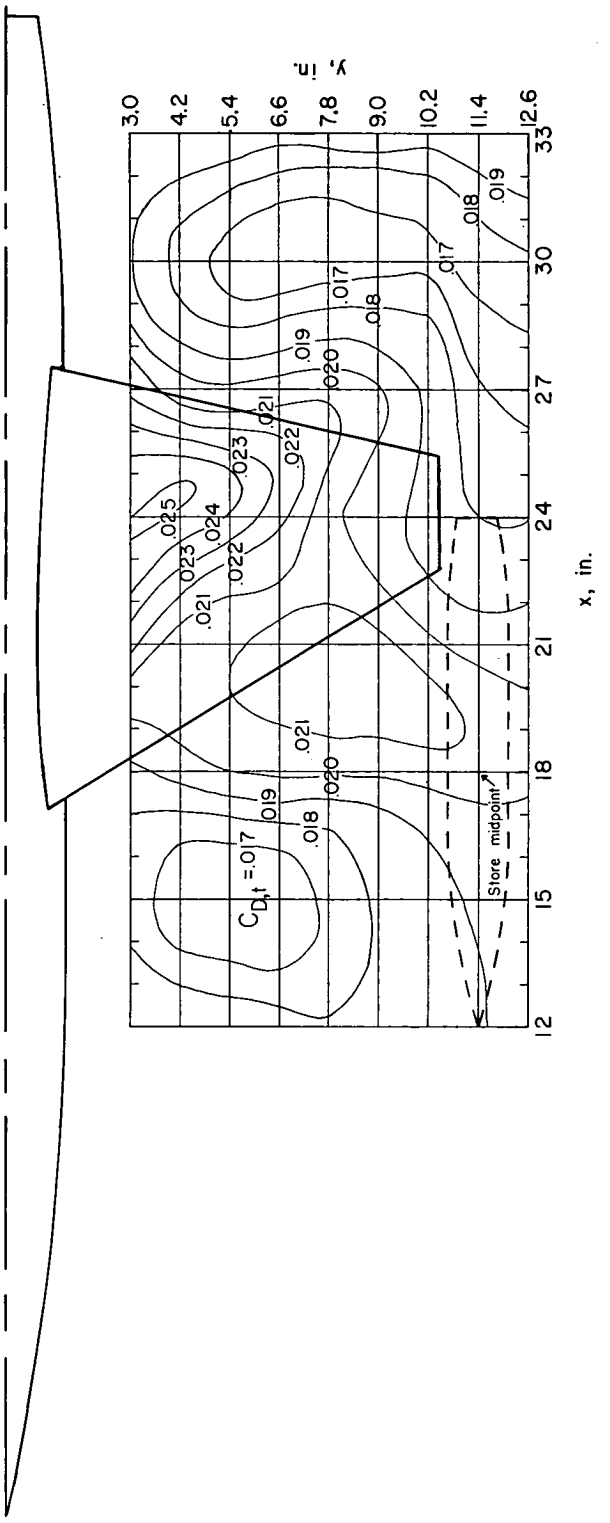

(a) $z = 1.15$ in.; $\alpha = 0^\circ$.

Figure 20.- Contour plot of the total-drag coefficients of the complete configuration (wing-fuselage combination plus store) at $M = 1.61$. Total-drag coefficients for the isolated configuration ($\alpha = 0^\circ$, $C_{D,i} = 0.0193$; $\alpha = 4^\circ$, $C_{D,i} = 0.0361$).

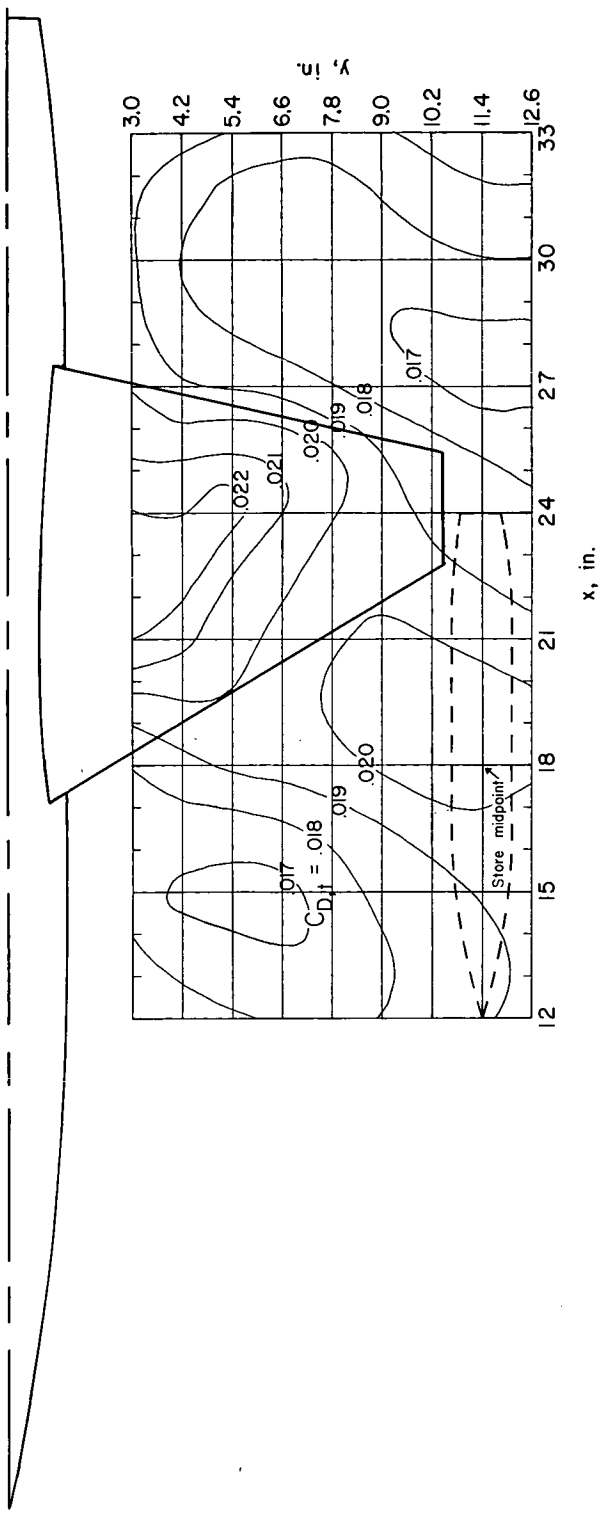

(b) z = 2.09 in.; $\alpha = 0^{\circ}$.

Figure 20.- Continued.

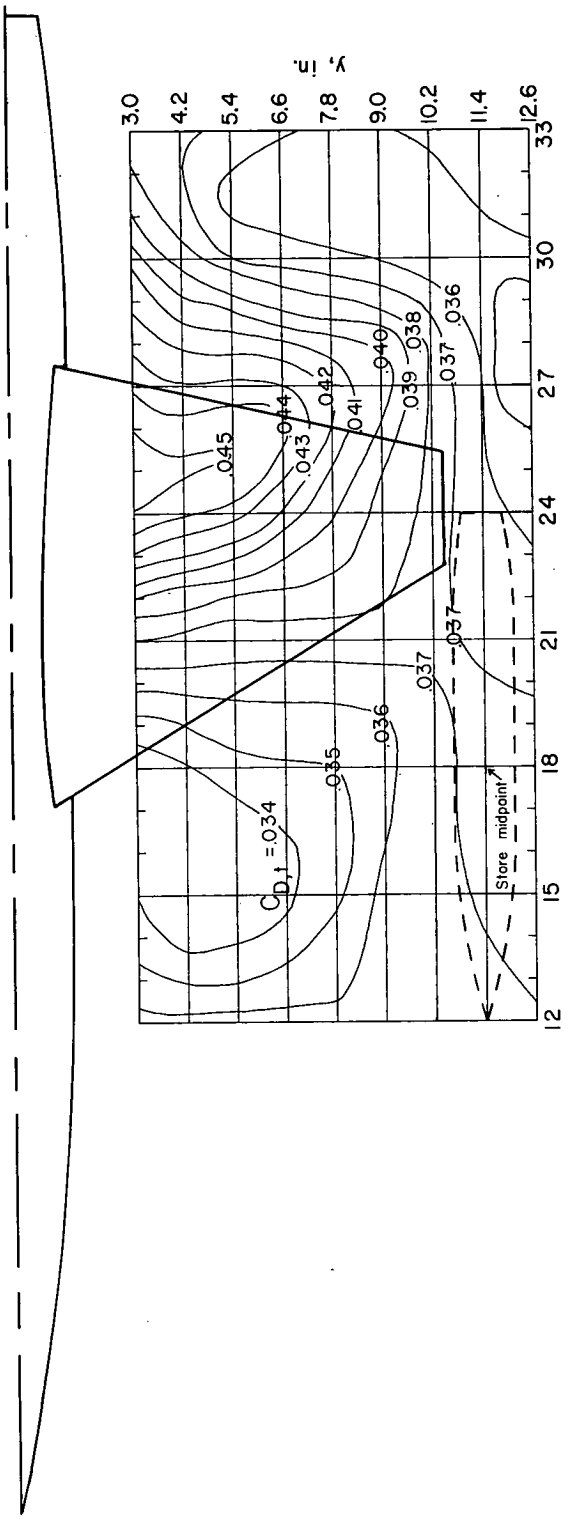

(c) $z = 2.09$ in.; $\alpha = 4^{\circ}$.

Figure 20.- Concluded.

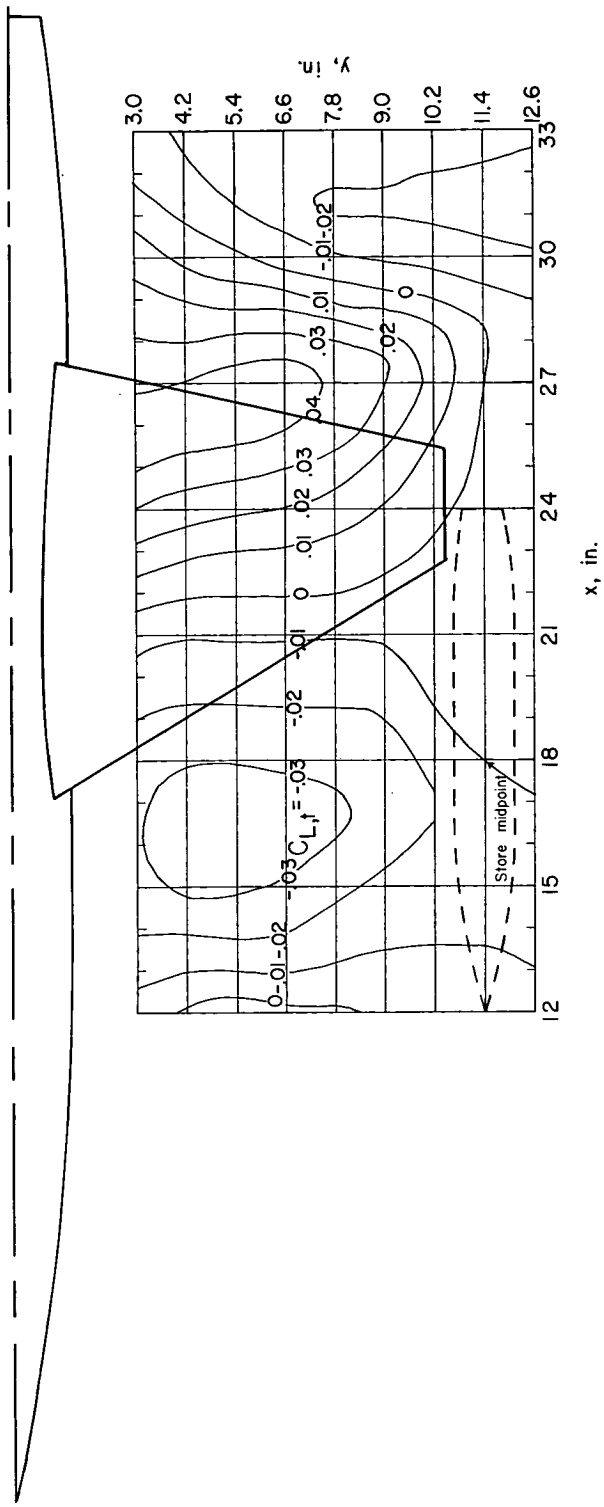

(a) z = 1.15 in.; $\alpha = 0^\circ$.

Figure 21.- Contour plot of the total-lift coefficients of the complete configuration (wing-fuselage combination plus store) at M = 1.61. Lift coefficients for the isolated configuration ($\alpha = 0^\circ$, $C_{L,i}$ = -0.015; $\alpha = 4^\circ$, $C_{L,i}$ = 0.215).

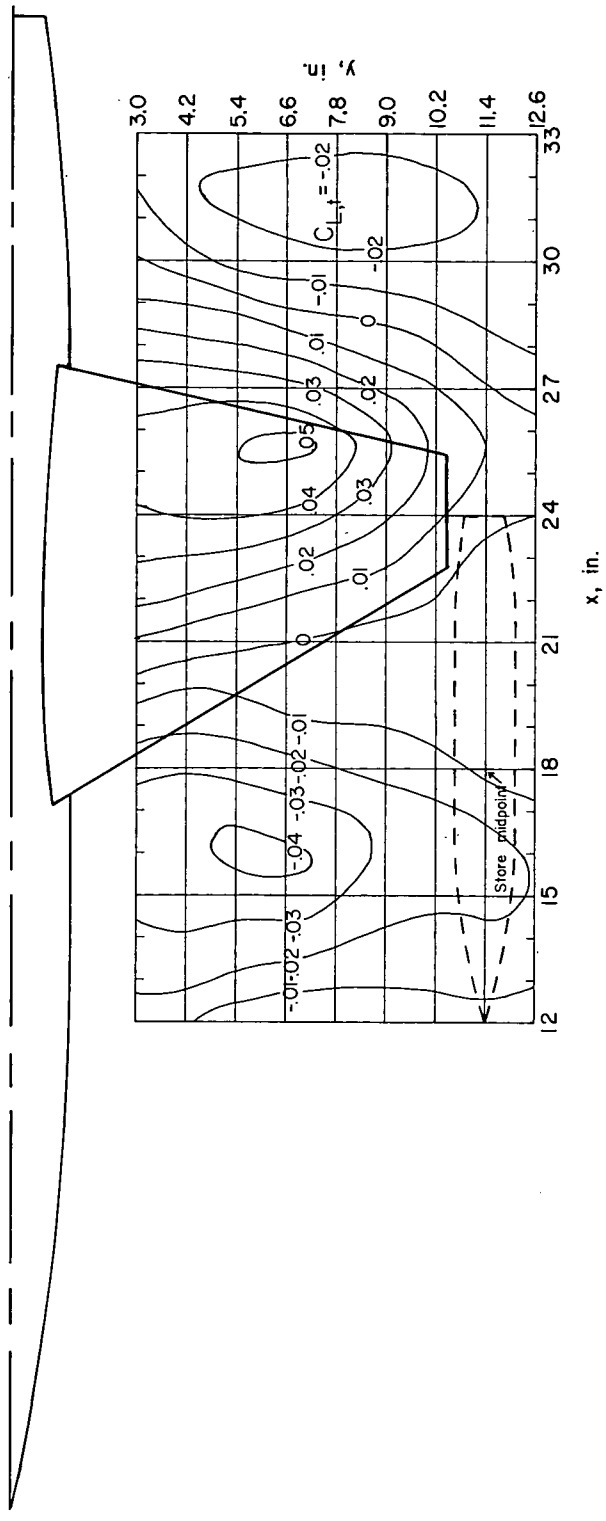

(b) z = 2.09 in.; $\alpha = 0^{\circ}$.

Figure 21.- Continued.

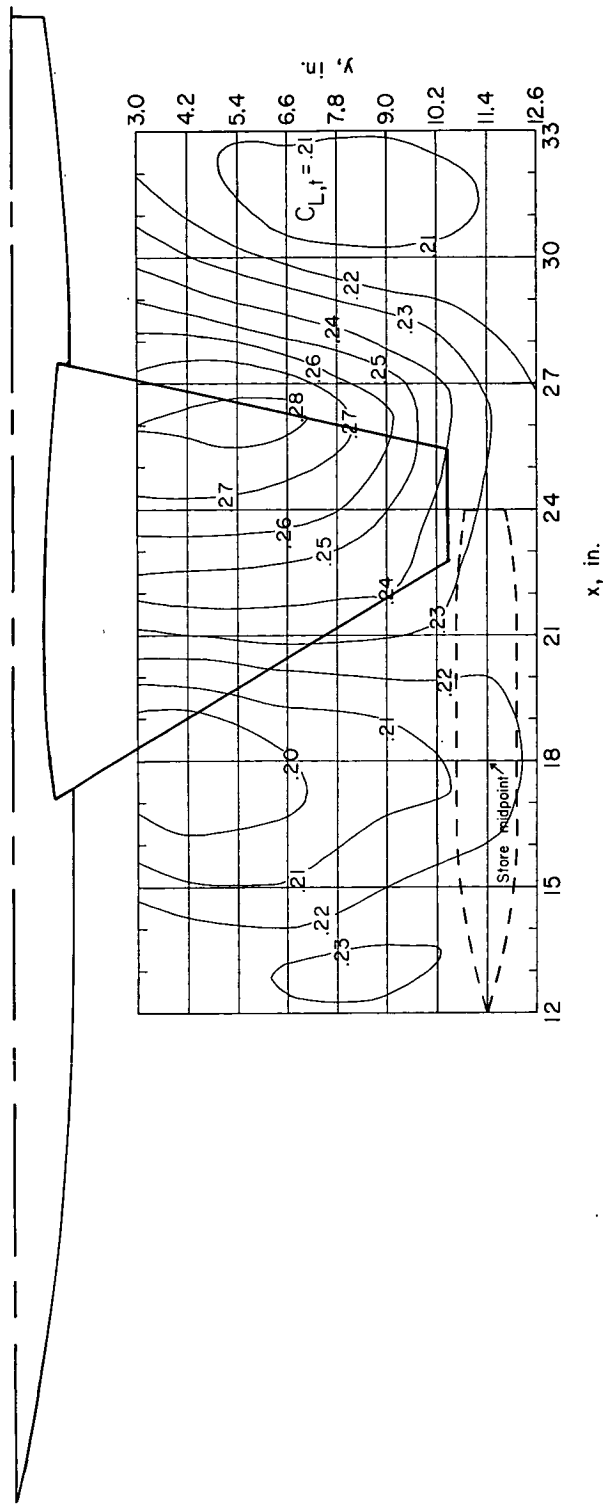

(c) z = 2.09 in.; $\alpha = 4^{\circ}$.

Figure 21.- Concluded.

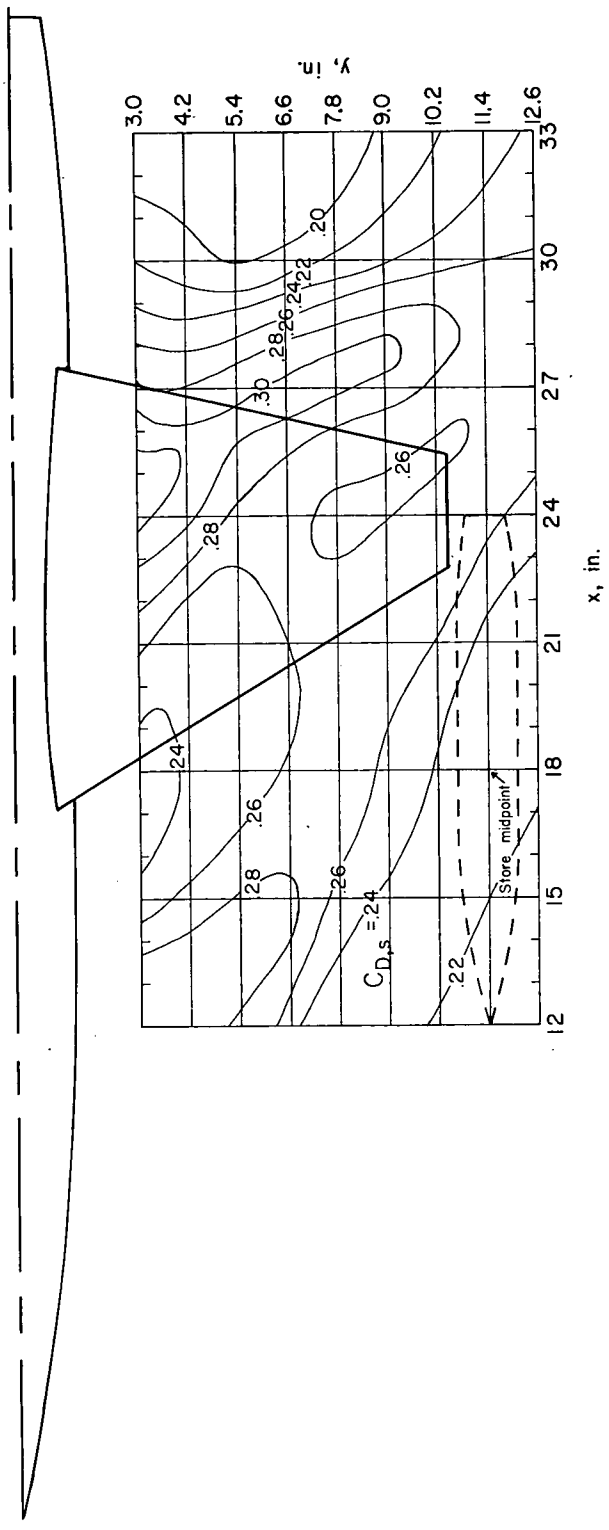

(a) $z = 1.15$ in.; $\alpha = 0^\circ$.

Figure 22.- Contour plot of the drag coefficients of the store in presence of the wing-fuselage combination at $M = 2.01$. Drag coefficients for the isolated store $\left(\alpha = 0^\circ,\ C_{D,i} = 0.232;\right.$ $\left.\alpha = 4^\circ,\ C_{D,i} = 0.250\right)$.

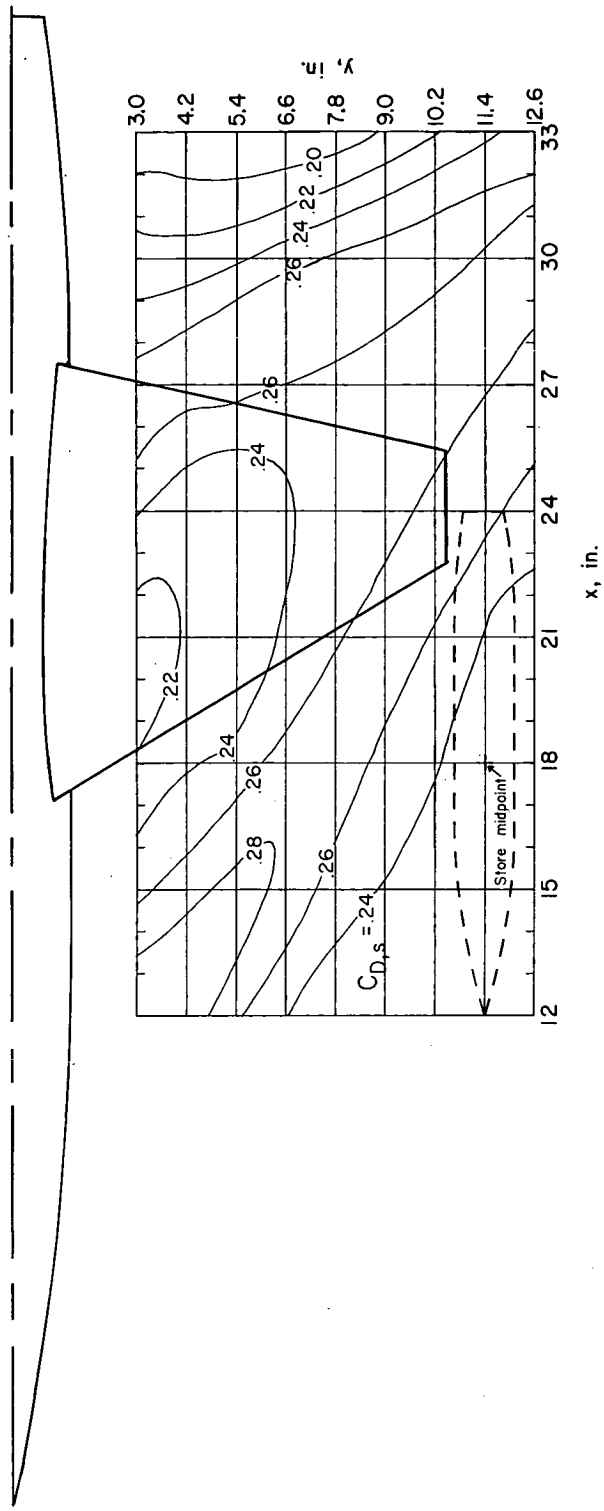

(b) z = 2.09 in.; $\alpha = 0^{\circ}$.

Figure 22.- Continued.

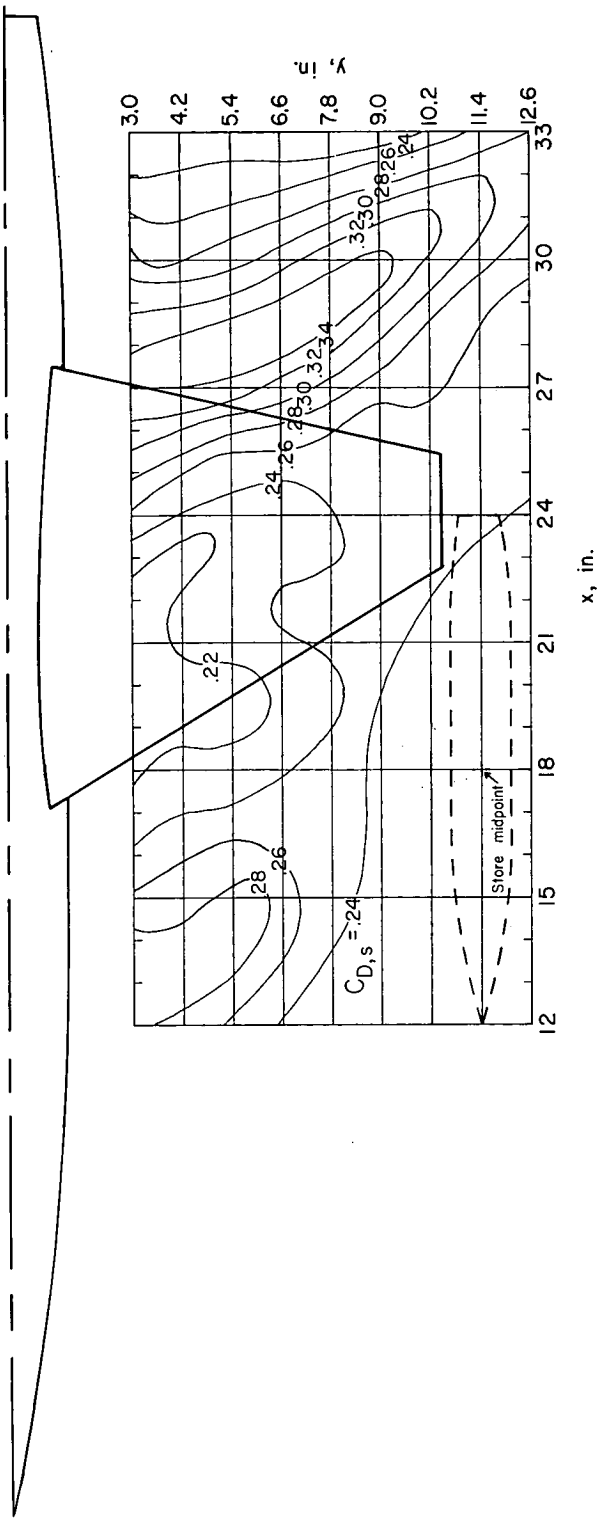

(c) z = 2.09 in.; $\alpha = 4^{\circ}$

Figure 22.- Concluded.

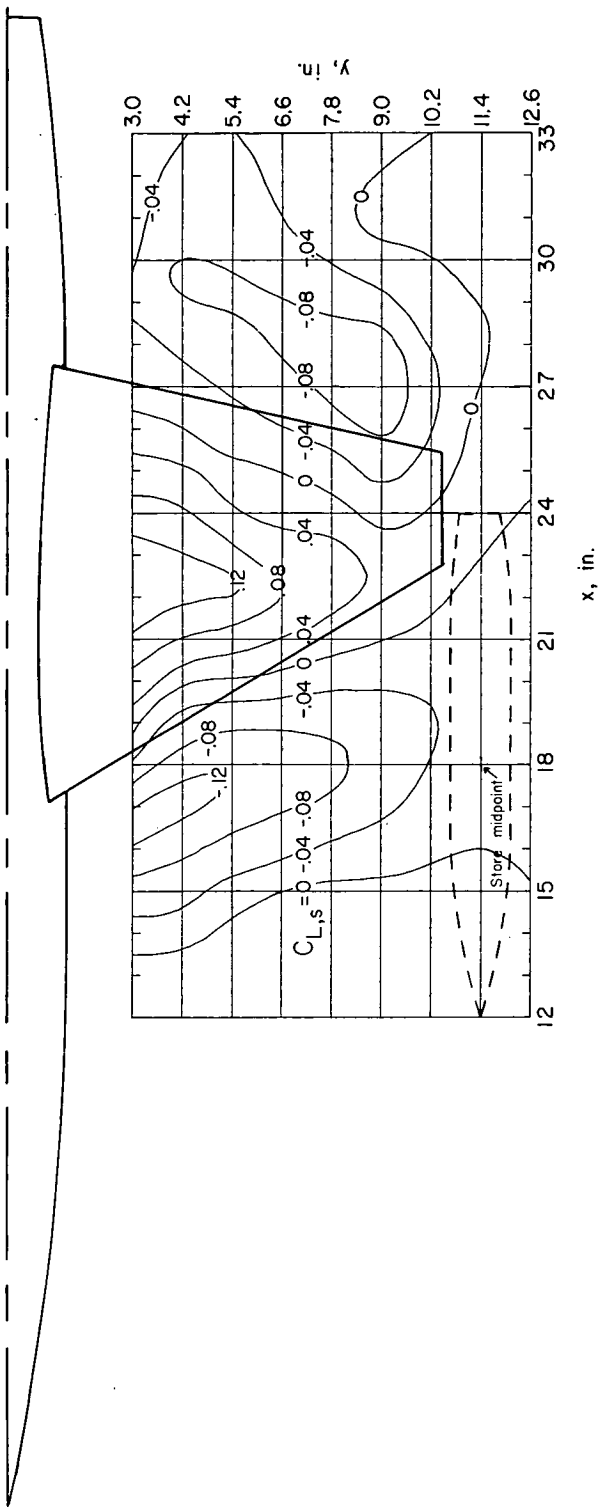

(a) z = 1.15 in.; $\alpha = 0^{\circ}$.

Figure 23.- Contour plot of lift coefficients of store in presence of the wing-fuselage combination at M = 2.01. Lift coefficients for the isolated store ($\alpha = 0^{\circ}$, $C_{L,i} = 0.000$; $\alpha = 4^{\circ}$, $C_{L,i} = 0.1700$).

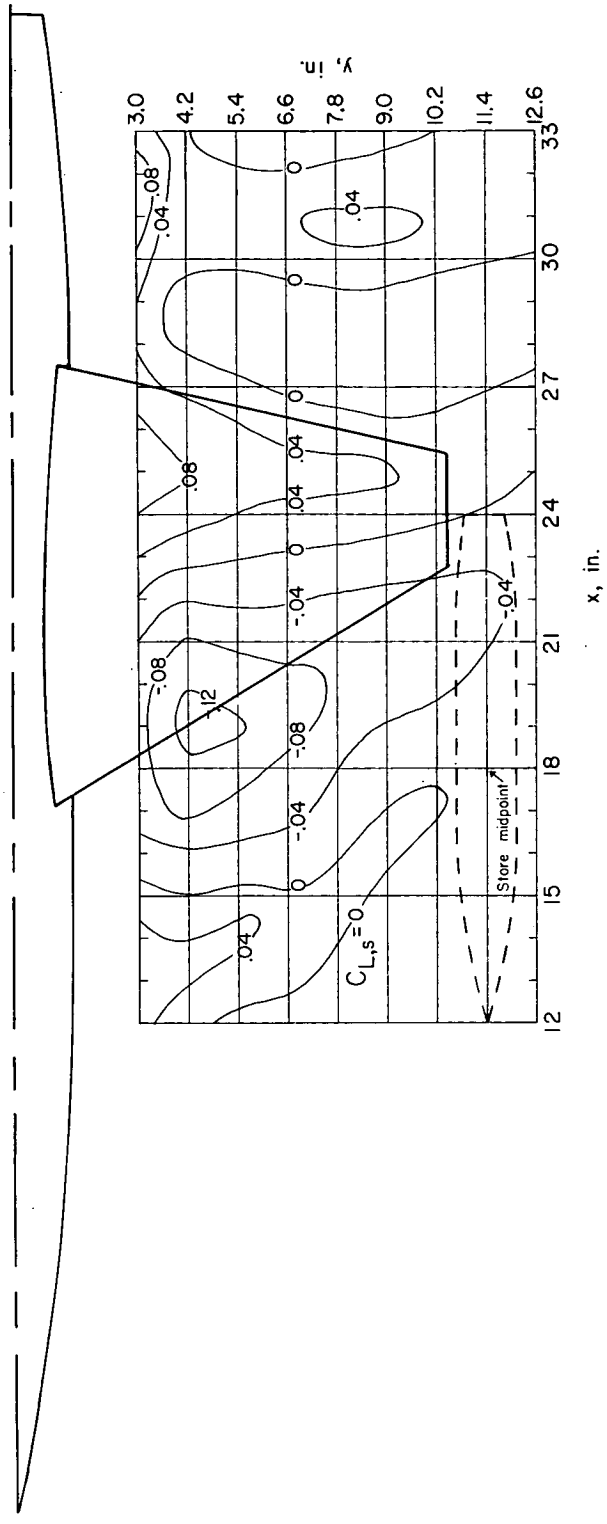

(b) z = 2.09 in.; $\alpha = 0^{\circ}$.

Figure 23.- Continued.

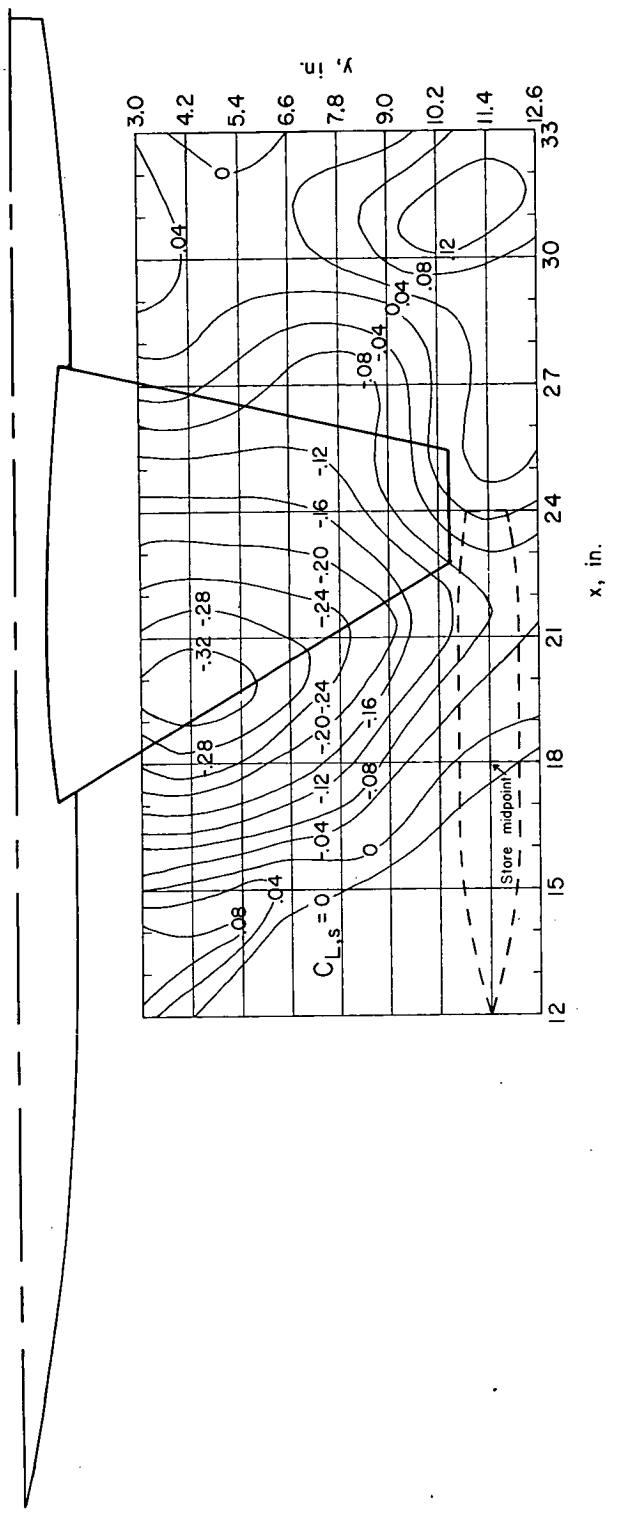

(c) $z = 2.09$ in.; $\alpha = 4^{\circ}$.

Figure 23.- Concluded.

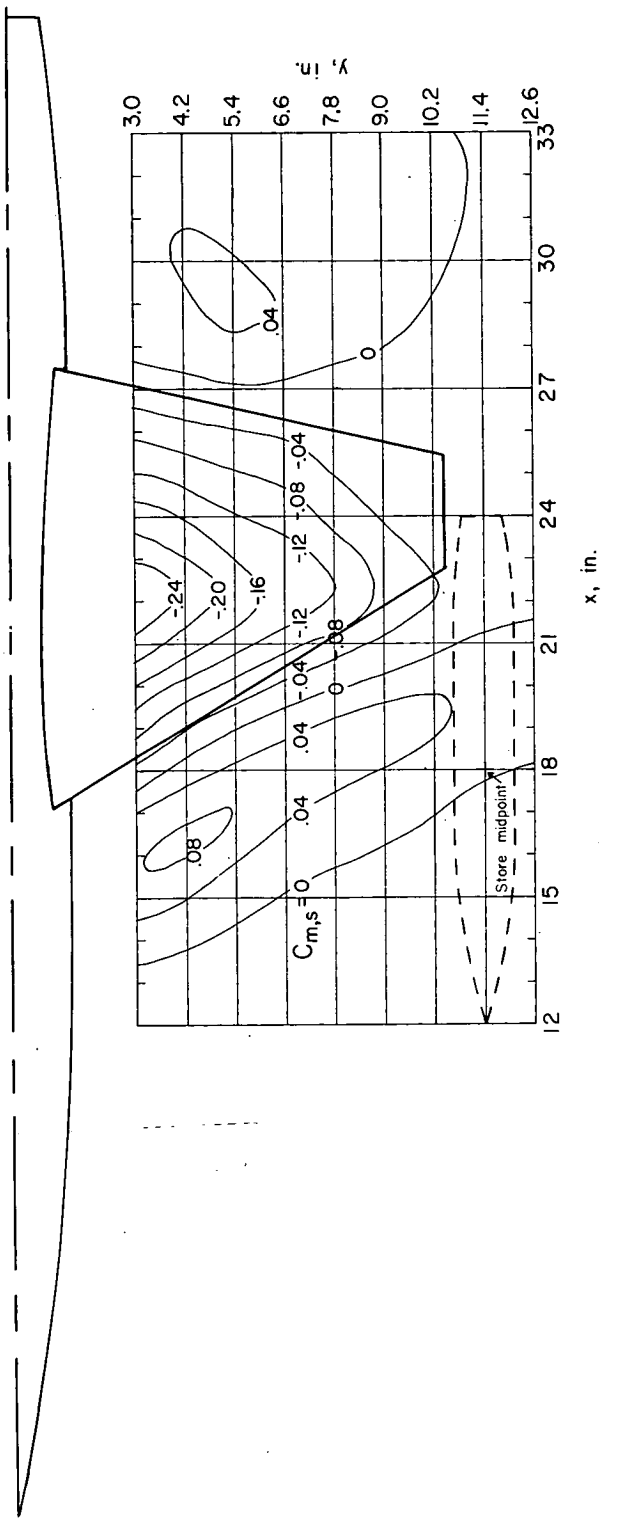

(a) $z = 1.15$ in.; $\alpha = 0^{\circ}$.

Figure 24.- Contour plot of pitching-moment coefficients of store in the presence of the wing-fuselage combination at $M = 2.01$. Pitching-moment coefficients for the isolated store ($\alpha = 0^{\circ}$, $C_{m,i} = 0.000$; $\alpha = 4^{\circ}$, $C_{m,i} = -0.025$).

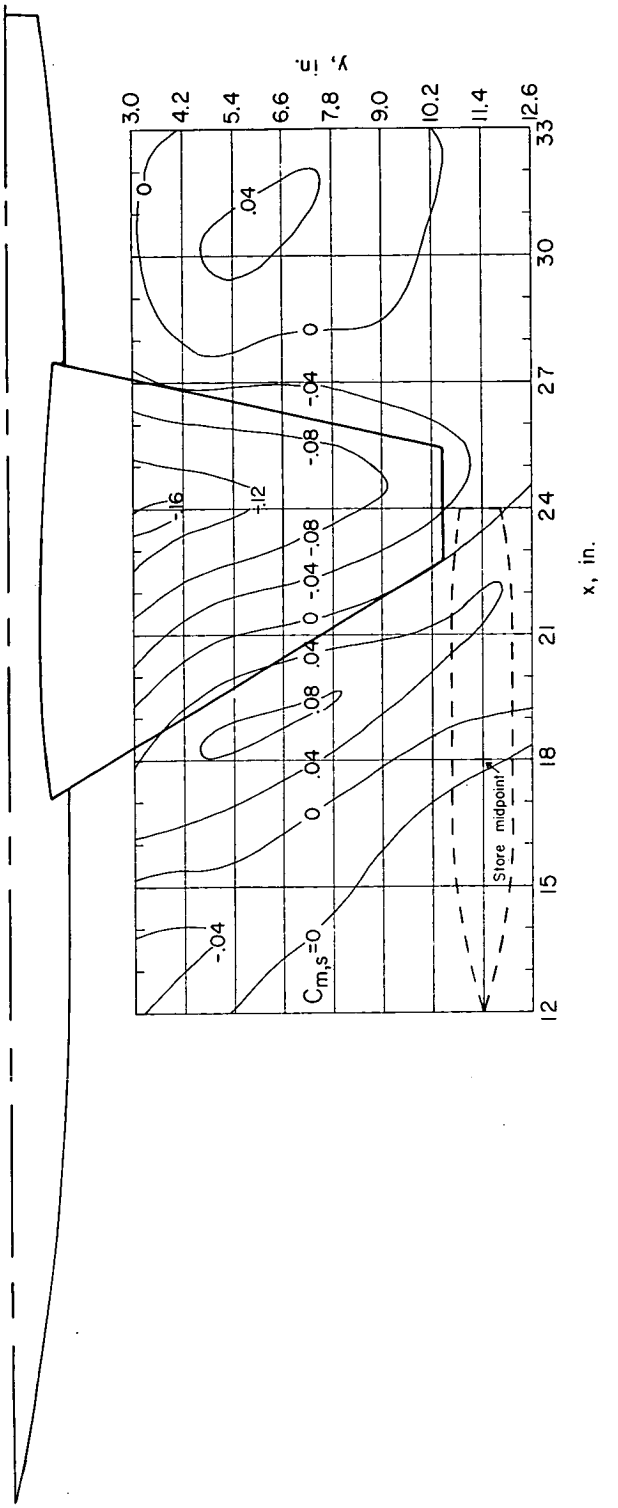

(b) z = 2.09 in.; $\alpha = 0^{\circ}$.

Figure 24.- Continued.

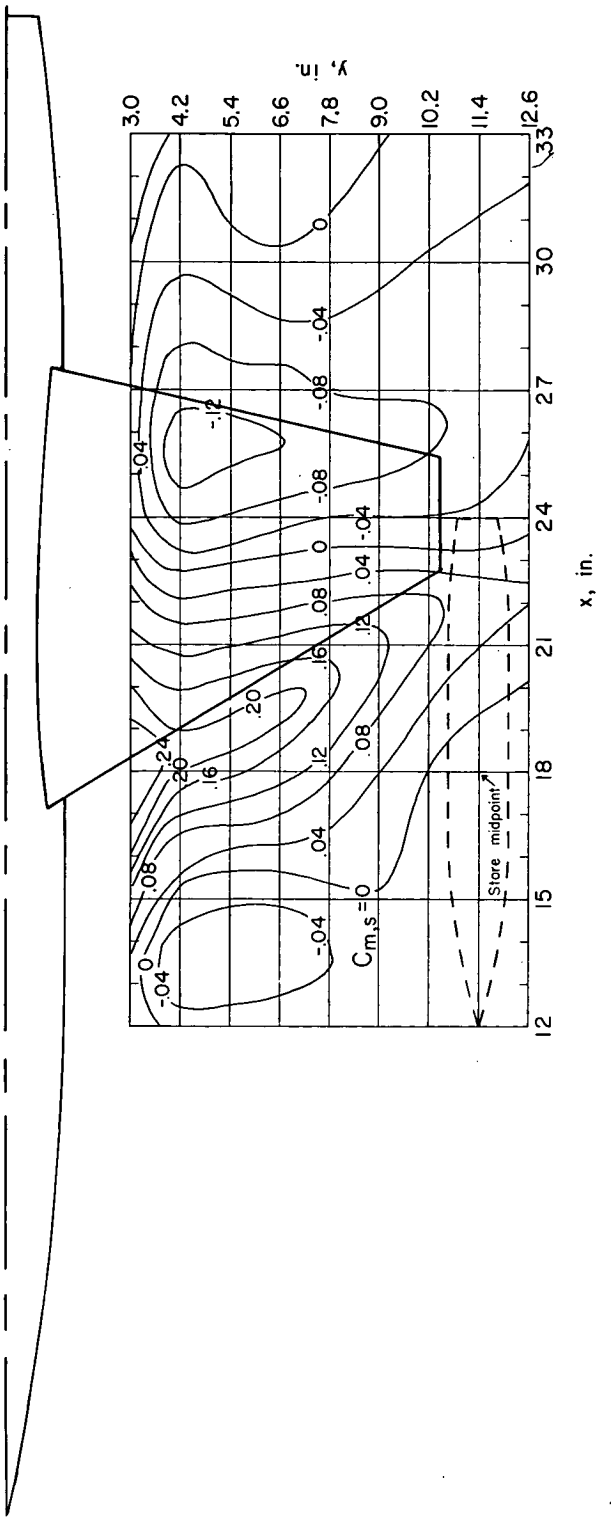

(c) z = 2.09 in.; $\alpha = 4^{\circ}$.

Figure 24.- Concluded.

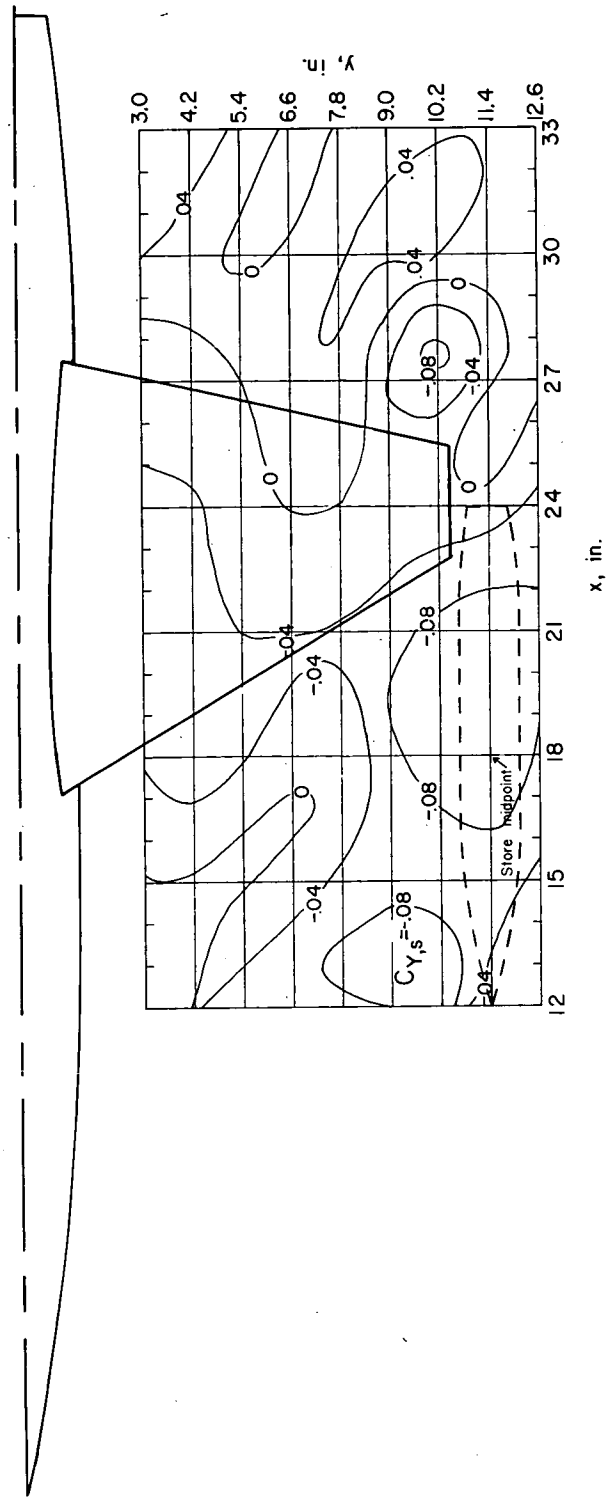

(a) z = 1.15 in.; $\alpha = 0^{\circ}$.

Figure 25.- Contour plot of side-force coefficients of store in presence of the wing-fuselage combination at M = 2.01.

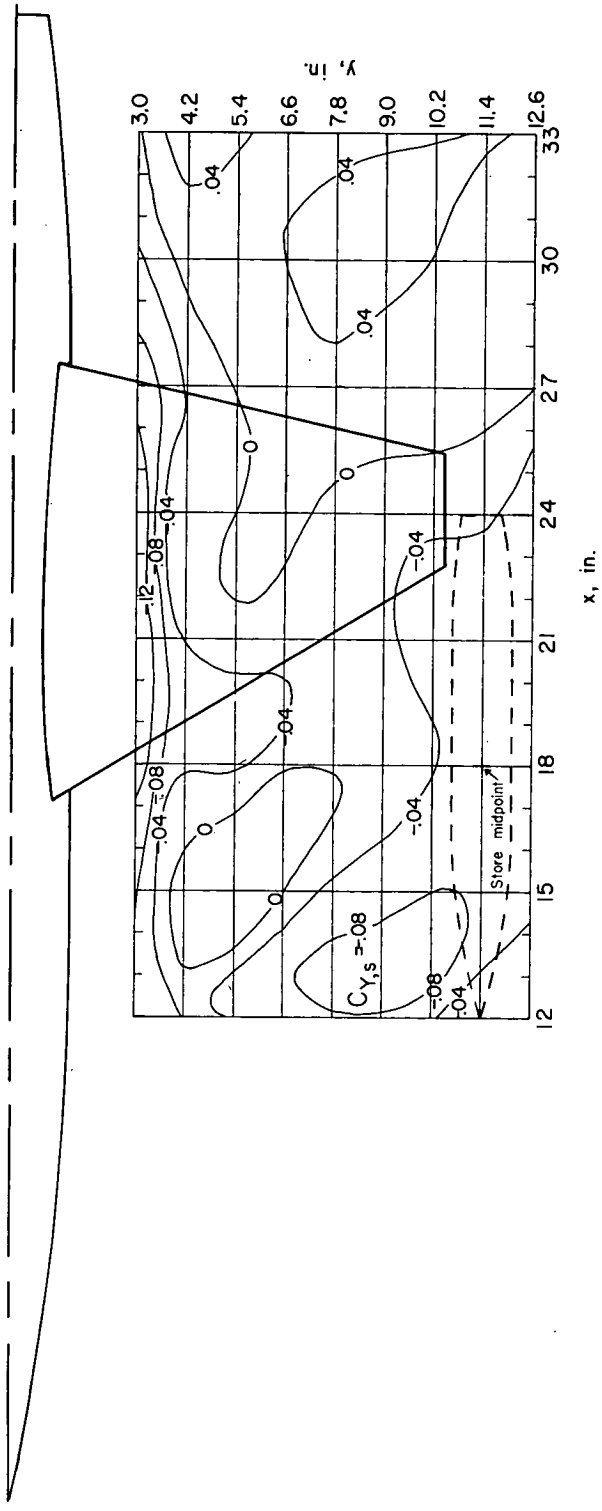

(b) z = 2.09 in.; $\alpha = 0^{\circ}$.

Figure 25.- Continued.

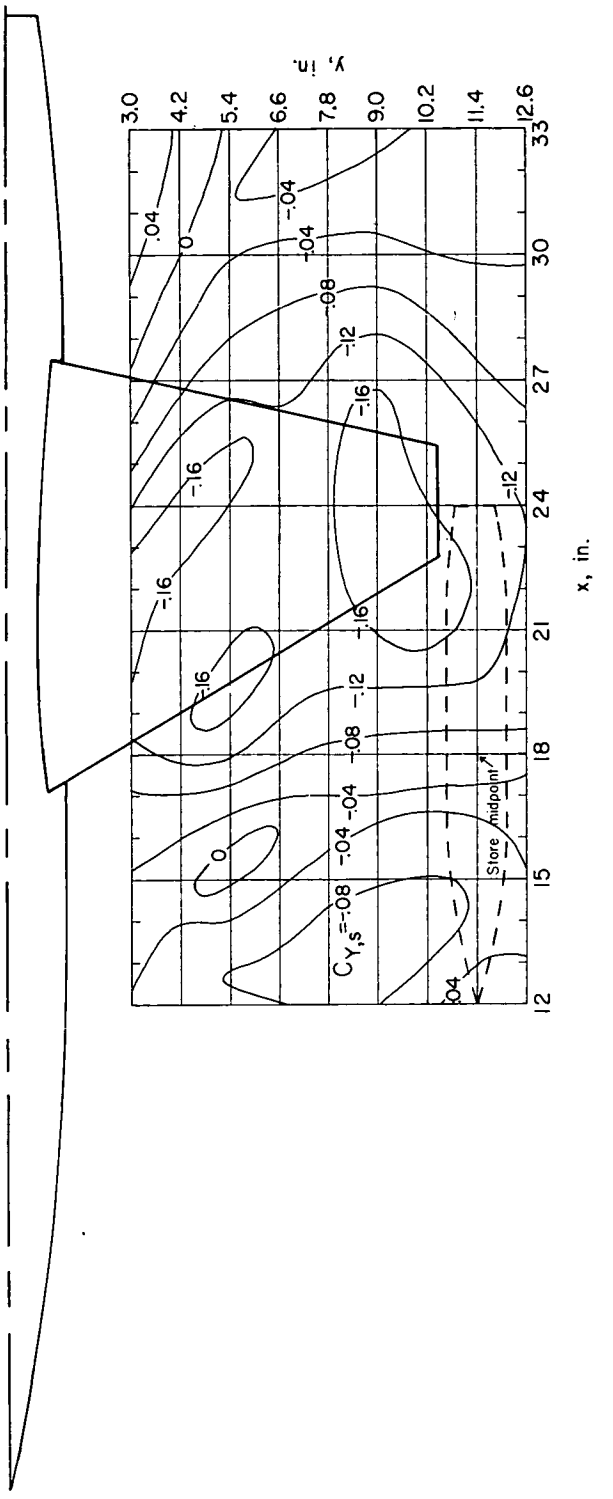

(c) $z = 2.09$ in.; $\alpha = 4^{\circ}$.

Figure 25.- Concluded.

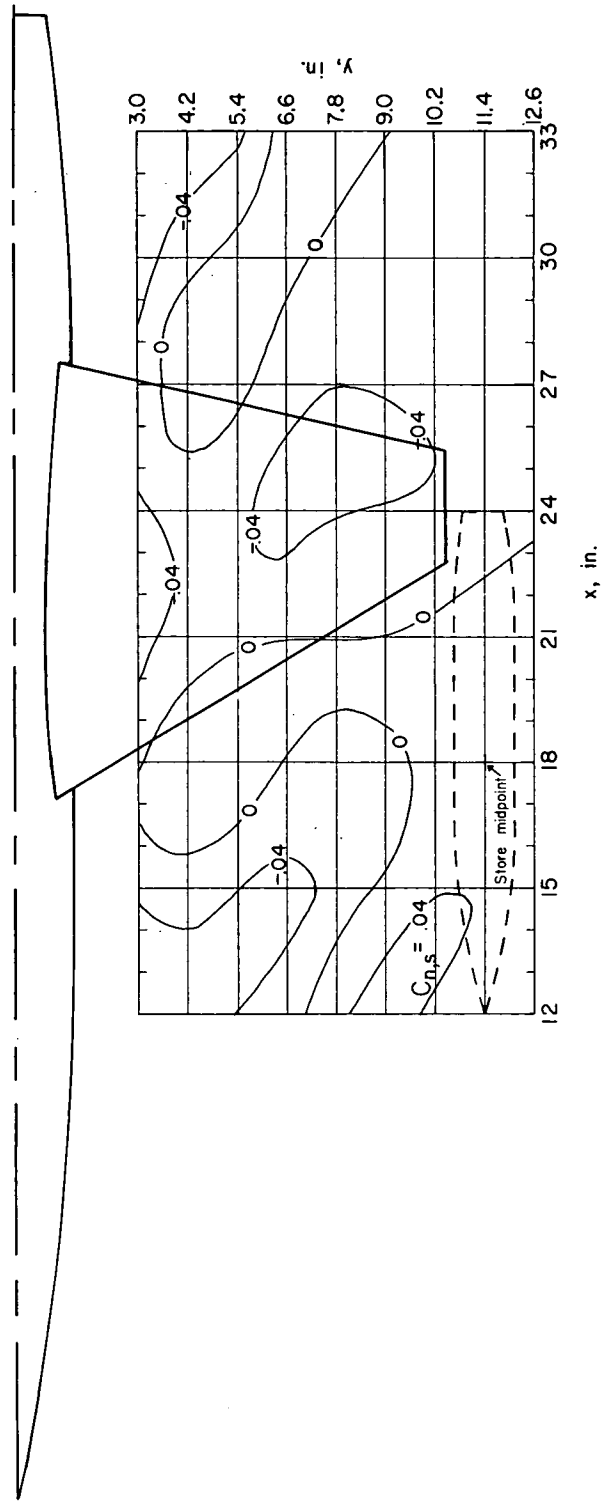

(a) $z = 1.15$ in.; $\alpha = 0^{\circ}$.

Figure 26.- Contour plot of yawing-moment coefficients of the store in presence of the wing-fuselage combination at $M = 2.01$.

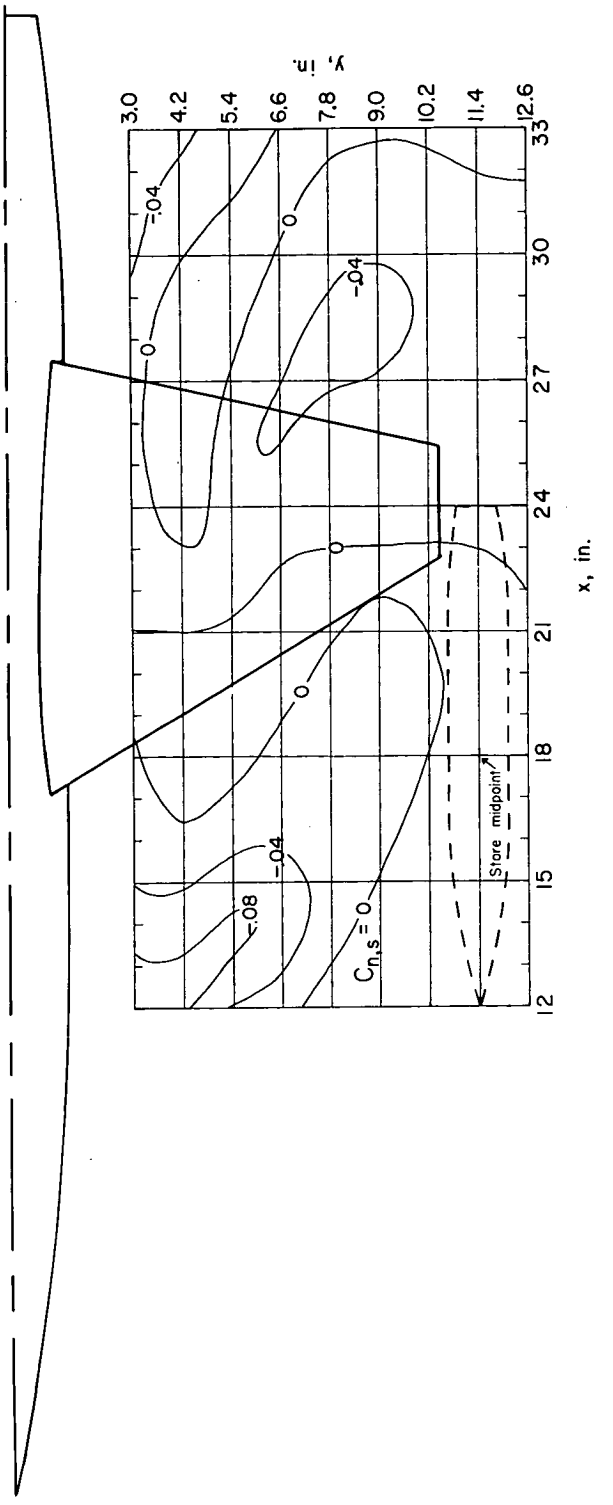

(b) z = 2.09 in.; $\alpha = 0^{\circ}$.

Figure 26.- Continued.

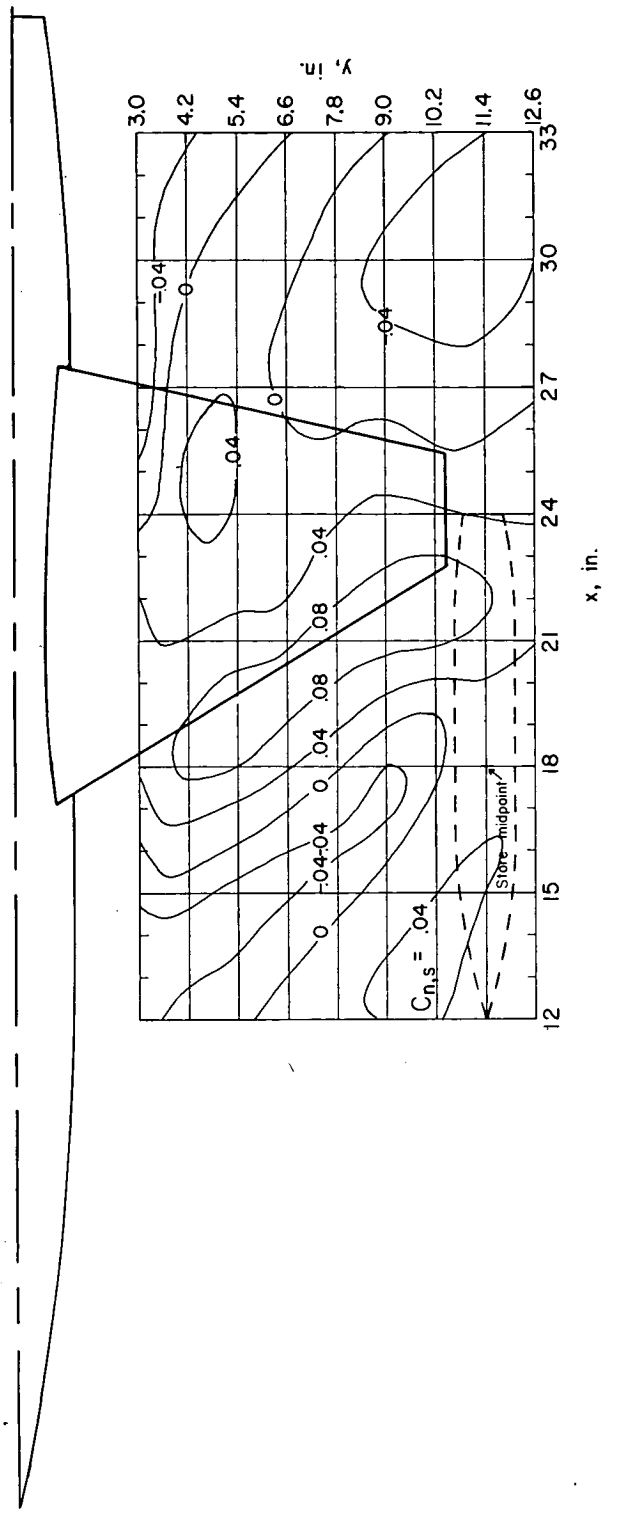

(c) z = 2.09 in.; $\alpha = 4^{\circ}$.

Figure 26.- Concluded.

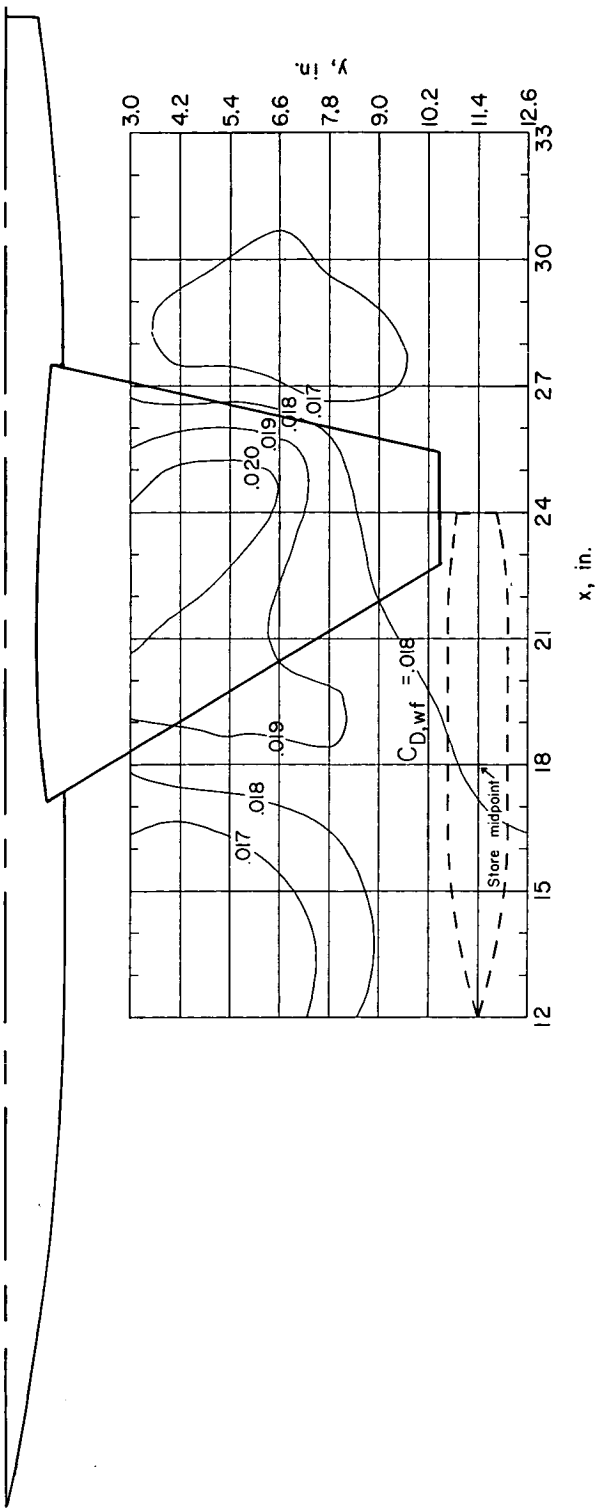

(a) $z = 1.15$ in.; $\alpha = 0^{\circ}$.

Figure 27.- Contour plot of drag coefficients of the wing-fuselage combination in presence of the store at $M = 2.01$. Drag coefficients for the isolated-wing—fuselage combination ($\alpha = 0^{\circ}$, $C_{D,i} = 0.0177$; $\alpha = 4^{\circ}$, $C_{D,i} = 0.0300$).

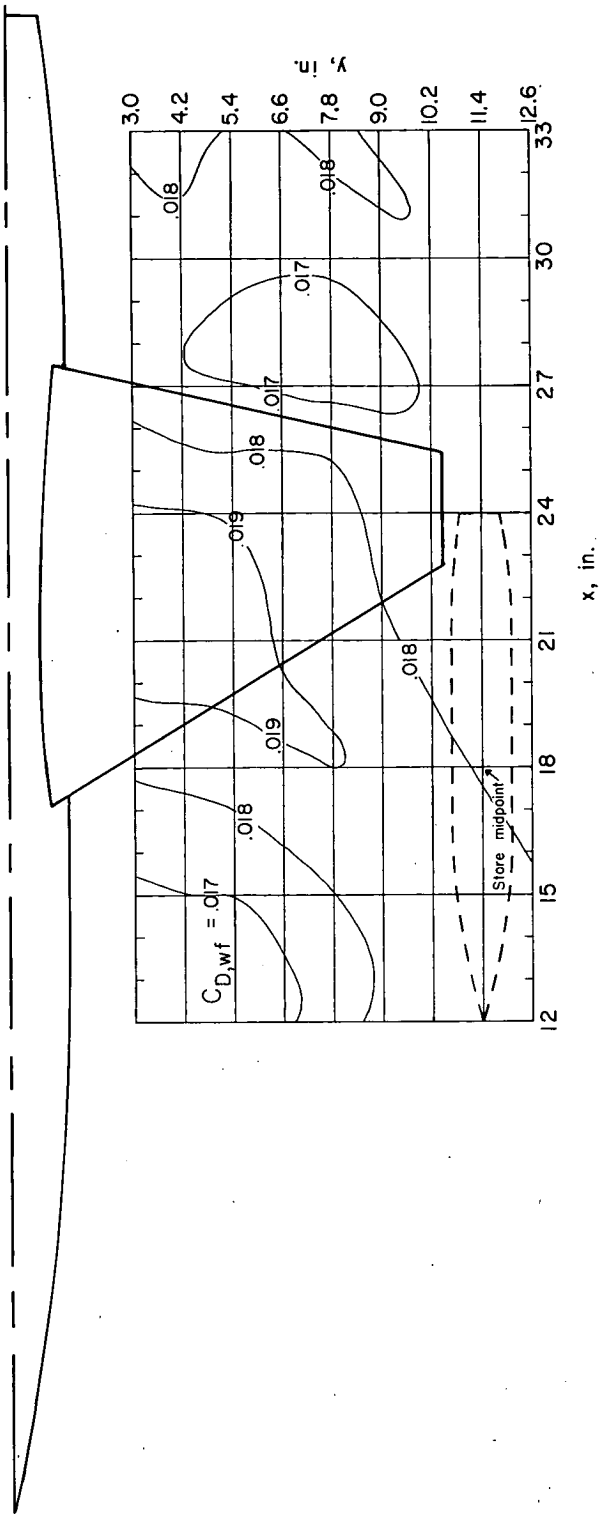

(b) z = 2.09 in.; $\alpha = 0^{\circ}$.

Figure 27.- Continued.

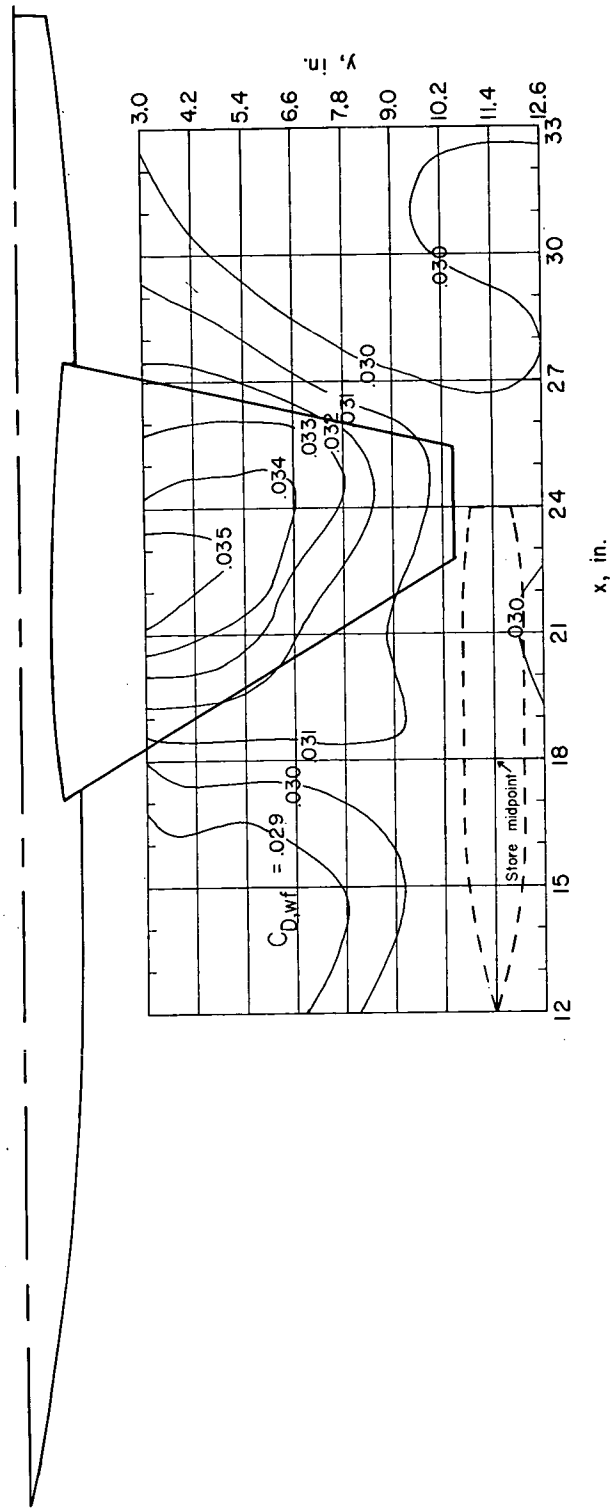

(c) z = 2.09 in.; $\alpha = 4^{\circ}$.

Figure 27.- Concluded.

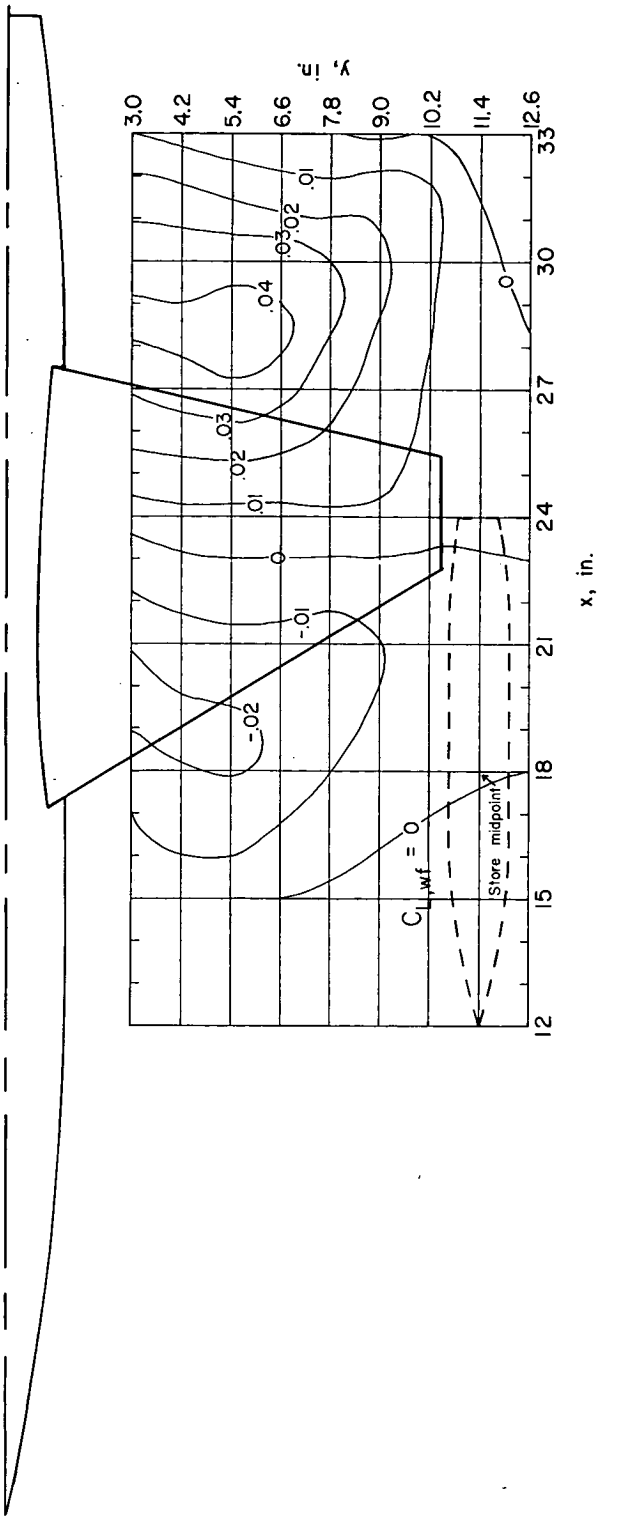

(a) $z = 1.15$ in.; $\alpha = 0^{\circ}$.

Figure 28.- Contour plot of the lift coefficients of the wing-fuselage combination in presence of the store at $M = 2.01$. Lift coefficients for the isolated-wing—fuselage combination ($\alpha = 0^{\circ}$, $C_{L,i} = -0.0039$; $\alpha = 4^{\circ}$, $C_{L,i} = 0.1638$).

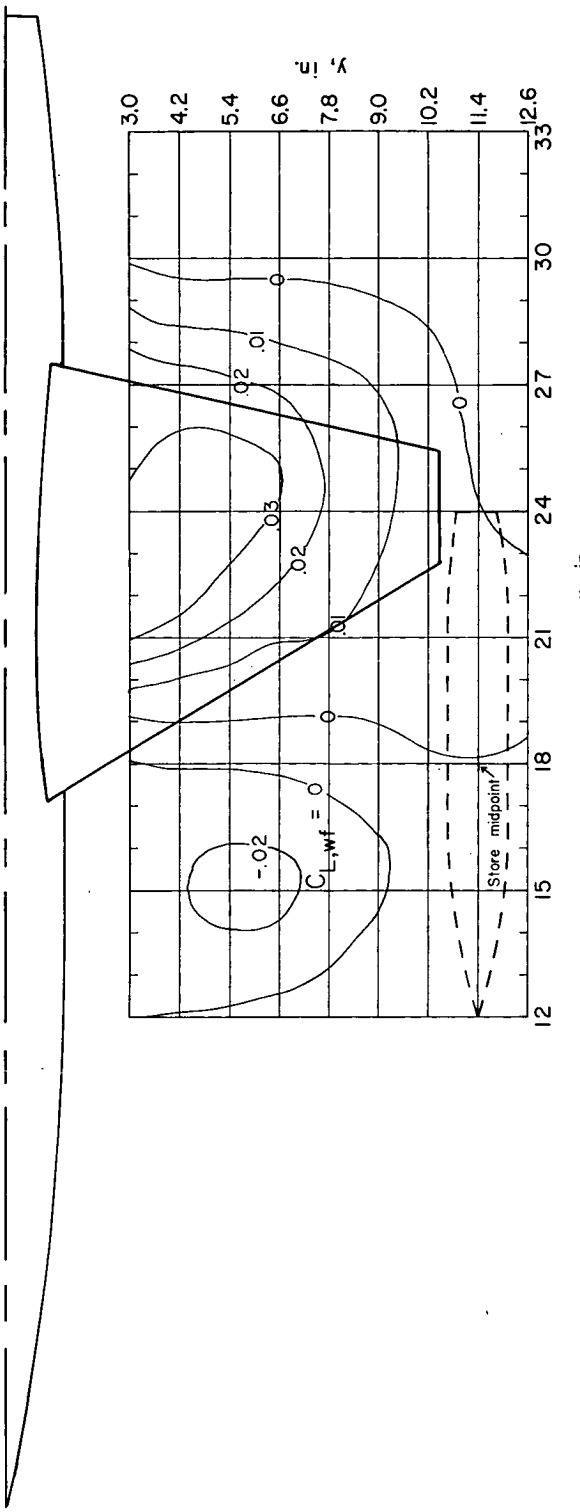

(b) $z = 2.09$ in.; $\alpha = 0^{\circ}$.

Figure 28.- Continued.

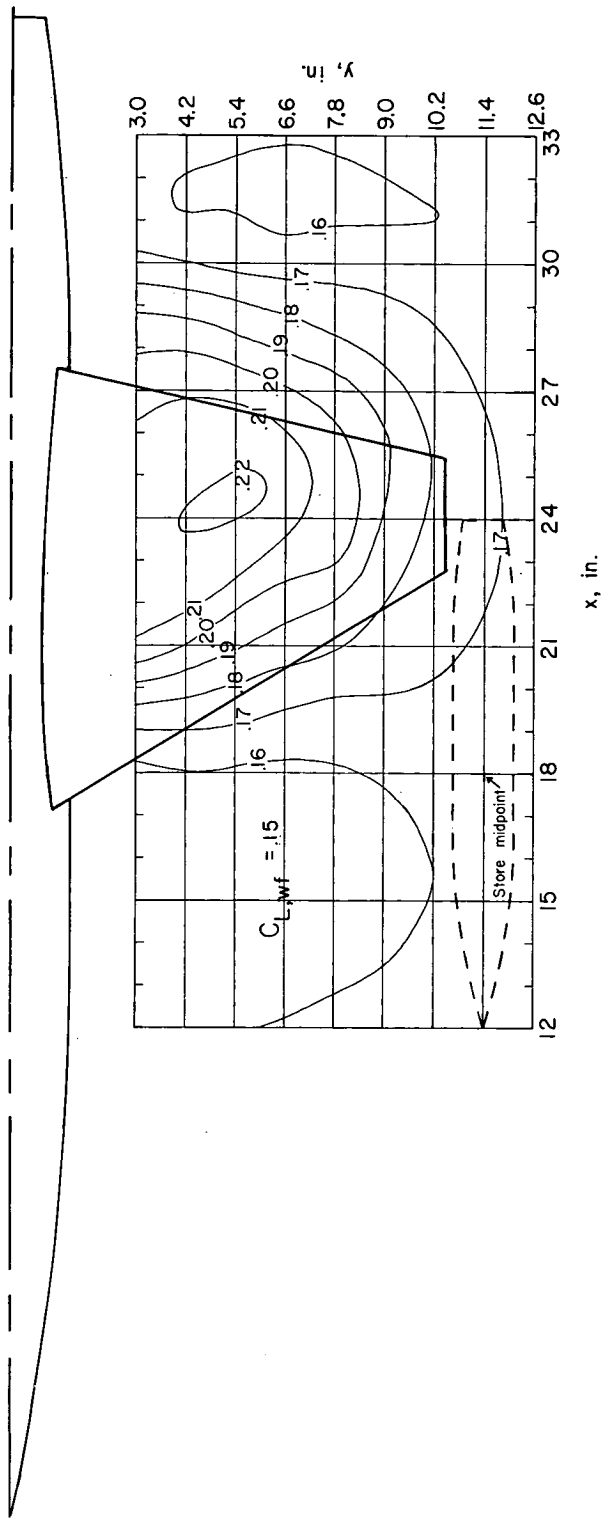

(c) z = 2.09 in.; $\alpha = 4^{\circ}$.

Figure 28.- Concluded.

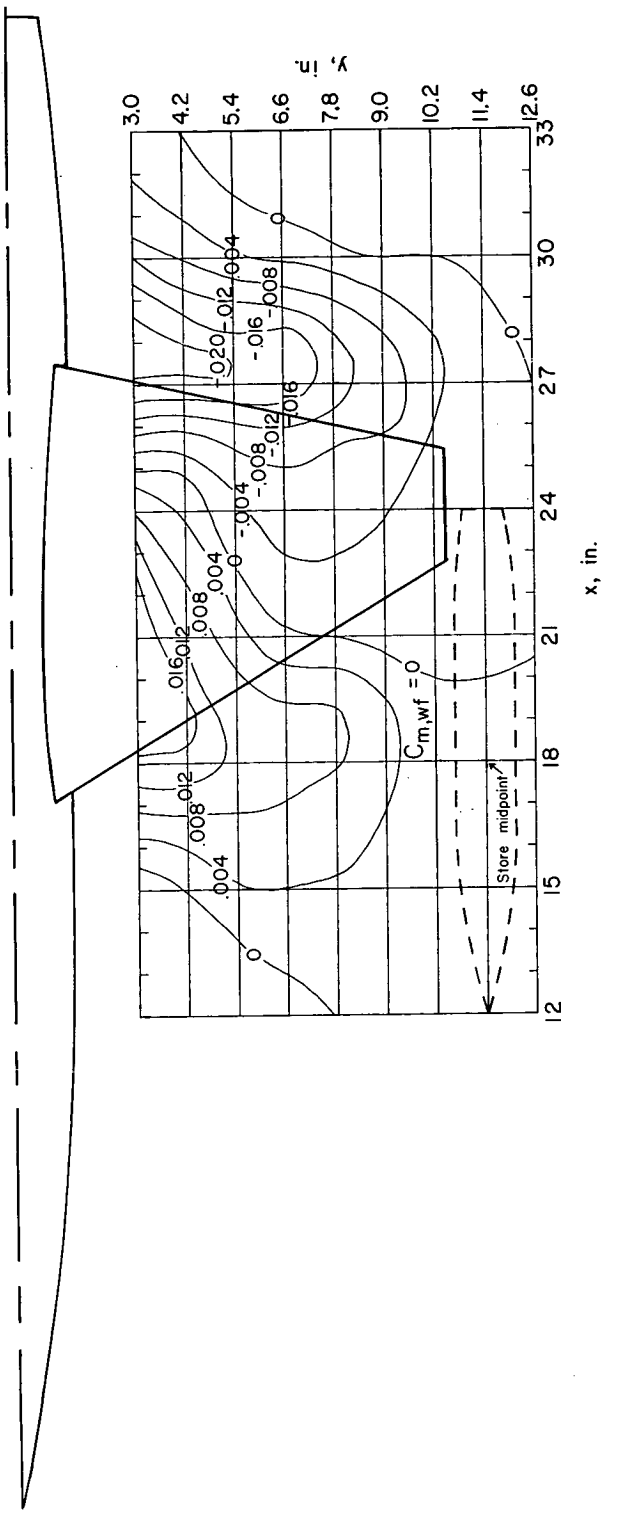

(a) $z = 1.15$ in.; $\alpha = 0^\circ$.

Figure 29.- Contour plot of pitching-moment coefficients of wing-fuselage combination in presence of the store at $M = 2.01$. Pitching-moment coefficient for the isolated-wing—fuselage combination ($\alpha = 0^\circ$, $C_{m,i} = 0.0003$; $\alpha = 4^\circ$, $C_{m,i} = -0.0267$).

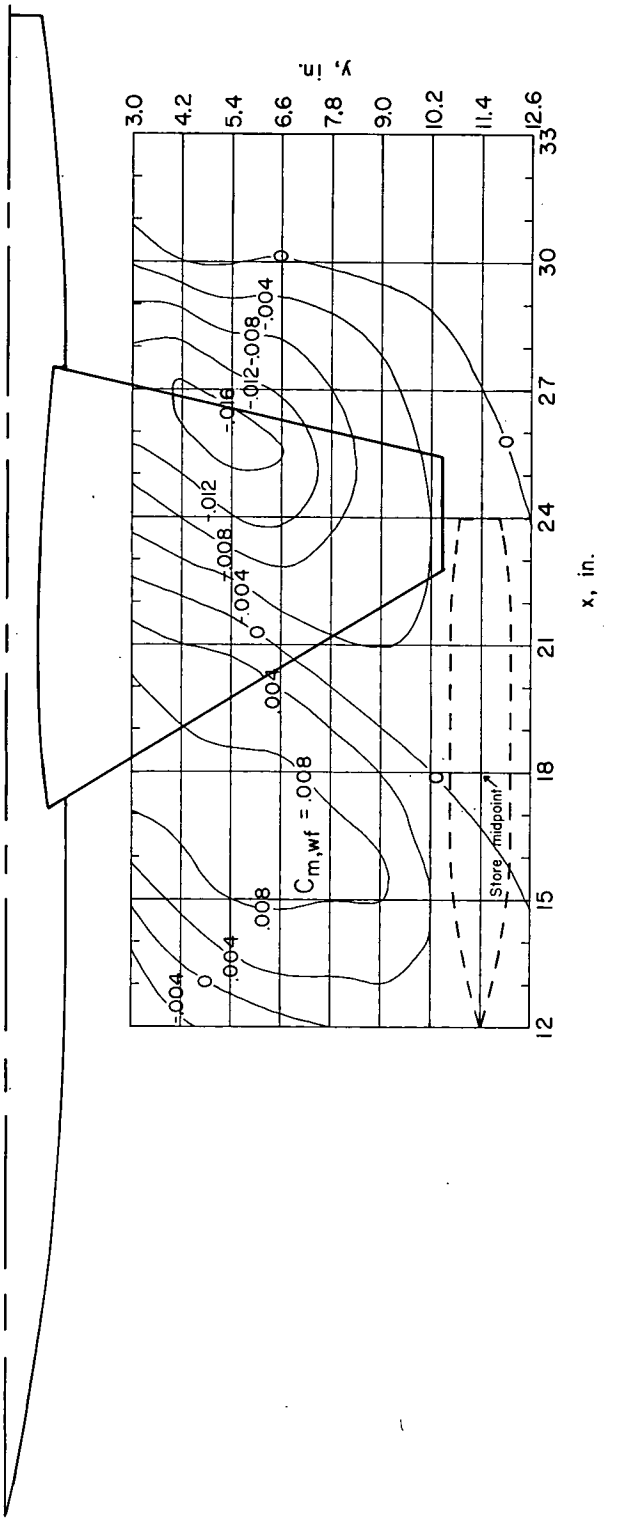

(b) z = 2.09 in.; $\alpha = 0^{\circ}$.

Figure 29.- Continued.

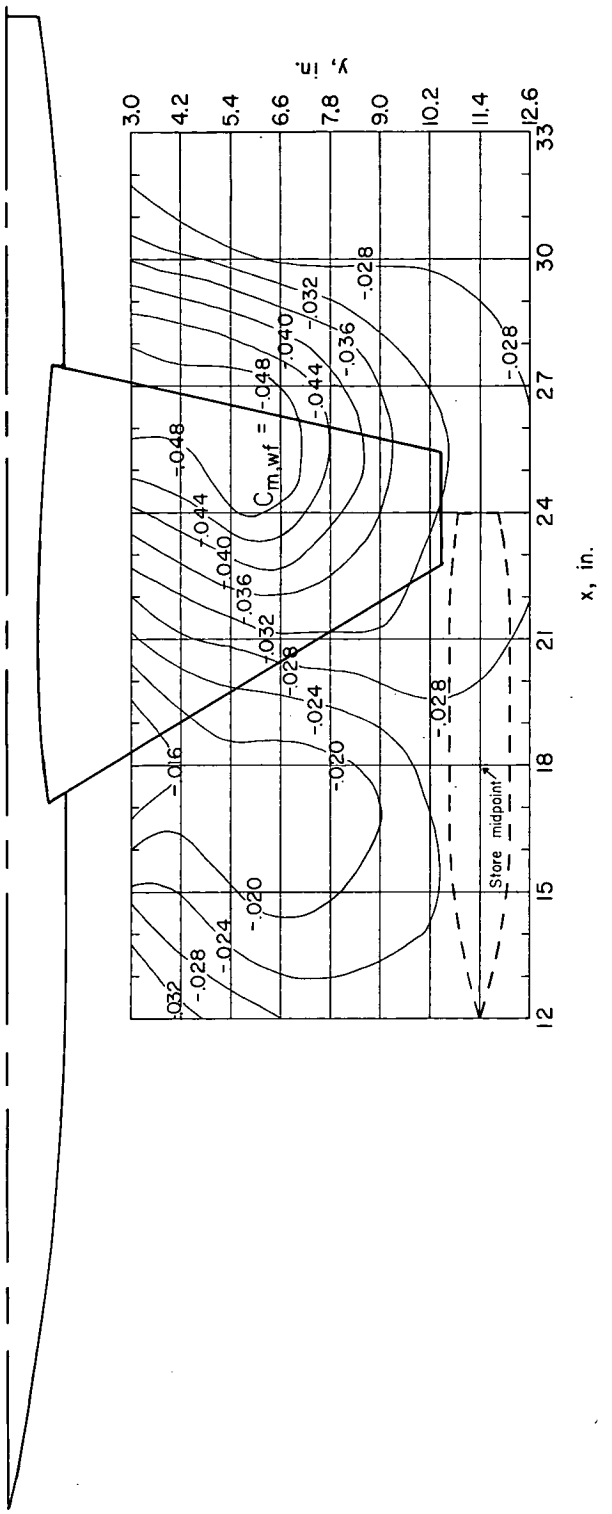

(c) $z = 2.09$ in.; $\alpha = 4^{\circ}$.

Figure 29.- Concluded.

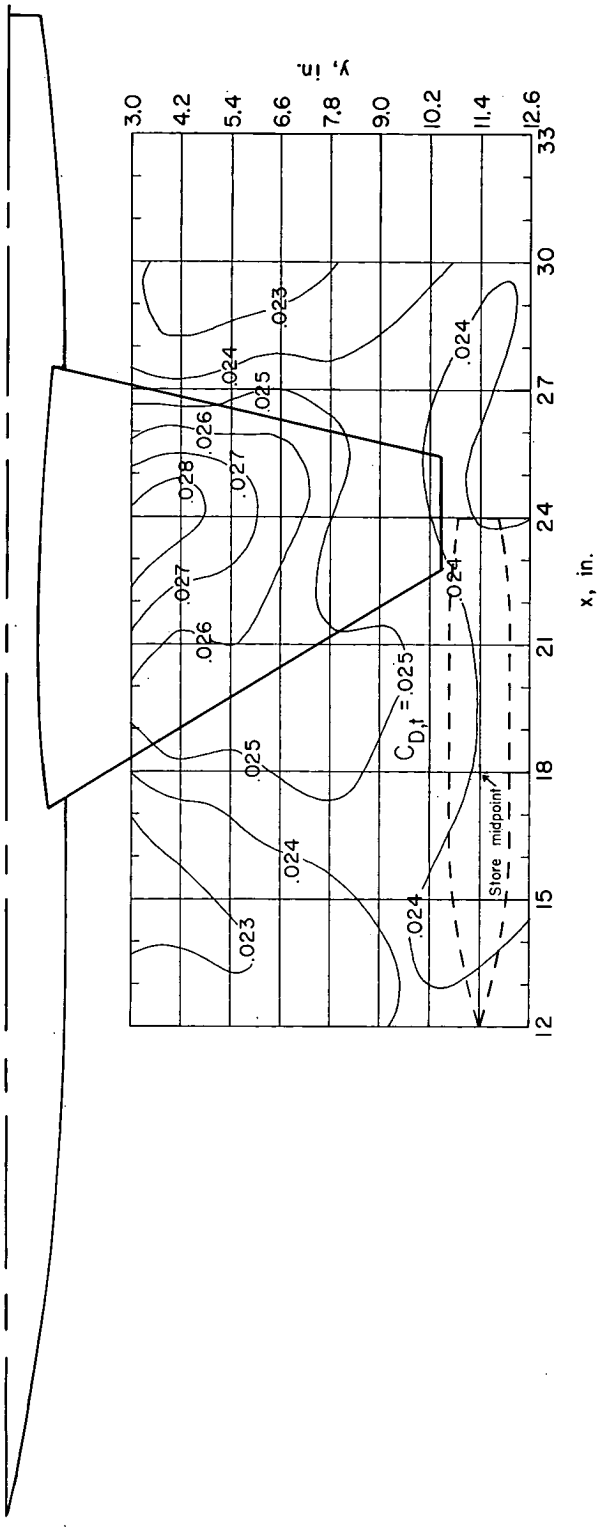

(a) $z = 1.15$ in.; $\alpha = 0^\circ$.

Figure 30.- Contour plot of the total-drag coefficients of the complete configuration (wing-fuselage combination plus store) at $M = 2.01$. Total-drag coefficients for the isolated configuration ($\alpha = 0^\circ$, $C_{D,i} = 0.0239$; $\alpha = 4^\circ$, $C_{D,i} = 0.0360$).

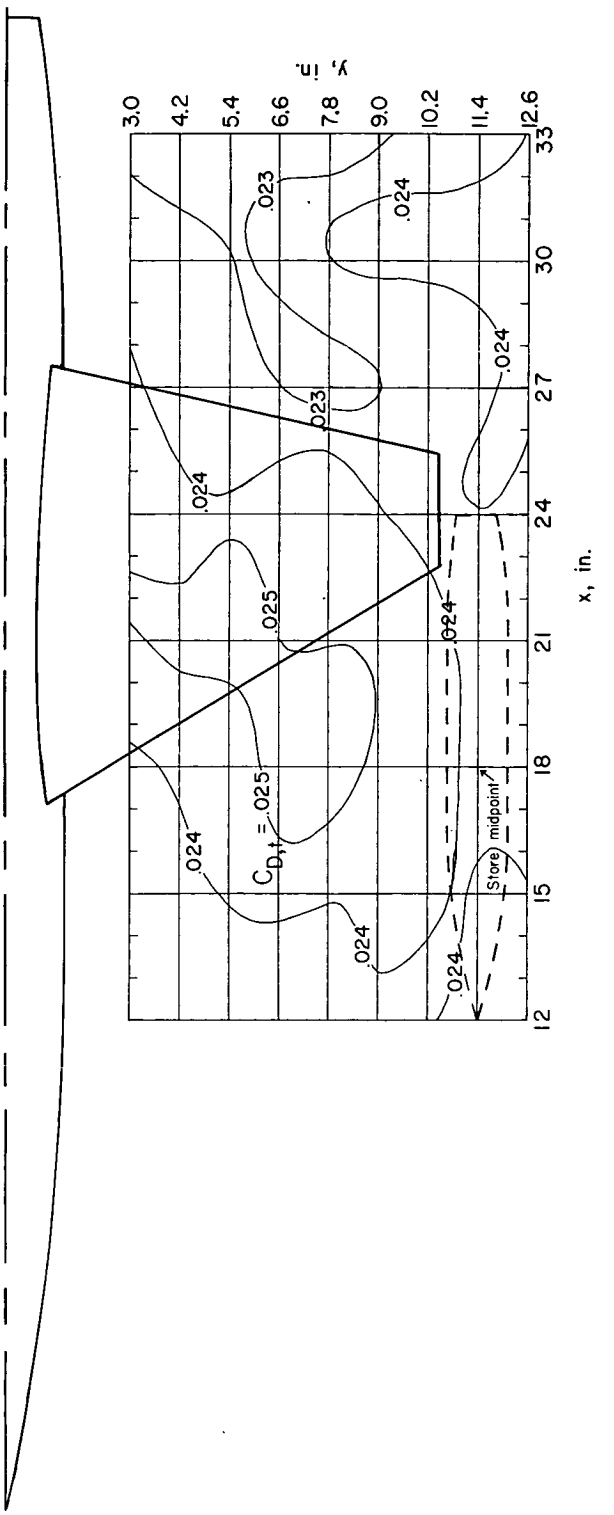

(b) z = 2.09 in.; $\alpha = 0^{\circ}$.

Figure 30.- Continued.

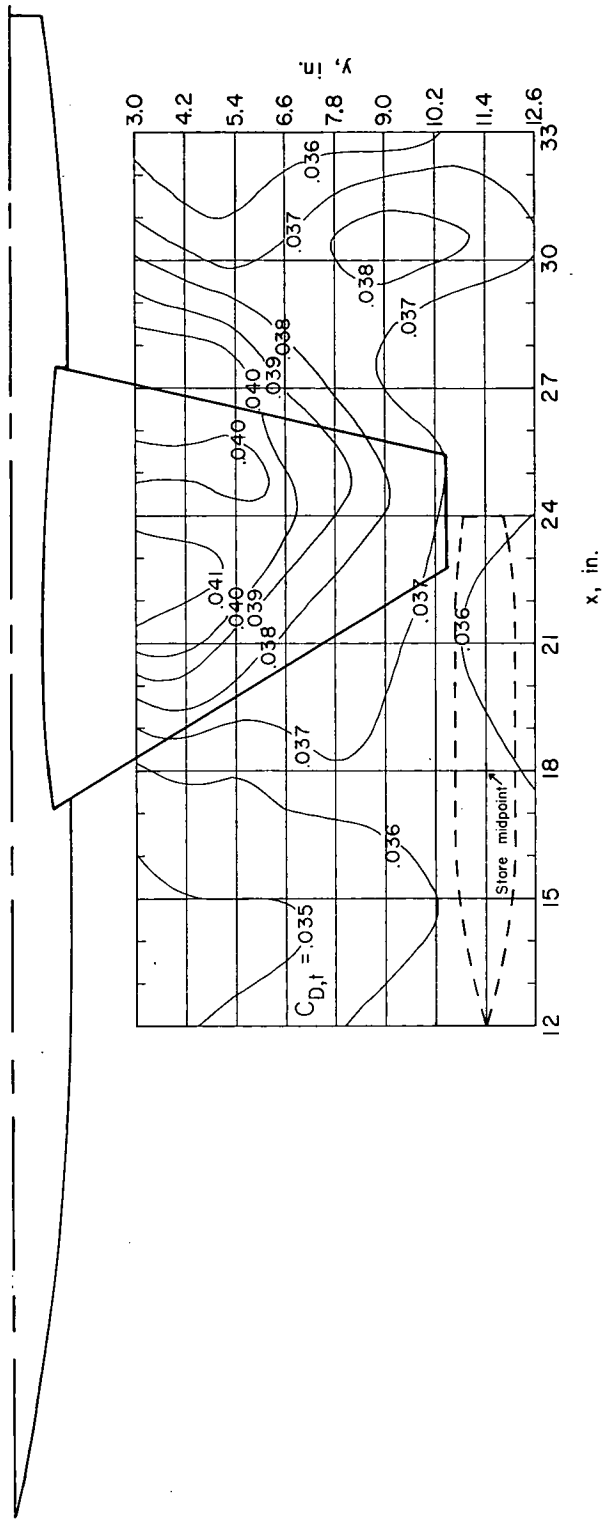

(c) z = 2.09 in.; $\alpha = 4^{\circ}$.

Figure 30.- Concluded.

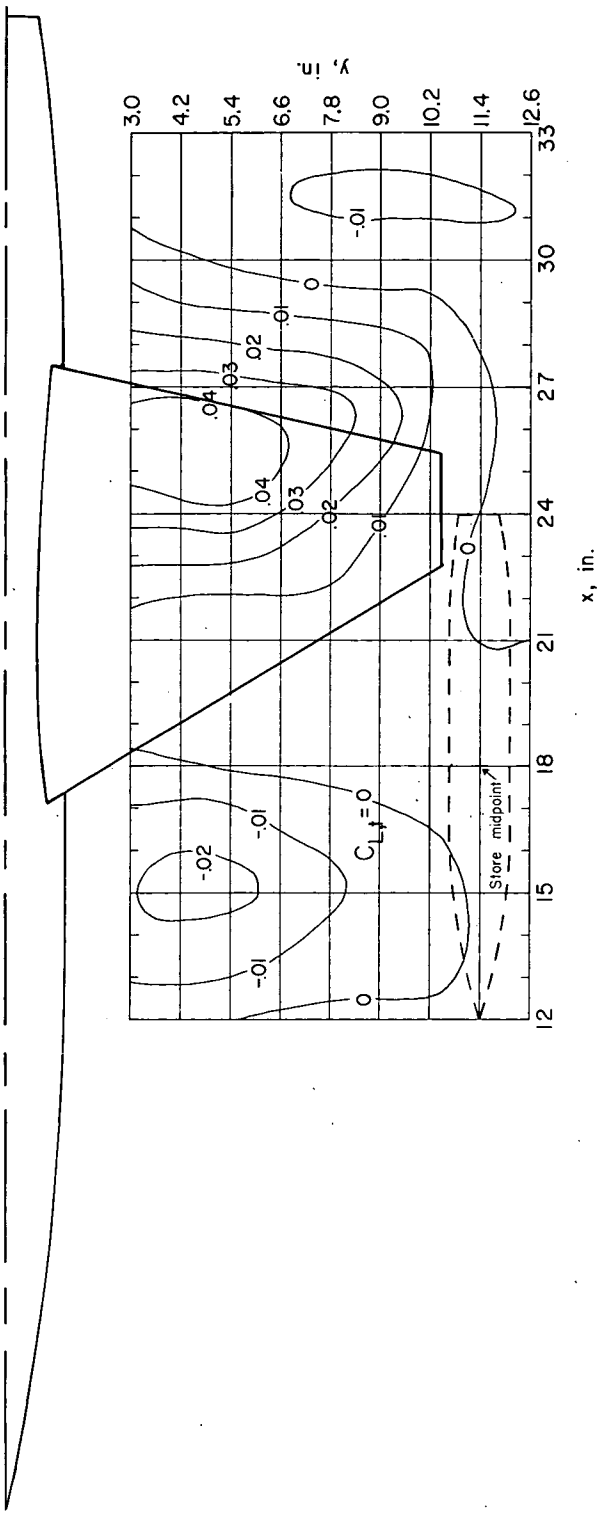

(a) $z = 1.15$ in.; $\alpha = 0^\circ$.

Figure 31.- Contour plot of the total-lift coefficients of the complete configuration (wing-fuselage combination plus store) at $M = 2.01$. Lift coefficients for the isolated configuration ($\alpha = 0^\circ$, $C_{L,i} = -0.0039$; $\alpha = 4^\circ$, $C_{L,i} = 0.1680$).

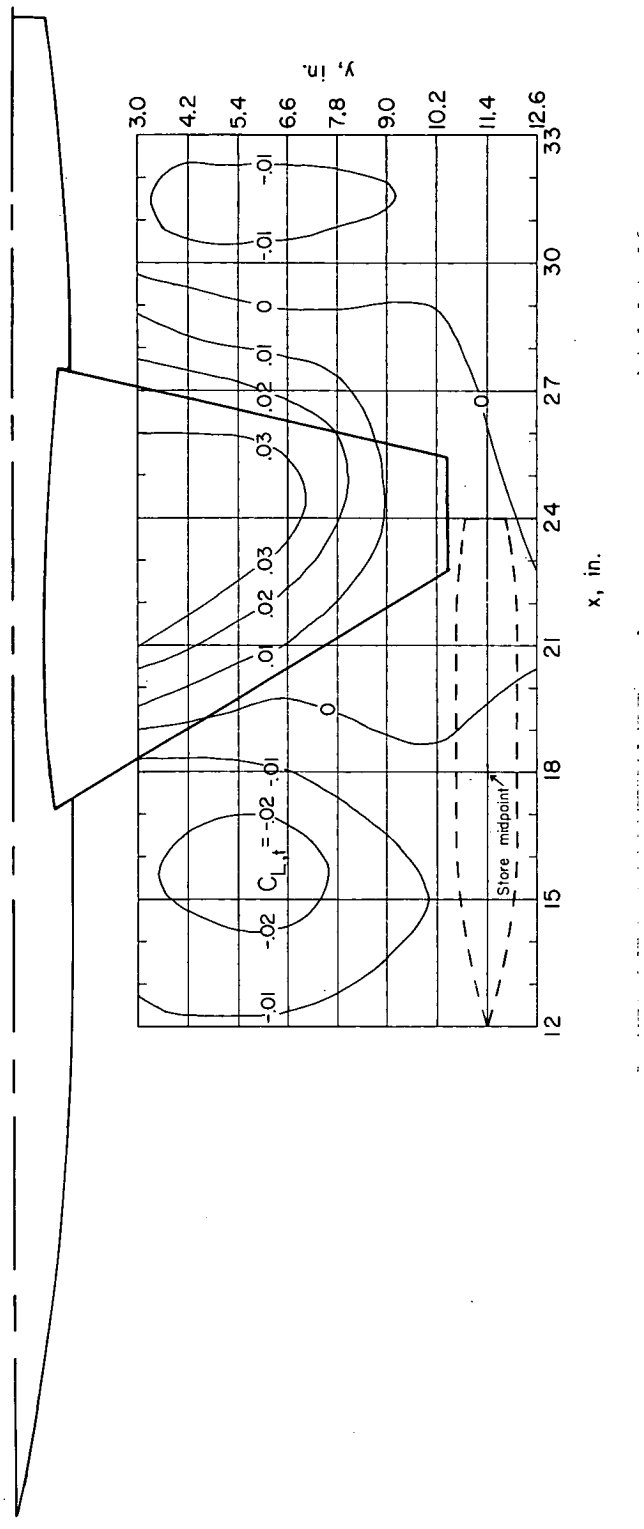

(b) z = 2.09 in.; $\alpha = 0^{\circ}$.

Figure 31.- Continued.

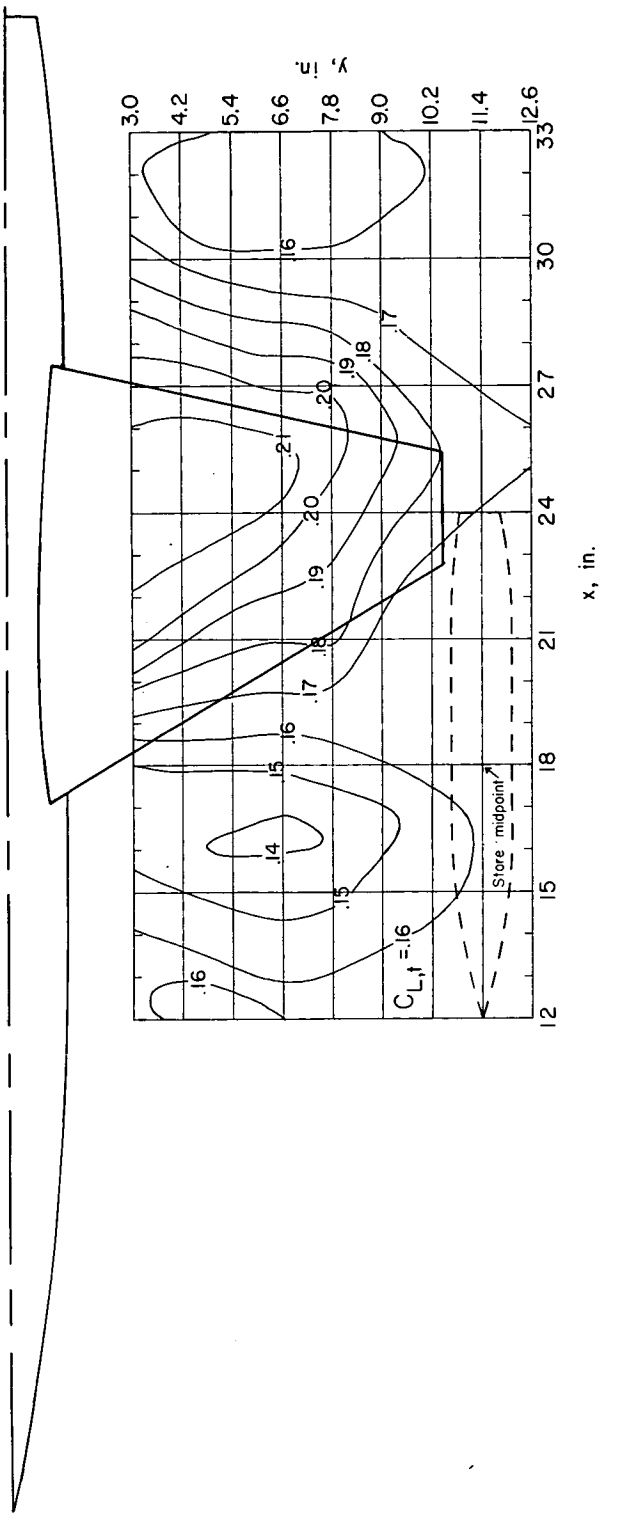

(c) $z = 2.09$ in.; $\alpha = 4^{\circ}$.

Figure 31.- Concluded.

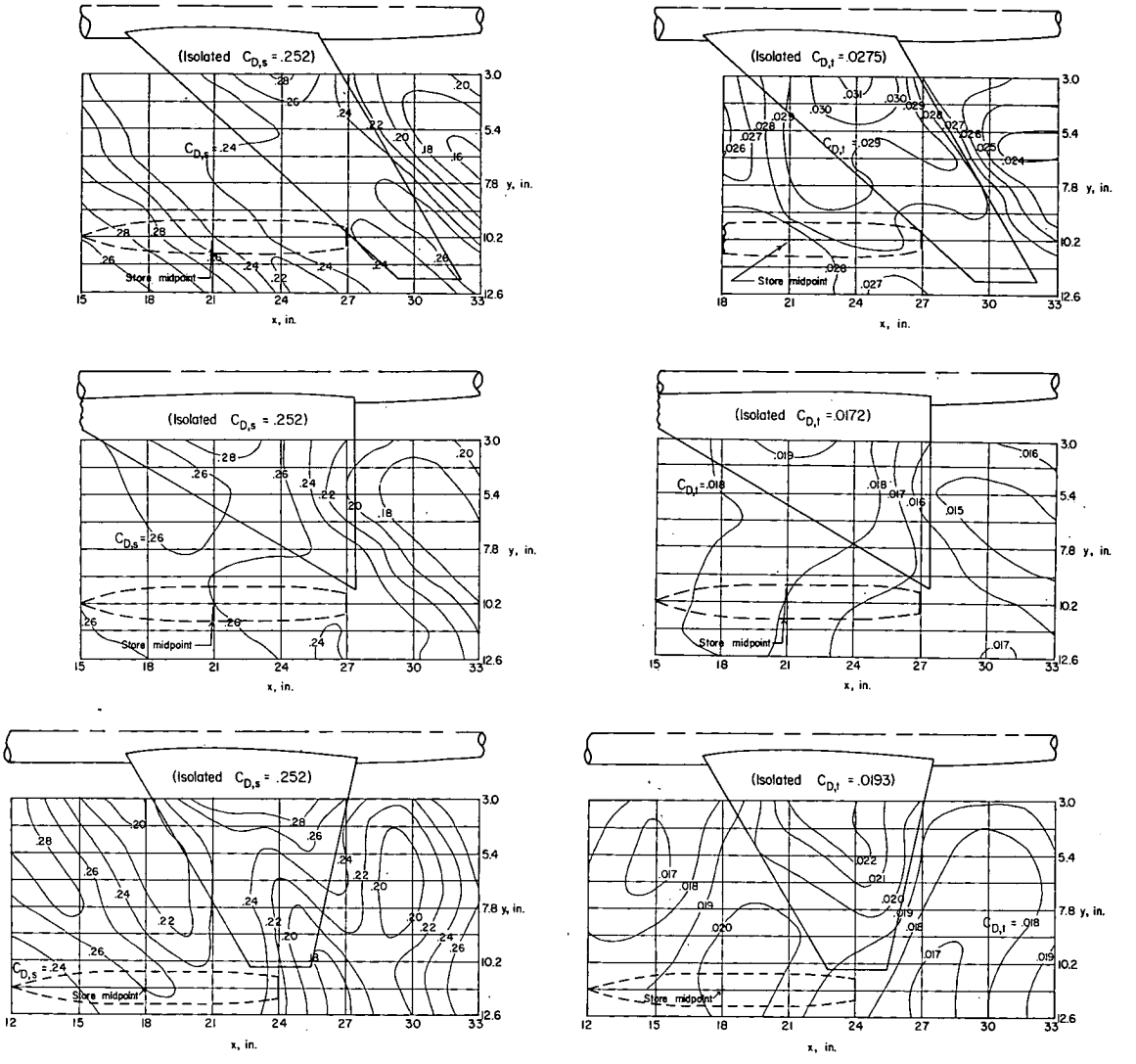

Figure 32.- Comparison of store-drag and total-drag contour plots for the 45° swept wing (refs. 1 and 2), 60° delta wing (ref. 4) and the 22° swept wing. z = 2.09 in.; α = 0°; M = 1.61.

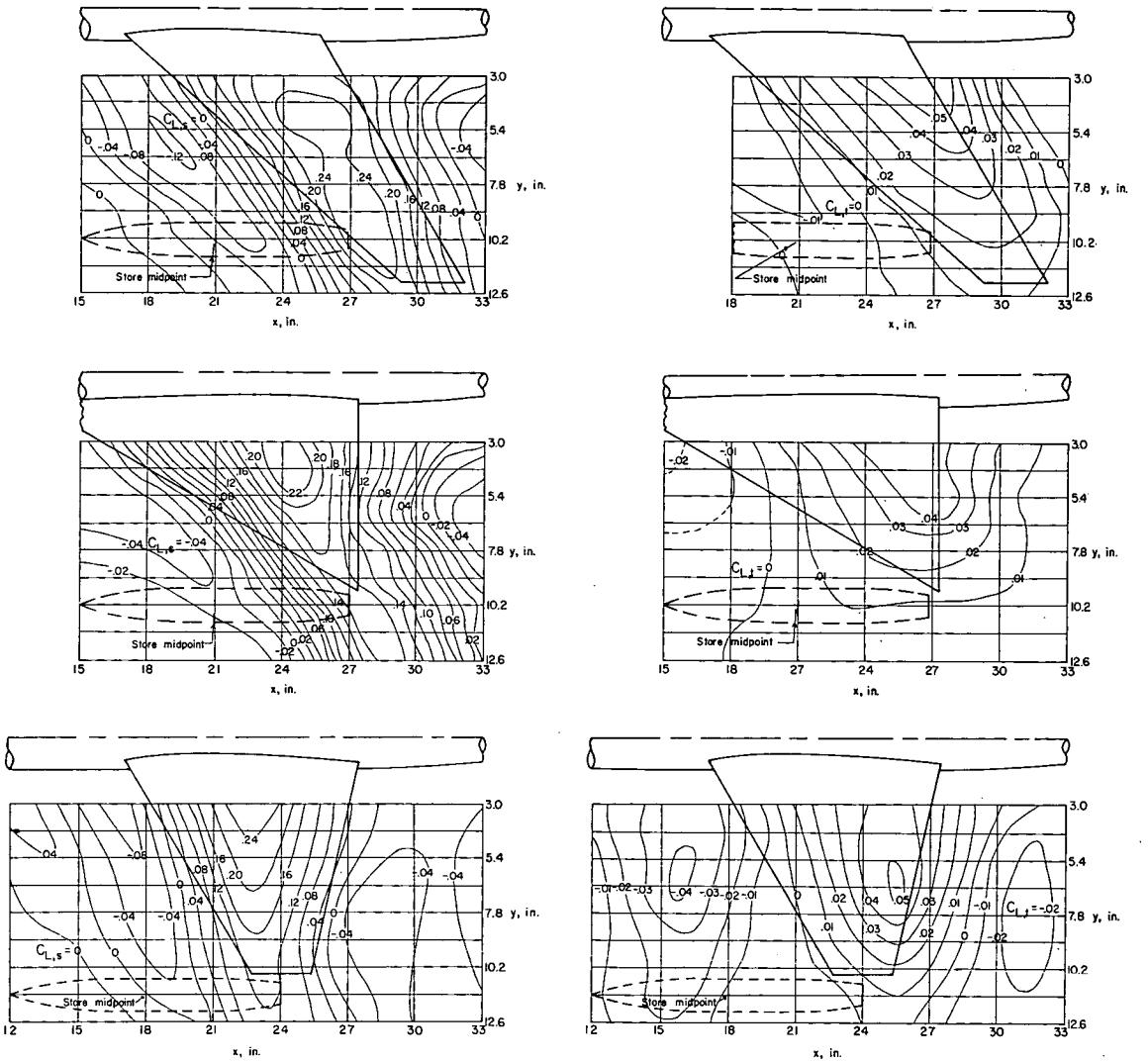

Figure 33.- Comparison of store-lift and total-lift contour plots for the 45° swept wing (refs. 1 and 2), 60° delta wing (ref. 4) and the 22° swept wing. z = 2.09 in.; α = 0°; M = 1.61.

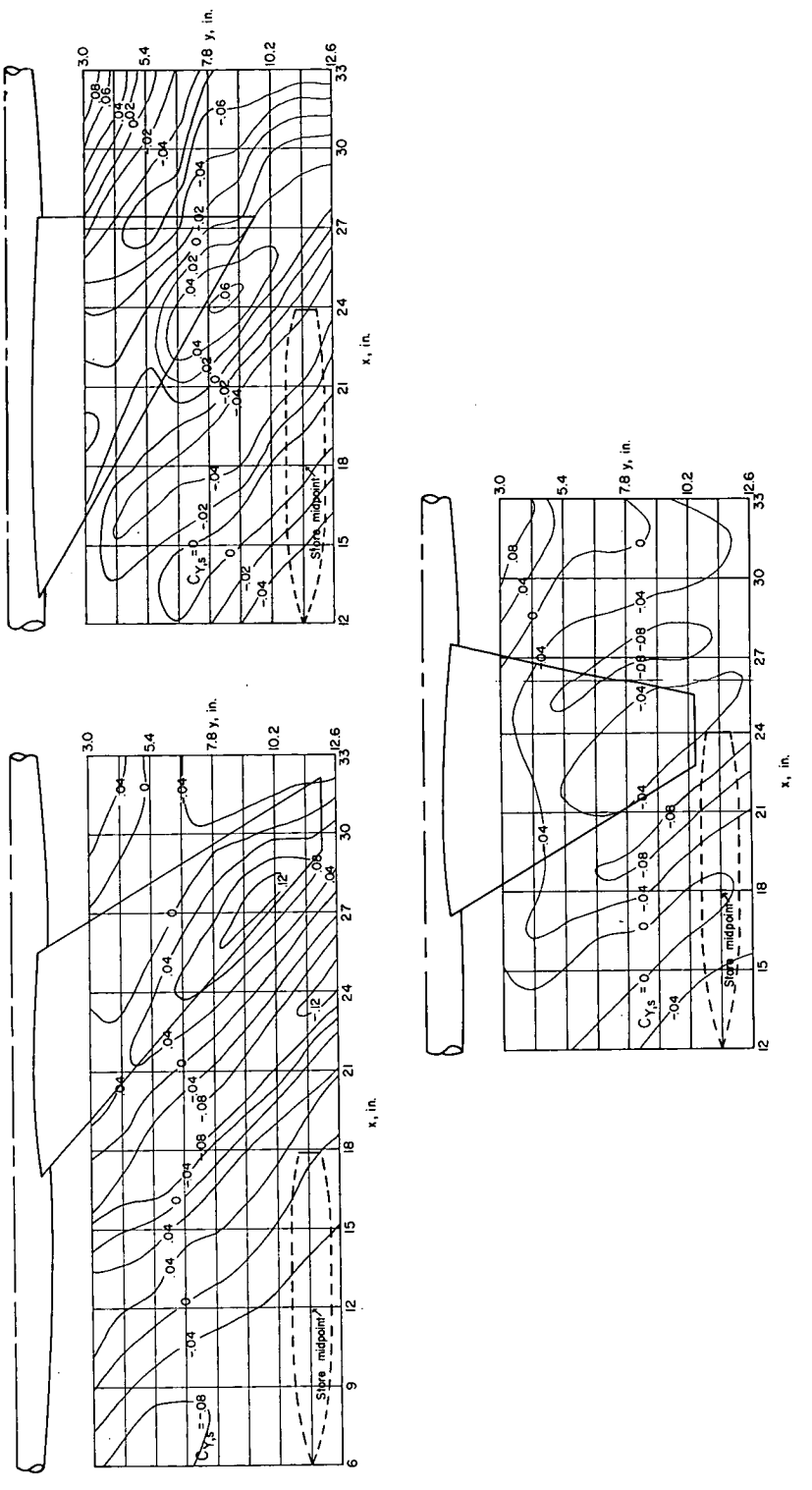

(a) $z = 2.09$ in.; $\alpha = 0^{\circ}$.

Figure 34.- Comparison of store side force in presence of the swept-wing—combination (refs. 1 and 2), delta-wing—combination (ref. 4), and 22° swept-wing—fuselage combination. $M = 1.61$.

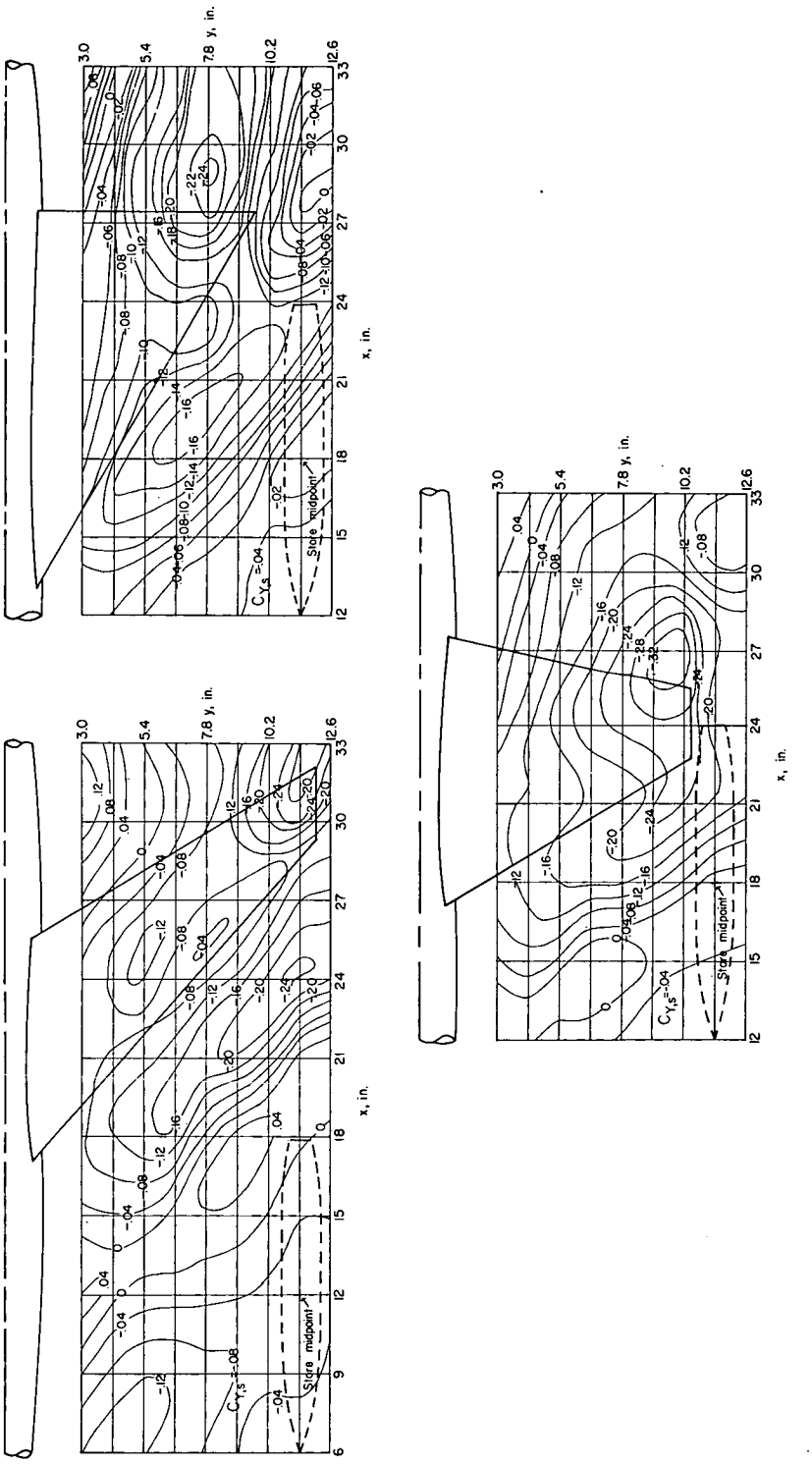

(b) z = 2.09 in.; $\alpha = 4^{\circ}$.

Figure 34.- Concluded.

NACA - Langley Field, Va.